esf european social fund in the czech republic
EUROPEAN UNION
MINISTRY OF EDUCATION, YOUTH AND SPORTS
OP Education for Competitivness
INVESTMENTS IN EDUCATION DEVELOPMENT

Ladislav Doležal, head of the Palacký University Medical Ultrasound Research Laboratory, graduated 1972 in Medical Engineering at the Brno University of Technology and received his PhD in 2000 with the Czech Academy of Science in Prague. He has practiced for more than 30 years in ultrasonographic engineering with the obstetrics and gynaecology clinic of the Medical Faculty Hospital at the Palacký University in Olomouc. During the last fifteen years he has practiced as an Assistant Professor in Medical Biophysics in both Czech and English medical education programmes. He is a member of the safety committee ECMUS, also, of the EFSUMB and he is secretary general of the CSUM. As a senior member of the IEEE he works in the Czech branch of the IEEE EMBS board as well as the board of the SBMILI. He represents the Czech Republic as an expert in the IEC TC87 WG9. He has published more than 120 scientific papers, 2 books and is the inventor of 6 patents.

Christian Kollmann is head of the UltraSound-Lab in the Center for Medical Physics & Biomedical Engineering, Medical University of Vienna. He graduated in Physics at the University of Goettingen in 1992. He received his PhD in Physics in 1998 from the Technical University of Vienna. Since 1993 he has been an Assistant Professor at the Center of ultrasound studies and as a lecturer at the University of Applied Sciences of Wiener Neustadt. As a nominated national expert of the Austrian ÖVE and the Austrian Standardisation bureau (ON) he is currently involved in the international normalisation work of the IEC TC 87 ultrasound group. He is a board member of the Austrian Society of Ultrasound in Medicine (ÖGUM), secretary of the European Committee of Medical Ultrasound Safety (ECMUS) of the EFSUMB, and a member of the Austrian AAA/ÖGA and ÖGMP. As an author he has published over 90 scientific papers and one teaching book in medical ultrasonics and biomedical techniques.

9 788024 431598

Efforts of Ultrasound in Medicine
Latest developments and efforts in medical ultrasound safety topics and bio-effects research
Ladislav Doležal
Christian Kollmann et al.

Ladislav Doležal
Christian Kollmann et al.

EFFORTS OF ULTRASOUND IN MEDICINE

Latest developments and efforts in medical ultrasound safety topics and bio-effects research

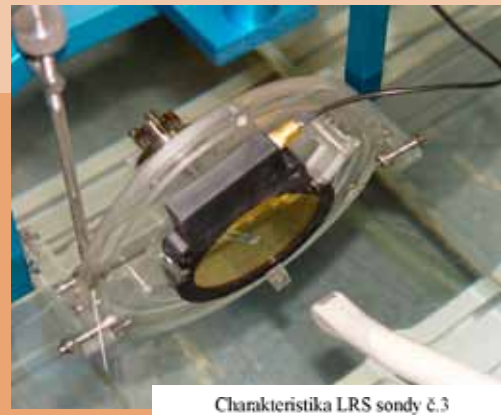

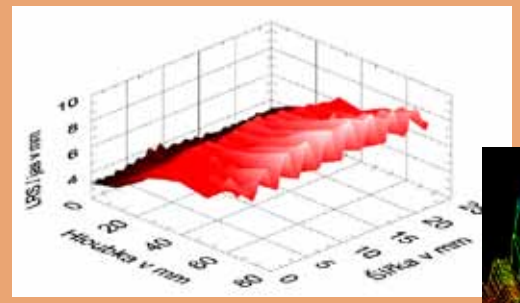

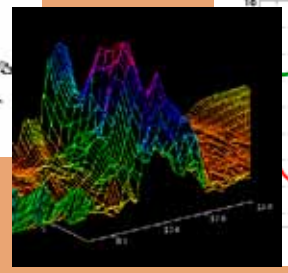

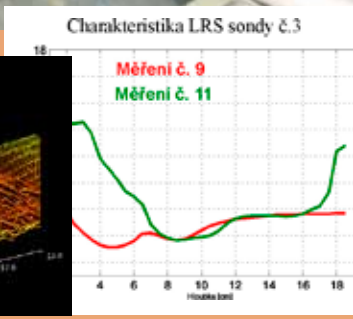

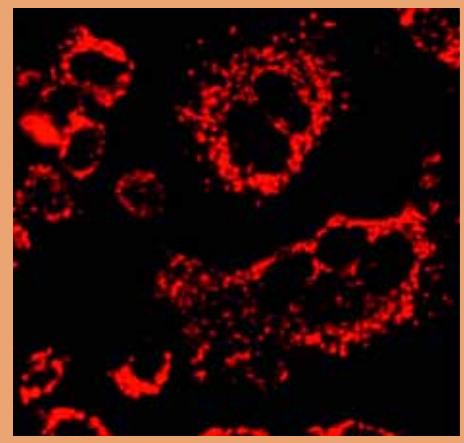

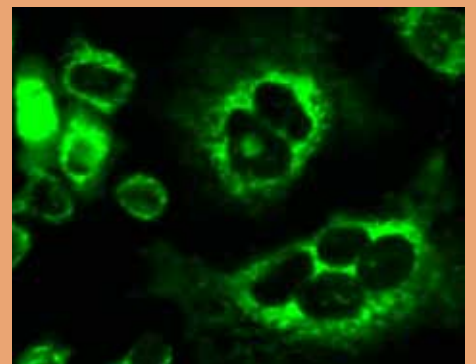

Efforts of Ultrasound in Medicine

latest developments and efforts in medical ultrasound safety topics and bio-effects research.

Efforts of Ultrasound in Medicine

Ladislav Doležal
Faculty of Medicine and Dentistry,
Palacký University, Olomouc, CZ

Christian Kollmann
Center for Medical Physics & Biomedical Engineering,
Medical University Vienna, A

at al

Reviewers:

Dr. Robert Morrison
Wheelers 20 Hill
Victoria 3150, Australia

Prof. Ing. Jan Hálek, Ph.D.
Palacký University, Olomouc, Czech Republic

Edited by Ing. Ladislav Doležal, Ph.D., Dr. Ing. Christian Kollmann
Executive Editor prof. MUDr. Milan Kolář, Ph.D.
Responsible Editor Mgr. Lucie Loutocká
Layout Mgr. Jaromír Vachutka
Cover Design Ing. Ladislav Doležal, Ph.D., Jiří Jurečka
Cover Photos from the archives of the autors

Published by Palacký University, Olomouc
Křížkovského 8, 771 47 Olomouc
www.upol.cz/vup
e-mail: vup@upol.cz

Printed by GRAFIA NOVA, s. r. o.
Lesní 2331, 756 61 Rožnov pod Radhoštěm
www.grafianova.cz

Olomouc 2012

First Edition

~~ISBN 978-80-244-2656-3~~

List of authors in alphabetical order

Wendy Berkers
Cablon Medical B.V., Leusden, NL
Jacinta E. Browne BSc. MSc. PhD. CPhys.
School of Physics, Medical Ultrasound Group, Dublin Institute of Technology, Dublin, IRL
jacinta.browne@dit.ie
Ing. Ladislav Doležal, PhD.
Palacký University in Olomouc, Faculty of Medicine, Olomouc, CZ
ladol@tunw.upol.cz
Dr. Andrew Hurrell, PhD., BSc (Hons)
Precision Acoustics Ltd, Dorchester, UK
andrew@acoustics.co.uk
Dipl.-Ing. Cosima Koch
Vienna University of Technology, Institute of Chemical Technologies and Analytics, Vienna, A
cosima.koch@tuwien.ac.at
RNDr. Hana Kolářová, PhD.
Palacký University in Olomouc, Faculty of Medicine, Olomouc, CZ
kol@tunw.upol.cz
Dr. Ing. Christian Kollmann
Medical University of Vienna, Center for Medical Physics & Biomedical Engineering, UltraSound-Lab, Vienna, A
christian.kollmann@meduniwien.ac.at
Dipl.-Ing. Stefan Radel, PhD.
Vienna University of Technology, Institute of Applied Physics, Vienna, A
radel@tuwien.ac.at
Ing. Kateřina Tománková, PhD.
Palacký University in Olomouc, Faculty of Medicine, Olomouc, CZ
katerina.tomankova@ upol.cz
Dr. Ing. Friedrich Überle
Hamburg University of Applied Sciences, Faculy of Life Sciences, Biomedical Technology Department, Hamburg, D
friedrich.ueberle@haw-hamburg.de

Preface

Ultrasound has been used for more than 60 years clinically, mainly not only in the modality of diagnostic imaging but also as a therapeutical method. Since very early on, it was and still is the aim of many scientists to understand and clarify the mechanism of interactions between the emitted ultrasound energy and biological tissues.

These efforts have ensured that ultrasound is regarded today as the tone of the safest imaging modality in use clinically to show tissue structures hidden in a patient's body.

Ultrasound societies, congresses and conferences have discussed and published the latest research results, concerning the ultrasound interactions with biological tissues. This along with the highlighting of relevant safety guidelines and policies emphasis the important merits they deserve.

The main aim of the book, in particular the concern of both editors, is the collating of the latest research results and meanings of ultrasound-induced bio-effects, interactions and related safety issues. Therefore the book is structured in two parts; - clinical issues and - technical-practical issues to bio-effects and medical device safety topics.

Last but not least the editors would like to thank

- the manuscript reviewers
- Dr. Robert Morrison for grammactical correction
- Mgr. Jaromír Vachutka for his patient work on formatting layout of this book.

Without their support we would not have been able to publish and issue this small book !

Ladislav Doležal
Christian Kollmann

Olomouc and Vienna, June 2012

Contents

1 Ultrasound Bio-Safety survey for practicians - the current ECMUS policy

Christian Kollmann

The topic ultrasound bio-safety and exposure is engaged in research and practice since the first scanning equipment was used for routine practice. It has been detected that the ultrasound waves are not only used to produce images but also interact with the medium or tissue being coupled. More and more research and interest has been spent on these various interactions, and over decades has generated different modern application devices using the special advantages of the wave components for therapeutic (physio-therapy, HIFU) and diagnostic purposes (Elastography, Harmonic Imaging, Intermittent Imaging etc.)

But nevertheless there are potential drawbacks combined with the emission of ultrasound waves and if modern equipment is used the practician must know what is going on and what could happen.

The following paragraphs will cover a comprehensive survey of possible ultrasound interactions, actual epidemiological outcomes and bio-effects as well as “state-of-the-art” safety guidelines and recommendations given by the European Safety Committee (ECMUS) of the European Federation of Societies for Ultrasound in Medicine and Biology (EFSUMB).

1.1 Ultrasound interactions

An ultrasound wave regardless if continuous or pulsed interacts with its mechanical or thermal wave component with tissue (Figure 1). Depending on the imaging mode and the selected user pre-sets and settings, different effects can occur. Within the last 4 decades of clinical use of ultrasound imaging along with each new scanner generation an enhancement of ultrasound power output could be detected. The pressure amplitudes [p_-, p_+, MPa] representing the mechanical component of the wave and the intensity [mW/cm^2] or total power emission [W] characterising the thermal component have been increased [1]. In the early 1990s the Food and Drug Administration (FDA) changed its paradigm of safety and stated a new

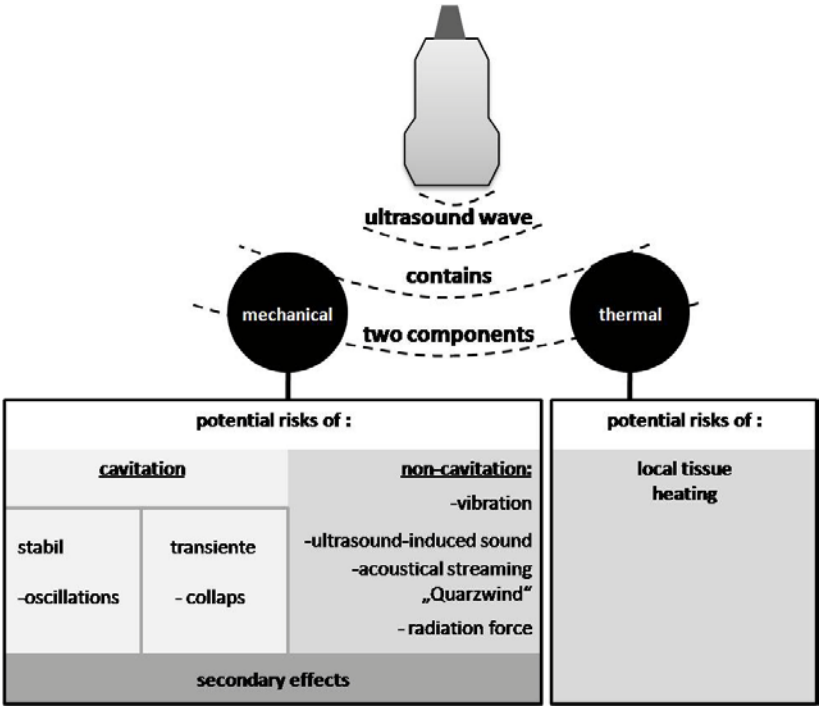

Figure 1 Ultrasound interactions.

upper limit for the maximum intensity output for diagnostic imaging scanners [2], allowing a new output exposure capable of perhaps causing side-effects that can imply a potential risk for body tissue.

1.1.1 Mechanical interactions

Cavitational interactions

One effect that is strongly related to the wave´s pressure amplitude is cavitation. Other medical ultrasound equipment using this effect are for instance Lithotripsy and ultrasound scalpels. If the pressure amplitudes are very high (several MPa) small cavities are generated within fluids or tissue, also free bubbles can act as such cavity seeds. Within the negative

pressure phase of the wave high traction forces are responsible for the generation of cavitation. Normally within a human being there are no free bubbles except when they are introduced invasively by a physican acting to enhance the ultrasound echoes. These ultrasound contrast agents (UCA) have the potential to produce cavitation on a lower pressure amplitude level [3-6].

Depending on the pressure amplitude of the ultrasound pulses such UCA answer with a special signature. At low pressure amplitude (low MI) the bubbles expand and contract linearly according to the pressure variation and it is named stable cavitation (Figure 2). The stabilized bubbles answer with a specific resonance frequency f according to

$$f \approx \frac{1}{2\pi r}\sqrt{\frac{3\gamma}{\rho}\left(p+\frac{2\sigma}{r}\right)} \text{ (de Jong et al. 1992)} \quad (1)$$

with r: bubble radius, ρ: density of fluid, σ: surface tension, γ: adiabatic gas constant, p: pressure of fluid.

In Table 1 mean bubble sizes and corresponding resonance frequencies are listed for commercially available UCA.

Table 1 Bubble sizes (diameter) of commercial Ultrasound Contrast Agents (UCA) and corresponding resonance frequencies [3, 7-11].

UCA name	EC accredited	Manufacturer	Mean bubble size [µm]	Resonance frequency [MHz]
Levovist	Yes	Schering	3	3.75
SonoVue		Bracco	2.5	4 – 4.5
Optison		GE Health Care	3.7	2
Luminity	No	Brystoll-Myers Squibb	2	1.5
Albunex	No	Molecular Biosystems	3 – 5	1.5- 2.2
Definity	No	Brystoll-Myers Squibb	1 - 4	10 – 20

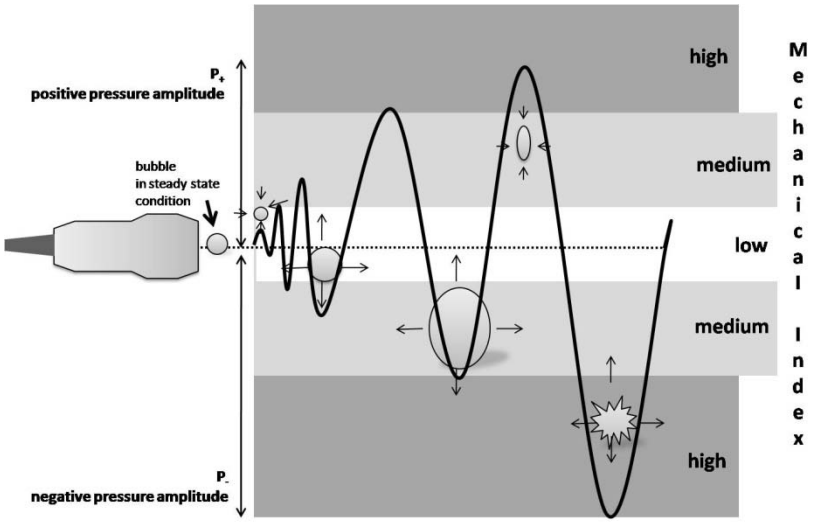

Figure 2 Schematical view of bubble behaviour within an ultrasound field with different amplitudes. Depending on the Value of the Mechanical Index there is linear, non-linear size shifting behavior or destruction (cavitation) of the microbubbles.

With increasing pulse amplitudes the bubble shifts its expanding and contracting phases to a higher non-linear manner and produces harmonic acoustical spectra as its signature. On the upper amplitude´s range (high MI) the stable cavitation turns into a transient cavitation, that is characterized by bubble destruction ("collaps") and fragmentation to smaller bubbles and further secondary effects (shock waves, local heating etc.) due to its incapability to change its shape during the fast wave cycles (Figure 2).

Normally within the human body cavitation does not occur because the pressure thresholds are relatively high (Table 2) and there are no free bubbles available but if ultrasound contrast agents (UCA) are present this threshold is decreased because micro-bubbles are introduced externally into the blood pool. Therefore a potential risk of cavitation can exist with actual ultrasound scanners that generate pressure amplitudes up to several MPa and working in low the frequency ranges.

The user of a scanner can recognize the amplitude by tracing the mechanical index (MI). A visible indicator or indice that is displayed online at the monitor or display. This indice will be explained subsequently.

Table 2 Thresholds from which cavitation can occur.

Medium	Threshold for cavitational effects [MPa]
Ultrapure water	ca. 100 (theor.) / 30 (exp.)
Normal water	ca. 0.1 – 0.5
Human body	ca. 1 – 10

The generation of cavitation is a complex process depending on scanner settings (e.g. pulse length, PRF, frequency) and medium properties (density, temperature, fluid pressure, viscosity).

At some ranges the user can manipulate the emitted pressure amplitude (MI-value) of the scanner by choosing particular set-up parameters:

- Mode (B, M, Doppler etc.)
- Acoustic output
- Penetration depth
- …
- Frequency
- Sample Volume size & depth
- PRF

However the set-up is chosen during an examination, the user is finally responsible for the potential risk and he/she should be aware of his/her action on the scanner optimisation.

Non-cavitational, non-thermal interactions

Another kind of mechanical interactions of the sound wave that are not related to cavitation are acoustic forces on particles that are smaller than the emitted wavelength and directed (acoustic) streaming along the wave propagation (Figure 3). These interactions have been monitored in clinical routine as reorienting or spinning of (blood) cells in suspensions and with Doppler ultrasound as low velocity measurements within the bladder or fluid-filled lesions [12-15].

In plane wave conditions the force F that attaches a particle or generates acoustic streaming can be calculated as:

$$F = \frac{2\alpha I_{TA}}{c} = \frac{W}{c} \text{ (Nyborg 1965, [15])} \quad (2)$$

with α: absorption coefficient of the fluid, I_{TA}: temporal average intensity at this point/depth, c: speed of sound in the fluid, W: total power.

Depending on the modality and output power used these forces can differ within a wide range (Table 3) but is capable of having some impact on tissue or cellular structures. Within the imaging modalities Doppler applications with their small detection area (sample gate, color window) result in comparable higher emitted forces. In Table 3 these emitted forces are calculated for different clinical ultrasound modalities.

Table 3 Acoustical forces that can be producing by different ultrasound equipment in tissue (c= 1540 m/s).

Equipment / mode	**Pressure** [MPa]	**Output power W** (range) [mW]	**Emitted Forces** (calculated) [µN]
B-Mode	1 - 8	5.7 – 57.6	3.7 – 37.4
M-Mode		1.5 – 14.7	1.0 – 9.5
Spectral Doppler	1 - 5	8.8 – 250	5.7 – 162.3
Color Doppler		23 – 225	14.9 – 146.1
CW-Doppler		21 – 109	14.3 – 70.8
Physio-Therapy	0.1 – 0.7	125 – 15000	81.2 – 9740.3
Lithotripsy	10 - 100	10 - 100	6.5 – 65
HIFU	5 - 15	35000 - 155000	22727.3 – 100649.3
Compared to: headphone audio	7.9 (116 dB)	50	32.5

Remark: 1 N = 10^6 µN is the force giving a mass of 1 kg an acceleration of 1 m/sec^2.

Another interaction is ultrasound-induced vibration or noise (Figure 3) that have been reported in obstetrics [16, 17]. It has been observed that fetal movements during scans increased and the authors concluded that

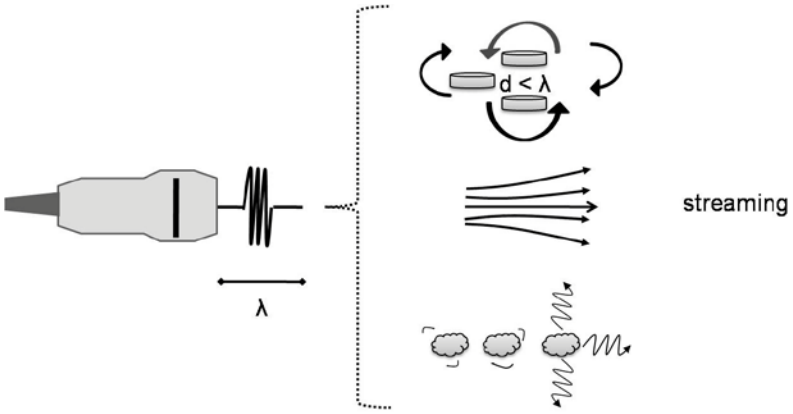

Figure 3 Non-cavitational, non-thermal interactions that can occur if an ultrasound wave is emitted. Particles can be rotated, a micro-streaming occurs or/and particles can vibrate and emit noise.

the repeated ultrasound wave emission (PRF) can generate an oscillating force on objects which induces vibration or noise that have frequencies lying within the audio spectrum and can be detected by the fetus who is reacting to that unusual impact.

It is important to note the potential of bio-effects arising from radiation forces, particularly when ultrasound is used to scan in early or first trimester pregnancies where cell movements and development are prominent.

1.1.2 Thermal interactions

Each ultrasound wave deposits energy in terms of local heating to the human body due to absorption processes. The longer a region (A) is locally sonicated the greater the energy (P) is introduced and the region heats up. The amount of thermal energy increase depends on the pulse length, the pulse repetition rate (PRF) and characterisation of the total energy deposition into the body region (Figure 4). Continuous waves produce the highest thermal increase, followed by Doppler (Spectral and Color) pulse regimes. The pulses used for B-mode are not as frequently emitted as Doppler pulses and the length is shorter (Figure 4).

Another aspect for thermal interactions is the shape or the size of the focal region of the three-dimensional ultrasound beam. An unfocused beam of the same output power of a probe covers a larger tissue region in a special depth (Figure 5 left) than a focused beam (Figure 5 right); but the ultrasound intensity, I, at that region is higher according to the equation (3):

$$I = \frac{P}{A} \left[\frac{\mathrm{mW}}{\mathrm{cm}^2}\right] \tag{3}$$

with P: ultrasound power, A: insonified area.

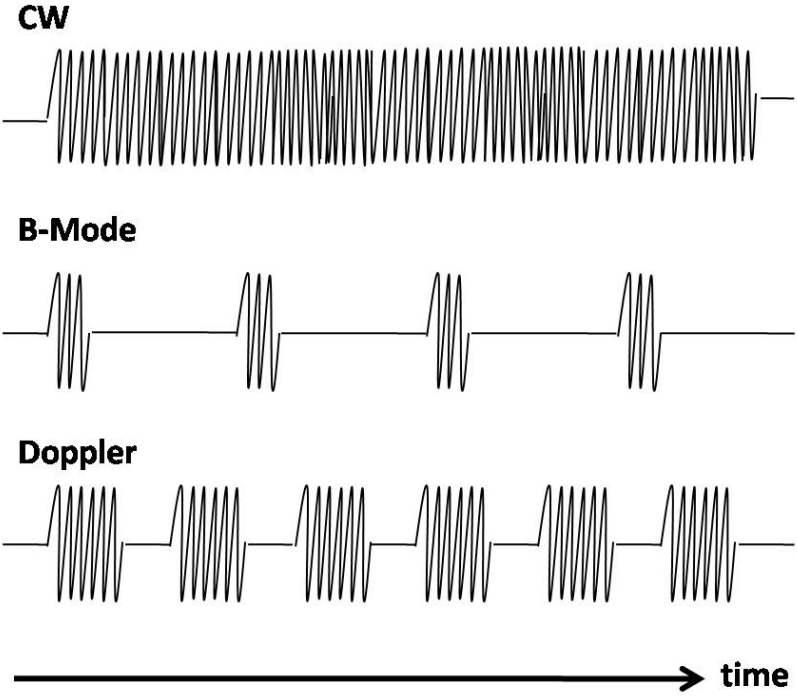

Figure 4 Schematical representation of emitted pulse length and pulse repetition frequency (PRF) for different ultrasound imaging modes.

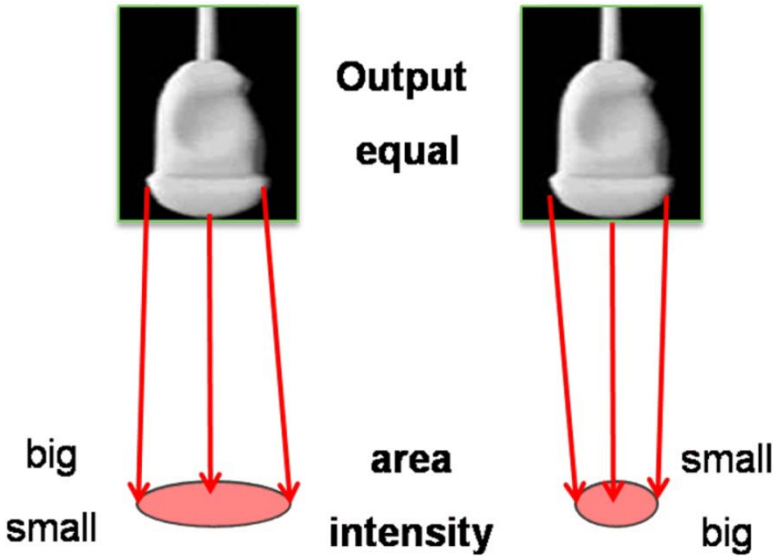

Figure 5 Schematical comparison of the intensity delivered in a special depth according to equation (3) using the same ultrasound output but an unfocussed (left) or focused beam (right).

Various scanner manipulations by the user can influence the outcome of the thermal component of the ultrasound beam as well as the conditions of the patient (e.g. tissue perfusion, absorption). Additionally the probe handling i.e. long stationary stops or long examination times can lead to an increase of tissue temperature. The highest increase of temperature can be expected at the skin surface with high frequency probes due to the different acoustic impedances between tissue and probe surface. While using intravascular or transoesophageal probes the heating of the probe itself must be taken into account. The temperature is monitored to minimise harm in the adjacent tissue.

Modern scanners calculate a special thermal index (TI) that gives the user a rough idea about the potential heating risk.

1.2 Epidemiological investigations and adverse biological effects

In the literature, namely from large Scandinavian studies, it is reported that almost all kinds of speculations of epidemiological change within the human´s development due to influence by early routine ultrasound scanning could not be interpreted as being significant [18, 19]. A survey of different epidemiological investigations and their outcome is listed in Table 4.

Table 4 Epidemiological items and potential influence by ultrasound.

Item	Proved influence of ultrasound
- Malignity of children	None
- Reduced birth weight	None
- Reduced birth body size	None
- Dyslexy	None
- Neurological changes	None
- Hearing / optical adverse effects	None
- Scholastic development	None
- Left-handerness / non-right handerness / Ambidextry	Open (potential influence for boys)

However, one study concerning the distribution of left-hander under male newborns is influenced by early ultrasound scanning. The latest evaluation of the available database data leads to this assumption. But this is not yet firmly proven and needs further data for a significant statement.

Another limitation of the future reliability of this epidemiological data is the change of allowed maximum output announced by the Food and Drug Administration in 1992 [2]. Since that date the manufacturers are allowed to sell ultrasound equipment with a maximum intensity output of 720 mW/cm^2. Only for the application in opthalmology is the output restricted to 50 mW/cm^2. This was not possible before 1992, therefore most of the epidemiological data is based on equipment with restricted maximum output up to 95 mW/cm^2.

Within the next few years we might have new and sufficient data acquired with modern equipment under FDA 1992 regulation and using new imaging methods. This will allow a greater evaluation of differences or various imaging methods on epidemiological outcome. Additionally in modern publications detailed information is given of the apparative exposimetry data used that was not standard in the recent past but which is essential to interpret the outcome of the wave/body interaction.

Under worst case conditions or conditions that rarely occur or are applicable in clinical use, in-vitro and in-vivo studies could show adverse bio-effects in animals or cell cultures using partly normal ultrasound imaging settings [20, 21]. These adverse effects are strengthened or, by using ultrasound contrast agents, result in capillary bleeding and microlesions occurring at all inner organs or premature ventricular contraction of the heart only by using intermittent ultrasound equipment. Distortions in migration of neural cells in mice have been reported or influence on membrane permeability and different concentration rates of ions in free cell cultures due to shear and pressure forces of the wave. Experimental studies for heating effects in animals demonstrate a significant increase in temperature for sensitive tissue (brain), which can result in potential harm of that tissue region and further implications.

1.3 Potential risk rating for different ultrasound imaging modes

In general the risk of harm due to diagnostic imaging equipment that operates under FDA limits is very low. On the other hand modern equipment has the potential to initiate mechanical or thermal effects in worst case conditions. It has been shown for thermal effects that there is a linear increase in risk with duration of exposure but an exponential increase with temperature concerning sensitive organs or tissue [18, 21]. The thermal risk depends on the dwell time of the scanner above a specific body region and the texture of that region, i.e. if a bone lies within the sound path. A simple classification for the thermal risk of different imaging modes can be given with (very low risk left, high risk right):

B-Mode < Color Doppler < Spectral Doppler

For the other applications modes (e.g. 3D; M; CW) available the potential of harming and the occurrence of effects is listed in Table 5.

Table 5 Potential risk rating for different ultrasound modes.

Mode	Risk of harm	Potential occurance for effects related to	
		Mechanic / cavitation	Heating
A	Very low	No	No
M			
B			
3D / 4D			
CW-Doppler			
CTG (CardioTocoGram)			
Color Doppler	Low but possible		Yes
Power Doppler			
Spectral Doppler			
Harmonic Imaging (Echo contrast)		Yes	No
Elastography		No	Yes

1.4 Indices to estimate the potential risk

Since 1991 there has been an obligatory standard to calculate, in real-time, a mechanical and thermal index and to display it [22-24]. For the user this is the only possibility to have feedback or rough estimation of

potential risks related to the settings applied. Therefore their meaning should be known and their changes observed during an examination.

1.4.1 Mechanical Index (MI)

With this mechanical index the likelihood of caviation occurance in tissue is estimated. The index is without units and based on a theoretical model involving an overall tissue attenuation ($_{-0.3}$), the emitted acoustic working frequency f_{awf} [MHz] and the negative pressure amplitude $p_{-0.3}$ [MPa] of the scanner according to equation (4):

$$\mathrm{MI} = \frac{p_{-0.3} \cdot {f_{awf}}^{-1/2}}{C_{MI}} \tag{4}$$

with C_{MI} = 1 MPa [19, 20].

It is assumed that above a threshold of MI = 0.7 a potential risk exists due to mechanical effects (caviation) to harm the tissue. In a case of application on very sensitive or gas-filled organs it is recommended to minimise the exposure and dwell time even when MI is in a range 0.7>MI>0.3 [25]. It must be noted that the MI is not valid while using ultrasound contrast agents, in this case the highest attention is needed for the equipment exposure settings because of the artificial introduction of gas-filled bubbles into the blood pool.

1.4.2 Thermal Index (TI)

The second indice to estimate the thermal risk is called the thermal index (TI). This index is displayed on the equipment screen if Doppler modes are chosen and changes its value for different set-ups in real-time. Because of the involved complex 6 theoretical models to count for the thermal conditions of the sound propagation within different tissues, the index is divided into 3 categories (TIS, TIB, TIC) that are displayed if the user selects a specific application program:

TI**S** **S**oft tissue within the sound path (e.g. renal examination)

TI**B** **B**one or parts of bone or bone under the surface but within the sound path (e.g. abdominal heart examination)

TI**C** **C**ranial bone or parts of bone at the surface of the sound

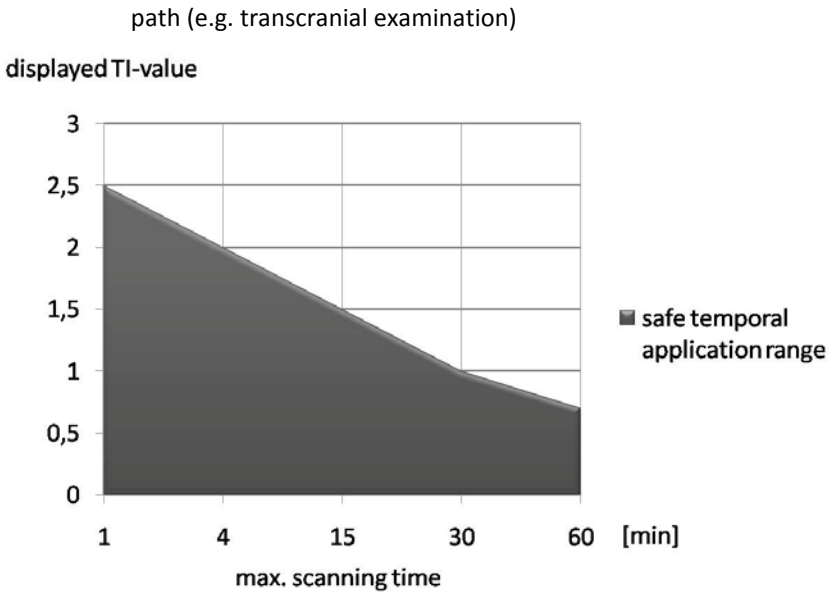

Figure 6 Maximum scanning times for displayed thermal index (TI) values as recommended by BMUS (2008).

While using Doppler modes the index should be watched and the exposure time must be reduced or the procedure changed if the TI value exceeds 0.7 if sensitive organs or fetuses are scanned [25] so not to provoke thermal harm (Figure 6). It is very difficult to estimate the thermal risk with TI alone. It has been shown that the real temperature increase within the tissue region is underestimated by a factor of 2 or more to avoid excessive dwell time or overall scanning duration in this model; in conclusion more care should be paid on Doppler examinations in practice.

1.4.3 Survey of TI / MI-values measured in routine scanning

A pilot study was performed in 2008 within different medical clinics of the General Hospital Vienna (AKH Vienna) to determine the TI/MI-values applicable in routine scanning situations. In total 496 routine ultrasound examinations have been recorded in detail during the course of the

project. [26]. With this time intensive procedure the exact duration of each examination and – what was most important – the TI/MI changes due to shifting user settings could be detected along a time line and the duration of each value was measured as well as the maximum and starting values together with the used modes.

A complete set of the statistical data for this study for the different clinical applications is listed in Table 6.

Table 6 Results of measured TI/MI- values and scanning times of routine examinations in the General Hospital Vienna in 2008 [26].

	TI range	MI range	TI mean±SD	MI mean±SD	Scan time [min] mean±SD
Angiology n=109	0,1–2,4	0,1–1,9	0,36±0,3	1,49±0,14	8,62±5,09
Obstetrics n=116	0,1–0,6	0,3–1,2	0,17±0,06	0,99±0,15	6,23±4,05
Cardiology n=104	0,2–3,0	0,09–1,9	1,72±0,18	1,73±0,28	8,47±6,15
Pediatrics n=104	0,1–1,8	0,25–1,4	0,42±0,15	0,76±0,26	3,93±2,16
Radiology n=63	0,1–2,2	0,1–1,6	0,39±0,11	0,83±0,27	12,85±4,52

It can be clearly seen that most of the routine clinical applications have covered almost the full MI index range available for the equipment concerning the mechanical component. For the thermal index TI the range is relatively low in obstetrics but high in fields where Doppler modes are more often or normally used, i.e. angiology, cardiology. In average all examinations exceed the limit for the MI-value (see 1.4.1) where user action is needed; this is also true for the TI-value in cardiological applications (see 1.4.2).

Normally after observing a high TI/MI-value the user should alter the equipment settings to get lower energy output and lower TI/MI-values on the display.

However, it can be noticed that users in "sensitive" medical fields like pediatrics or obstetrics are generally in charge of their patients while performing the ultrasound examinations or the equipment programs and set-ups are set initially on low levels by the manufacturer.

For cardiological examinations it seems as if the highest output is essential, needed to generate an excellent image. Under these equipment conditions the users must know about the potential risks they can provoke and should have an optimal knowledge of safety-related principles; in particular because of additional contrast agents administration increases the risk for bio-effects enormously!

1.5 ECMUS Recommendations for routine use

The European Federation of Societies for Ultrasound in Medicine and Biology (EFSUMB) have established a special experts committee for medical ultrasound safety (ECMUS – www.efsumb.org/ecmus), that scans and evaluates the actual published literature and technical equipment available concerning ultrasound safety aspects and bio-effects. The committee´s policy is to work continuously on different technical and clinical topics and has access to the latest "*State-of-the-art*" knowledge to inform the member societies and individuals of potential risks or with safety guidelines related to clinical ultrasound by:

- Clinical Safety Statement for diagnostic ultrasound (yearly actualized)
- Guidelines for safe use of modern applications for practicians (e.g. extracorporeal shockwave Lithotripsy (ESWL) devices or Doppler ultrasound)
- Tutorial papers on different and hot ultrasound applications
- Literature reviews to international research results in journals
- Patient leaflet to inform the public about ultrasound and its clinical procedure in common
- Data base of recommendations and statements from other bodies and similar committees(e. WFUMB, BMUS, FDA, ÖGUM)

The ECMUS committee´s motto: *ALARA – As Low As Reasonable Achievable* is placed in decisions and implemented in all guidelines to keep the risk of application problems for patient and physician/user as small as

possible and to help ultrasound to be one of the safest imaging modality and therapy methods.

All information is available on the internet via the ECMUS MicroSite (www.efsumb.org/ecmus) or via the EFSUMB Newsletter published in the journal Ultraschall in der Medizin (www.thieme.de/ultraschall) the official European Ultrasound journal.

The latest information is provided by ECMUS for clinical practicians to be sure that ultrasound applications in routine can be performed without harm or risk for patients.

1.5.1 Clinical Safety Statement

The actual ECMUS Clinical Safety Statement provided by EFSUMB can be downloaded via www.efsumb.org/ecmus.

It describes and summarizes in brief the latest "state-of-the-art" knowledge for the safe use and application for diagnostic procedures in clinical practice:

ECMUS Clinical Safety Statement (shorted version) - www.efsumb.org/ecmus

- Cardiotocograms (CTG) are not restricted in use.
- Ultrasound examinations shall be performed by trained personnel with actual safety knowledge only.
- Periodic control of TI & MI - and if needed adjustments (ALARA!) - during the examination.
- Keep the examination as short as possible for the clinical outcome.
- Beware of scanning neonatal brain, eyes and spinal cord due to increased thermal risk over the total pregnancy time.
- No routine Doppler examinations during the 1. Trimenon (only if clinical indicated).
- Ultrasound contrast agents application shall be avoided 24 hrs before shockwave procedures.

1.5.2 Souvenir images

After 3D/4D ultrasound methods have been introduced and established in clinical routine applications mainly within the obstetrics, allowing to

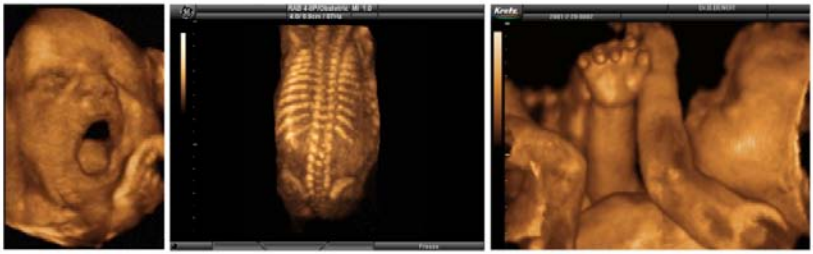

Figure 7 Representation for the 3D-images of the fetus or so-called *Souvenir* images.

view plastical representation of the fetal´s body surface or the head, the offer for the pregnant woman and parents to get and buy these three-dimensional images or movies were marketed (Figure 7).

These *Souvenir-images* or *–movies* on CD/DVD for non-diagnostic all day use have shaped up to a big market that is known in the English speech areas as "*Keepsake image*" and offered by many commercially oriented persons or institutions that are not doing any diagnostic screening. Their only purpose and business is to perform good quality 3D-pictures or -movies.

From the ethical point of view these examinations are questionable and are refused by all medical ultrasound societies and federations [27-29]. No profit can be demonstrated for the fetus and its development, rather an additional exposure risk added to the normal clinical screening due to a new scanning date that can be long to get an optimal 3D-image or movie.

ECMUS introduced in 2006 as first committee the first international statement on that topic to guard the fetal´s rights [28].

ECMUS Statement on souvenir images – www.efsumb.org/ecmus

- Ultrasound scanning shall not be performed for this reason only.
- During a diagnostic scan this is tolerated as long as the necessary exposition is not increased and the scanning duration is not prolonged to a large extent.

1.6 Practical ultrasound exposure estimation, safety awareness and safety related equipment maintenance

In a practical routine it is almost impossible for the physician and operator to know exactly the output of the equipment, TI and MI values are the only ways that indicate if the output after manipulation at the console is increasing or decreasing. Additional information about limits as given within the BMUS Guidelines [25] are essential to recognise possible risky settings during an examination.

Normally the equipment comes with a defined pre-set program together with the application specialist of the manufacturer. These pre-sets generate in most cases and for different application modes medium TI/MI-levels right from the beginning and an experienced operator has to reduce the level (output) actively to comply with the guidelines or to reduce voluntarily the patient´s exposure dose while the diagnostic outcome is still the same. Therefore it would be desirable to start each examination with low initial pre-set settings to generate low output and low TI/MI-values. During the examination the operator has to change actively the receiving gain and postprocessing settings to get an optimal diagnostic relevant image while the patient´s exposure is still unchanged and low.

Various surveys to exposure aspects and safety guidelines between operators and physicians have shown that a basic knowledge of application risks due to this modality exists but not in detail or what is needed specificly for their daily routine [26].

It is essential today and “state-of-the-art” for each operator of an ultrasound equipment to have knowledge about

- The normal handling of the equipment
- Possible ultrasound interactions with tissue
- Acoustical limits and safety concepts (TI, MI)
- Settings producing the highest output levels (highest TI/MI-values)
- Procedures if exposure limits are exceeded to fulfill the obligation of legislative carefulness during the examination.

Another aspect that is not performed at the moment on a regular scheme and on each equipment is regular technical maintenance including console, probes and display (apparative quality control). Not only the obligatory electrical safety checks are needed but also the optimal function of each element within the probe or the electronics within the console that are defining in total the image quality.

The outcome of only a few broken or destroyed scanner elements or losses within amplifiers can be that the operator is provoked to increase the output due to a worse image quality; finally this results in an increase risk to the patient for inducing bio-effects. However, periodical probe function tests and additional performance tests would detect this kind of losses or alterations in an early stage unambiguously.

Different concepts and procedures have been published in the literature over the years. A practical guideline for quality assurance are the *AUStrian 5-min checks* available as download from the Austrian Ultrasound Society (www.oegum.at) as well as more specific information listed there to this topic.

1.7 References

[1] EFSUMB. *EFSUMB Newsletter*. 2003.

[2] Food and Drug Administration (FDA). *Guidance for Industry and FDA Staff - Information for Manufacturers Seeking Marketing Clearance of Diagnostic Ultrasound Systems and Transducers*; Sep. 9 2008.

[3] KOLLMANN, C.; PUTZER, M. Ultraschallkontrastmittel – physikalische Grundlagen. *Radiologe*. 2005, 45, pp. 503-512.

[4] KOLLMANN, C.; New sonographic techniques for harmonic imaging— Underlying physical principles. *European Journal of Radiology*. 2007, 64, pp. 164–172.

[5] KOLLMANN, C. Basic Principles and Physics of Duplex and Color Doppler Imaging. In MOSTBECK, G.H. (ed.). *Duplex and Color Doppler Imaging of the Venous System, Medical Radiology*. Springer, 2004, pp. 1-18.

[6] TERHAAR, G. Safety and bio-effects of ultrasound contrast agents. *Med Biol Eng Comput.* 2009, 47, pp. 893–900.

[7] SCHNEIDER, M.; ARDITI, M.; BARRAU, M.B.; BROCHOT, J.; BROILLET, A.; VENTRONE, R. et al. BR1: a new ultrasonographic contrast agent

based on sulfur hexafluoride- filled microbubbles. *Invest Radiol*. 1995, 30(8), pp. 451-7.

[8] MILLER, D.L. Overview of experimental studies of biological effects of medical ultrasound caused by gas body activation and inertial cavitation. *Progress Biophysics and Molecular Biology*. 2007, 93, pp. 314-330.

[9] STRAUSS, A.L. (ed.). *Farbduplexsonographie der Arterien und Venen: Atlas und Leitfaden*. 2. ed. Berlin : Springer, 2001.

[10] GOERTZ, D.; de JONG, N.; Van der STEEN, A. Attenuation and Size Distribution Measurements of Definity™ and manipulated Definity™ Populations. *Ultrasound in Medicine & Biology*. 2007, 33, 9, pp. 1376-1388.

[11] HERMENS, B.; MISCHI, M.; BÖHMER, M.; AARTS, R.M.; KORSTEN, H.H.M. Nonlinear propagation of ultrasound through varying contrast agent concentrations. *IEEE Benelux EMBS Symposium.* 2007, pp. 42-45.

[12] BARNETT, S. (ed.). Other Non-thermal Mechanisms: Acoustic Radiation Force and Streaming in Conclusions and recommendations on thermal and non-thermal mechanisms for biological effects of ultrasound. Proceedings of the World Federation for Ultrasound in Medicine and Biology Symposium on Safety of Ultrasound in Medicine. *Ultrasound Med Biol*. 1998, 24, Supplement 1, pp. S23-S28.

[13] NIGHTINGALE, K.R.; KORNGUTH, P.J.; TRAHEY, G.E. The use of acoustic streaming in breast lesion diagnosis: a clinical study. *Ultrasound Med Biol*. 1999, 25, 1, pp. 75-87.

[14] O'BRIEN, W.D. Ultrasound – biophysics mechanisms. *Progress in Biophysics and Molecular Biology* 2007, 93, pp. 212–255.

[15] NYBORG, W. Acoustic streaming. In MASON, W. (ed.) *Physical Acoustics Vol. IIB*. New York : Academic Press, 1965, pp. 265-331.

[16] FATEMI, M. et al. Fetal stimulation by pulsed diagnostic ultrasound. *J Ultrasound Med.* 2001, 20, pp. 883-889.

[17] FATEMI, M.; ALIZAD, A. et al. Characteristics of the audio sound generated by ultrasound imaging systems. *J Acoust. Soc. Am*. 2005, 117, pp. 1448-1455.

[18] EFSUMB. *European Committee of Medical Ultrasound Safety (ECMUS) Safety Tutorial paper 18* [online]. 2003. WWW: <www.efsumb.org/ecmus>.

[19] SALVESEN, K.A. Epidemiological prenatal ultrasound studies. *Prog. in Biophysics and Molecular Biology*. 2007, 93, pp. 295-300.

[20] DUCK, F.A. Hazards, risks and safety of diagnostic ultrasound. *Medical Engineering & Physics*. 2008, 30, 1338–1348.

[21] CHURCH, C.C.; MILLER, M.W. Quantification of risk from fetal exposure to diagnostic ultrasound. *Prog Biophys Mol Biol*. 2007, 93(1-3), pp. 331-353.

[22] AIUM/NEMA. *Standard for Real-time display of thermal and mechanical acoustic output indices on diagnostic ultrasound equipment.* Rev. 2. USA, 2004, UD 3-2004.

[23] ABBOT, J.G. Rationale and derivation of MI and TI – a review. *Ultrasound Med. Biol*. 1999, 25, pp. 431-442.

[24] IEC 61157. *Standard means for the reporting of the acoustic output of medical diagnostic ultrasonic equipment.* Ed.2. Geneva, Switzerland : International Electrotechnical Commission, 2007-08.

[25] British Medical Ultrasound Society (BMUS). *Guidelines for the safe use of diagnostic ultrasound equipment* [online]. 2008. WWW: <www.bmus.org>.

[26] SABITZER, H.; KOLLMANN, C. TI/MI-Werte bei Routine-Untersuchungen. *Ultraschall in Med*. 2009, 30, pp. S14.

[27] WFUMB. Safety Committee [online]. 2008. WWW: <www.wfumb.org>.

[28] EFSUMB. *European Committee of Medical Ultrasound Safety (ECMUS) Souvenir Scanning Statement* [online]. 2006. WWW: <www.efsumb.org/ecmus>.

[29] Food and Drug Administration (FDA). *Avoid Fetal "keepsake" images, heartbeat monitors* [online]. FDA Consumer Health Information March 24, 2008. WWW: <www.fda.gov>.

2 Methods for Ultrasound Scanners Performance Evaluation

Ladislav Doležal

Problems related to the safety of ultrasound applications are judged from the point of view of patients, nursing and examining personnel. Also, ultrasound biological effects have predominated for more than 50 years of ultrasound use in medicine. The direct effects of ultrasound energy on living tissue have been examined intensively. The danger inherent in the possibility of incorrect treatment resulting from erroneous diagnosis based on misinterpretation of the sonogram has only been taken into consideration in the last decade of the 20th century. Misinterpretation is possible owing to artifacts. Artifacts, i.e. faulty interpretation of the image during ultrasound diagnosis, can lead to incorrect harmful treatment. When evaluating the risks of such artifacts, it is necessary to differentiate objective and subjective factors.

a) Objective risk factors include:

Imaging physical artifacts and inadequate quality of equipment imaging caused by low technical standards, poor maintenance or the age of the equipment.

b) Subjective factors relate to the skills of the examiner. These include:

Unfamiliarity with the physical mechanisms of ultrasound image creation, lack of skill in operating the equipment and hence inability to set the optimal working parameters, lack of knowledge of the topographic anatomy necessary for correct image interpretation, inborn characteristics of the observer such as spatial imagination and the ability to abstract what is seen.

Physical artifacts are based on the physical properties of ultrasound waves and the environment in which they are propagated. As such they are unequivocally definable according to physical laws and to eliminate them, it is necessary to apply appropriate procedures and imaging methods. If these recommended appropriate methods do not exist, the physical laws must be accepted and taken into consideration. In this case eliminating the risks is totally dependent on the experience and knowledge of the examiner and the above subjective characteristics. On the other

hand, the sonograph imaging quality is a factor completely dependent on the technical parameter of the equipment. In order to increase the imaging quality or eliminate imaging defects and thus reduce the potential risks of sonogram misinterpretation, it is necessary to create a complex system for determining and objectively evaluating the relevant qualitative parameters [1].This is very difficult to achieve and requires the definition of the parameters of sonographic imaging quality, development of suitable measuring methods, procedures for their evaluation and the creation of a graded system of sonograph quality criteria and last but not least strong legal regulations are necessary to apply the methods to practice.

Some international standards and recommendations e.g. [2] and [3] have been introduced over the last decade and commercial testing objects mostly for the B-mode of imaging are becoming available even on a commercial basis. These contain defined non-homogeneities and the image is analyzed subjectively by the operator or the use of computer aided analysis. To fulfill the all important physical criteria for correct mimicking of the tissue [4], the test object construction has to be rather sophisticated. This kind of testing method is fast and relatively inexpensive, but obviously measurements are burdened with an error resulting from subjective assessment of image quality and sonograph adjustment, even with the use of computer technology support.

It is obvious that quantitative and accurate evaluation of the imaging quality is very difficult and, internationally, there are only very few institutes dealing with the problems using the methods mentioned above.

2.1 Standards and official recommendations

There are several regulatory bodies and professional societies concerned about technical parameters and quality assessment of sonographs world wide. The International Electrotechnical Commission (IEC) administers technical standards even for medical applications. The U.S. Food and Drug Administration serves as a sample of a governmental office having the power to control the safety, quality and effectivity of medical instruments. The World Federation for Ultrasound in Medicine and Biology (WFUMB) heads medical oriented staff. WFUMB federates continental federations like the European Federation of Societies for Ultrasound in Medicine and Biology (EFSUMB) or the Asian Federation of Societies for Ultrasound in Medicine and Biology (AFSUMB). In America in

general the American Institute of Ultrasound in Medicine (AIUM) exist while in Central America the Latin American Federation for Ultrasound in Medicine (FLAUS) is important. Australasion Society for Ultrasound in Medicine (ASUM) and Mediteranean and African Society of Ultrasound (MASU) also exist. Presently the total number of individual members is more than 54.000, and these are physicians, scientists, engineers and mostly ultrasonographers [5].

Regulatory bodies

The International Electro-technical Commission (IEC) [6] is the leading global organization that prepares and publishes international standards for all electrical, electronic and related technologies. These serve as a basis for national standardization and as references when drafting international tenders and contracts.

Through its members, the IEC promotes international cooperation on all questions of electro-technical standardization and related matters, such as the assessment of conformity to standards, in the fields of electricity, electronics and related technologies.

The IEC charter embraces all electro-technologies as well as associated general disciplines such as terminology and symbols, electromagnetic compatibility, **measurement and performance**, dependability, design and development, **safety** and the environment. There are two technical committees dealing with ultrasonography equipment under the IEC. The first is the TC62 – Electrical equipment in medical practice, the other one is TC87 - Ultrasonics. The TG62 is responsible for electrical safety standards. The committee manages very comprehensively the document “IEC 60601: Medical electrical equipment” dealing with different medical instruments. The TC62 has published and maintains about 120 documents related to safety use of medical electrical instruments. However, few of the standards are related just to the ultrasonography appliances. Those **ultrasound** medical application concerning parts of the IEC 60601 are listed in Table 1.

Table 1 List of selected IEC safety standards (family of the IEC 60601: Medical electrical equipment) related to **ultrasonic** medical equipments.

IEC 60601-1 Ed. 3.0: Medical electrical equipment - Part 1: General requirements for basic safety and essential performance.
IEC 60601-1-1 Ed. 2.0: Medical electrical equipment - Part 1-1: General requirements for safety - Collateral standard: Safety requirements for medical electrical systems.
IEC 60601-1-2 Ed. 3.0: Medical electrical equipment - Part 1-2: General requirements for basic safety and essential performance - Collateral standard: Electromagnetic compatibility - Requirements and tests.
IEC 60601-1-4 Ed. 1.1: Medical electrical equipment - Part 1-4: General requirements for safety - Collateral Standard: Programmable electrical medical systems.
IEC 60601-1-9 Ed. 1.0: Medical electrical equipment - Part 1-9: General requirements for basic safety and essential performance - Collateral Standard: Requirements for environmentally conscious design.
IEC 60601-2-5 Ed. 3.0: Medical electrical equipment - Part 2-5: Particular requirements for the basic safety and essential performance of ultrasonic physiotherapy equipment.
IEC 60601-2-37 Ed. 2.0: Medical electrical equipment - Part 2-37: Particular requirements for the basic safety and essential performance of ultrasonic medical diagnostic and monitoring equipment.
IEC 60601-2-62 Ed. 1.0 (in preparation stage): Medical electrical equipment - Part 2-62: Particular requirements for basic safety and essential performance of high intensity therapeutic ultrasound (HITU) systems.

There it is another set of the IEC standards related to the ultrasonography and ultrasonic medical applications. These standards do not relate directly to the patient and operator safety, but to the equipment's technology; measurements of applied ultrasound energy physical properties and ultrasonic medical equipment particular parameters measurement methods. Due to their impact on the patients with quality of application during examination, some of the standardized objects may affect safety too.

Table 2 demonstrates the IEC standards (excluding the IEC 60601 family) that may be connected with safe use of ultrasonic medical equipment.

Table 2 The list of the IEC standards exception the IEC 60601 family related to the ultrasound medical applications.

IEC/TR 60854 Ed. 1.0: Methods of measuring the performance of ultrasonic pulse-echo diagnostic equipment.
IEC 61157 Ed. 2.0: Standard means for the reporting of the acoustic output of medical diagnostic ultrasonic equipment.
IEC 61205 Ed. 1.0: Ultrasonics - Dental descaler systems - Measurement and declaration of the output characteristics.
IEC/TS 61206 Ed. 1.0: Ultrasonics - Continuous-wave Doppler systems - Test procedures.
IEC 61266 Ed. 1.0: Ultrasonics - Hand-held probe Doppler foetal heartbeat detectors - Performance requirements and methods of measurement and reporting.
IEC/TS 61390 Ed. 1.0: Ultrasonics - Real-time pulse-echo systems - Test procedures to determine performance specifications.
IEC 61391-1 Ed. 1.0: Ultrasonics - Pulse-echo scanners - Part 1: Techniques for calibrating spatial measurement systems and measurement of system point-spread function response.
IEC 61391-2 Ed. 1.0: Ultrasonics - Pulse-echo scanners - Part 2: Measurement of maximum depth of penetration and local dynamic range.
IEC 61685 Ed. 1.0: Ultrasonics - Flow measurement systems - Flow test object.
IEC 61689 Ed. 2.0: Ultrasonics - Physiotherapy systems - Field specifications and methods of measurement in the frequency range 0,5 MHz to 5 MHz.
IEC 61828 Ed. 1.0: Ultrasonics - Focusing transducers - Definitions and measurement methods for the transmitted fields.
IEC 61846 Ed. 1.0: Ultrasonics - Pressure pulse lithotripters - Characteristics of fields.
IEC 61847 Ed. 1.0: Ultrasonics - Surgical systems - Measurement and declaration of the basic output characteristics.

IEC/TS 61895 Ed. 1.0: Ultrasonics - Pulsed Doppler diagnostic systems - Test procedures to determine performance.
IEC/TS 61949 Ed. 1.0: Ultrasonics - Field characterization - In situ exposure estimation in finite-amplitude ultrasonic beams.
IEC 62126 Ed. 1.0: Ultrasonics - Fields: Methods for computing temperature rise in homogeneous soft tissue for diagnostic ultrasonic fields.
IEC 62359 Ed. 2.0: Ultrasonics - Field characterization - Test methods for the determination of thermal and mechanical indices related to medical diagnostic ultrasonic fields.
IEC 62377 Ed. 1.0: Ultrasonics - Colour flow imaging systems - Test procedures to determine performance.

Some national regulatory governmental agencies are oriented to medical care. Among the worldwide national regulatory agencies is the FDA (Food and Drug Administration), which is an agency within the Department of Health and Human Services of the USA government. The FDA is responsible for protecting the public's health by assuring the safety, efficacy, and security of human and veterinary drugs, biological products, medical devices, the nation's food supply, cosmetics, and products that emit radiation [7].

The FDA is also responsible for advancing the public health by helping to speed innovations that make medicines and foods more effective, safer, and more affordable and by helping the public to get the accurate, science-based information they need to use medicines and foods to improve their health. Other national regulatory agencies around the world mostly accept the FDA-established guidelines.

The FDA regulations system is arranged and coded according to Subject Title, Chapter of title, Subchapter, Part, and Section. A sample of the Code of Federal Regulations concerning the ultrasound medical applications is on Table 3.

Particular FDA bodies involved in medical applications of ultrasound are listed on the FDA website [8]:

The FDA places the ultrasound imaging appliances into a subgroup of Medical Imaging with Radiation-Emitting Products and Procedures. The Ultrasound Imaging clause consists of the following paragraphs:

* Description
* Procedures
* Risks/Benefits
* Information for Patients
* Information for Professionals
* Laws, Regulations & Performance Standards
* Industry Guidance
* Other Resources

These contain brief but comprehensive information for both, patients and professionals. There is a note in the paragraph concerning laws and standards declaring that "there are no federal radiation safety performance standards for diagnostic ultrasound". But it concludes in the Risk/Benefits analysis, within the first sentence: "Ultrasound imaging has been used for over 20 years and has an excellent safety record. It is non-ionizing radiation, so it does not have the same risks as X-rays or other types of ionizing radiation".

The paragraph "Laws, Regulations & Performance Standards" states that Manufacturers of electronic radiation emitting products sold in the United States are responsible for compliance with the Federal Food, Drug and Cosmetic Act (FFDCA), Chapter V, Subchapter C - Electronic Product Radiation Control.

Manufacturers of ultrasound imaging products are responsible for compliance with all applicable requirements of Title 21 Code of Federal Regulations (Subchapter J, Radiological Health) Parts 1000 through 1005. The Table 3 overviews these Parts and specifies details of Part 1002 – Records and Reports for ultrasonic appliances as a sample. The regulations are arranged and coded according to Subject, Title, Chapter, Subchapter, Part, Subpart, Section, Table, application area and user.

Table 3 The FDA system of code of regulations applied to medical and nonmedical ultrasonic equipments with detailed list of Part 1002 – Records and Reports.

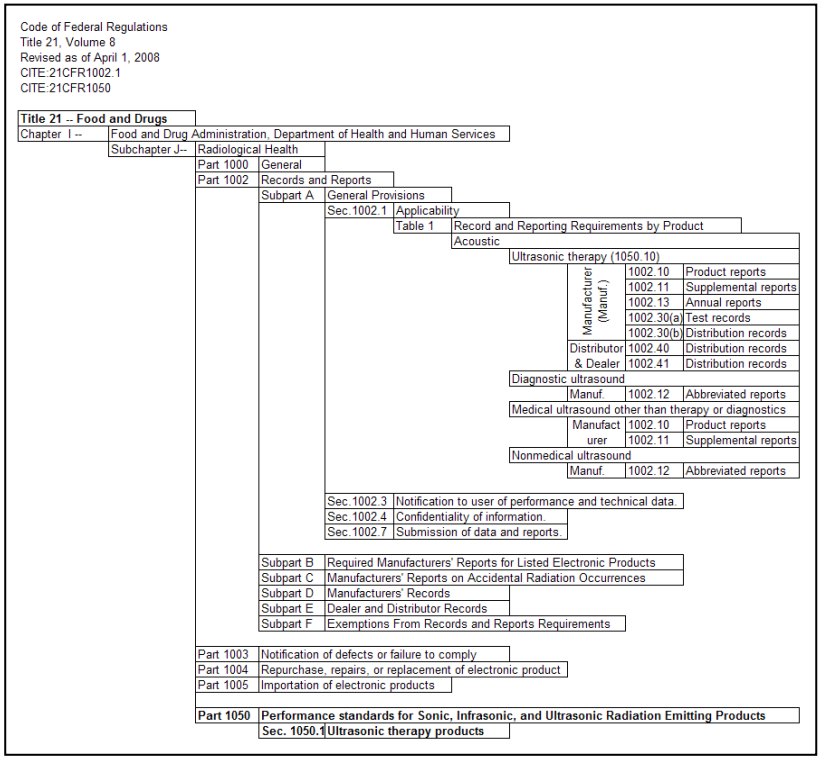

Situation in The European Union

Council Directive 93/42/EEC concerning Medical Devices covers areas such as placing on the market and putting into service. The directive establishes essential requirements and harmonized standards for the manufacture, design, and packaging of medical devices. A medical device is defined as any instrument, apparatus, appliance, software, material or other article used to support medical care. Since 14 June 1998 no medical device covered by the MDD 93/42/EEC could be placed on the market that did not carry a CE mark. The CE mark proves both to the authorities and to

the buyer -or user- that this product fulfills all essential safety and environmental requirements as they are defined in the so-called European Directives. There are two basic aspects to the CE mark the device. Firstly – any official responsible body in the EU (manufactures, distributor, service person, importer etc) should be labeled and secondly – a document "Declaration of Conformity" which states that the apparatus complies to the requirements of the directives as stated on the declaration, so following the standards as indicated and thus is safe for use.

The Medical Devices are classified by the MDD according to their invasivity and risk, into four classes. Class I, are not invasive with low risk equipment or devices without a monitoring function. Class IIa, classifies short-term usage, invasive medical devices with moderate risk. The next is the Class IIb, associated with long term usage, invasive medical devices with high risk. The most dangerous are the devices of Class III, being invasive, used long term with critical risk. Ultrasonographs and most of ultrasound therapeutical appliances belong to the Class IIa. A non-sterile coupling gel is a member of the Class I.

The Class I equipment is not invasive at all, and should not thus administer anything harmful to the patient, no medicines nor energy. For this type of medical equipment, the so-called manufacturer's declaration is applicable and no involvement of any certified or notified body is required. Class II equipment (and upwards) requires the involvement of a notified body that will approve customers documentation and/or Quality Management System.

The MDD 93/42/EEC has been modified by the 2007/47/EC, an amendment which was established on September 5, 2007 and the consolidated directive has been mandatory since March 21, 2010. The amendment changed the definition of a medical device, things now not considered a medical device, explanation of the Member State's role, etc.

The medical device quality and safety has the full responsibility of its distributor at the moment of purchase and installation. After sale, safety and quality aspects are transferred to the user. The user then has to ensure proper periodical maintenance and electrical safety checks.

A proper maintenance and quality assurance check is vital for effective use of medical technology with patient safety being paramount. However,

a serious problem is lack of authority and expertise in evaluating systems, to ensure periodical inspections, for quality assessment of the ultrasonographs. Industry and marketing are supported well with standards on technology and production quality management and in some countries even the law is used to enforce the appropriate standards. But the after-sale care isn't so well specified. The medical systems in use must be periodically inspected for electrical safety only, not to check quality and effectivity of their function. Periodic maintenance is recommended, but not exactly specified. The periodic maintenance range depends on a particular authorized service body and user owner. This is a management decision and it is not standardized.

International and Nation wide groups exist with interests in ultrasound; the ultrasound focussed professional societies:

WFUMB

The WFUMB [5] calls to federation continental federations such as the European Federation of Societies for Ultrasound in Medicine and Biology (EFSUMB) and the Asian Federation of Societies for Ultrasound in Medicine and Biology (AFSUMB). Also included are: The American Institute of Ultrasound in Medicine (AIUM), The Latin American Federation for Ultrasound in Medicine (FLAUS), The Australasion Society for Ultrasound in Medicine (ASUM) and The Mediteranean and African Society of Ultrasound (MASU). Presently the total number of individual members is more than 54.000, and these are physicians, scientists, engineers and ultrasonographers.

EFSUMB

The EFSUMB [9] is an European-wide Federation that encourages networking between ultrasound professionals of all disciplines throughout Europe, allowing them to benefit from the wealth of experience and knowledge from other countries and other health-care systems. The EFSUMB was established on February 11th, 1972, when delegates of 13 European societies met in Basel (Switzerland) for the formal foundation of the Federation. There were 1589 members when the Federation met for its third congress in Bologna on October 1-5, 1978. [10] It was at that meeting that, in an attempt to rule the interdisciplinary collaboration and

to create the base for establishing safety guidelines the famous Resolution of Bologna was agreed. Since then, the European Federation of Ultrasound in Medicine and Biology has remained responsible within Europe for matters of interdisciplinary collaboration in the field of diagnostic ultrasound and for the safety of ultrasound devices in medical use. It has successfully represented Europe within the World Federation of Ultrasound in Medicine.

ECMUS

According to the Resolution of Bolognia the European Committee for Medical Ultrasound Safety (ECMUS) [11] was constituted in Dubrovnik on the 2nd October 1979 when the first meeting of ECMUS was held. The committee comprises six members whose areas of special knowledge and expertise should cover as wide a range as possible of the fields related to bioeffects. The committee should liaise in association with the safety committees of the World Federation of Ultrasound in Medicine and any other relevant committee of other major national or international bodies affiliated with ultrasound. The committee should re-examine the EFSUMB Clinical Safety Statement in the light of new scientific findings every year. Safety Guidelines for shockwave lithotripsy and the use of Doppler ultrasound examinations are available as well as sixteen Tutorial Papers on the ECMUS Micro Site. [12] The ECMUS Micro Site contains the ECMUS documents including Literature Reviews, ECMUS Forum and considerably more interesting information.

The ECMUS cooperates very closely with safety oriented experts from sister societies under the ceiling of WFUMB.

Among others the BMUS - British Medical Ultrasound Society including its Safety Committee is very active. Also their work on the quality and safety policy is worthy of being highlighted. The BMUS provides a wide range of services for professionals, not only the doctors and sonographers, but also biomedical engineers. The society edits the quarterly official journal „Ultrasound“ in The Royal Society of Medicine Press, ISSN 1742-271X.

Another very important group of the ultrasound oriented medical staff are societies of three German speaking countries – from Germany the DEGUM, from Austria the ÖGUM and from Switzerland the SGUM. The first two societies are edited by Georg Thieme Verlag editor magazine „Ultraschall in Medizine“ ISSN 0172-4614 which commenced during the

year 2004 and is now connected to the official magazine of EFSUMB – the European Journal of Ultrasound. All three societies have been in existence since1976.

There is also an arrangement of very interesting meetings „Dreiländertreffen“ covering all important topics including education, exchange of experiences and safety and quality assessment which are focussed on all the time.

Covering medical practice, three kinds of ultrasound societies exist.

Firstly the societies previously discussed, cover all medical branches and deal with general problems of medical ultrasound applications. These are networked in the continental and World federations and to which, for example samples may be given by the Czech Society for Ultrasound in Medicine (CSUM) or the American Institution on Ultrasound in Medicine (AIUM) etc.

Other kinds of ultrasound dedicated medical specialised international societies include the International Society of Ultrasound in Obstetrics and Gynecology (ISUOG) [13] and the International Society of Cardiovascular Ultrasound (ISCU) [14]. These societies are oriented to highly specialised medical applications, in areas where ultrasonography is widely used.

The third type of society are professional societies for which medical ultrasound is not the main topic, but it supports their main work or is a part of their work range. They may have their own viewpoints dealing with ultrasonography, for example: the American Colleague of Radiology (ACR) [15], the American Association of Physicists in Medicine (AAPM) [16], the National Electrical Manufacturers Association (NEMA) [17], the National Council of Radiation Protection & Measurements (NCRP) [18], the International Commission on Radiation Units and Measurements (ICRU) [19] etc.

One goal held by these bodies is to manage the best professional level of ultrasound applications in medicine. In the diagnostic field of ultrasound applications the scanners performance evaluation contributes well to reaching this goal.

2.2 Methods used for quality performance assessment of ultrasound scanners and their parameters

Recently a few measuring methods for technicians, producers, designers and also metrologists have been made available for a wide range of ultrasound scanners, their parameters and assessments. Two main attempts to QA are important. They differ according to the scheme of use or by the way the results are utilised. The first classification, is the scaling measuring methods, with this classification being based on their frequency of application and level of use. Another one evaluates methods by accuracy and reliability. Indeed some parameters affecting measuring applications are the method's price and availability in practice!

2.2.1 Simple ("paperclip" or "coin") method

This is a very easy, cheap and effective method which is known as the electronic multielement transducer dead element(s) discovering. The method is not suitable for phased array transducers. The method is based on multiple back reflections generated at an irradiated metal object surrounded by air. The multiple reflections are imaged as an echogenic scanning lines of all the apertures containing the element irradiating the metal object. A simple metal object may be used e.g. paperclip wire or any narrow coin. The name of the method expresses this fact.

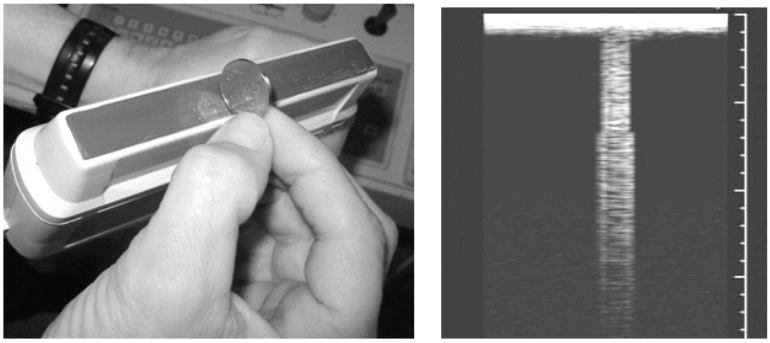

Figure 1 The „coin test" – simple test for transducer function, aperture width and dynamic focussing focal depth.

Even if the method is very simple, some important data concerning aperture width and range of focal areas for multiple dynamic focussing may be obtained. This information is derived from the fact that the signal received by one element is displayed as a signal from whole aperture. The multiple reflected signal is displayed by all the scanning lines having apertures containing the elements in contact with the metal object. The echogenic beam width is twice the width of the receiving aperture. See the Figure 1.

The dead element doesn't generate and/or receive the multiple reflection signal, therefore the echogenic lines disappear when the reflecting object is positioned in front of the dead element.

2.2.2 Daily Tests

The number of failures affecting the sonograph imaging quality may be discovered by simple every day tests performed by a sonograph operator or hospital engineer. Such tests may detect, for example: drop-out of crystals in the transducer, dead zone shift, a decrease of maximum depth of penetration, changes of contrast range, sensitivity and noise limits. Frequent (daily or weekly) periodical simple quality parameter testing is vital for safe and effective patient diagnostic imaging. This kind of test doesn't require expensive instruments and technically skilled person. The time needed to perform such a test is only a few minutes and doesn't interfere with a sonographer's routine working schedule. As an example of a complex and comprehensive test set, an AUStrian Test kit ™ designed by Kollmann [20] may be useful. This test set contains detail instructions and necessary tools allowing the following quick assessments of:

1. Aperture
2. Dead zone
3. Axial/lateral/functional resolution
4. Depth- & Measurement calibration, Scala/Coursor-consistency
5. Maximum penetration depth
6. Contrast range
7. Uniformity
8. Sensitivity
9. Noise limit

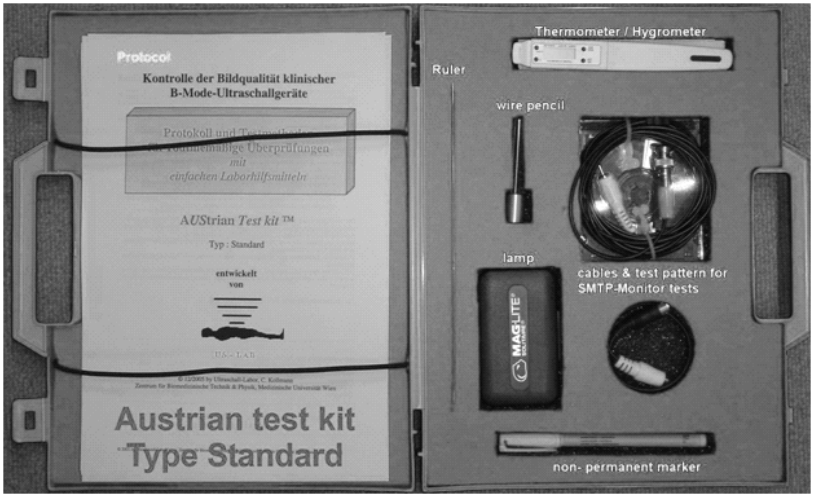

Figure 2 This is a very useful kit for short term periodical tests. It contains all necessary tools and instructions including result forms for simple tests with comprehensive diagnostic apability. (Used with courtesy of Ch. Kollmann).

It is clear, that such simple and quick tests cannot substitute accurate laboratory measurements. An argument for their use is the importance of a continuous periodical check on sonographs which are heavily loaded in a standard health care system. In such conditions the probability of any damage, namely of transducer or its cable is rather high. Also due to the complexity of the sonographic picture there is not really any chance for the operator to discover a problem unless regular testing is performed. All these facts support the idea of the periodical sonograph quick check, even if it is still very rare in a practice.

Another easy to use test employing comprehensive information, delivered in a simple test tool from Sonora Medical Systems, Inc. is called the Nickel test. The Nickel test is a simple and small ultrasound acoustic performance-testing tool for checking transducers as well as various modalities and functions within the imaging systems. A principle of its function is very similar to the „Coin test“ that is reflected by its name

Figure 3 The „Nickel tool“ and the test result images. The image on the left shows the response from a convex transducer where width of aperture and number of elements is observable. The right image was obtained by use of a phased array sector transducer. The centre frequency of this transducer is low (cca 2 - 3 MHz) therefore the third deep strip only is visible and the whole lateral area is marked because in the phased array system the signal received by one tested element is distributed to all receiving channels. (From Sonora leaflet.)

which is identical to a small US coin „Nickel”. The principle of how it works is as follows: - the Nickel test target is equipped with a small PDF sensor which receives a transmitted pulse from a measured transducer element and reacts by transmitting back 3 separate echo simulating pulses with different ultrasound frequency. The Nickel is not designed to be a calibration tool. It is an indicator of the overall functional health of both the probe and the various major electronic segments of the ultrasound system that define the performance of the various modes of operation (e.g. B-Mode, Doppler, Color Flow and M-Mode). The simulated echo signal that is inputted into the transducer from the Nickel also allows the testing of some special functions within any given ultrasound system, for example algorithms used for spatial compounding, second harmonic imaging, various pseudo-colour displays and dynamic focusing. See the [21].

2.2.3 Test objects for evaluation

The most well known and simple method for sonogram quality assessment uses different types of ultrasonography test objects also called phantoms. The phantoms are available in a wide range of types from

different producers and contain various types of reflectors; naturally they are filled using material of similar acoustic parameters to soft tissue. The test objects are used to estimate: spatial and contrast resolution, depth of penetration, elevation of focal area position, look-up table parameters and calliper accuracy etc. Simple test objects may also be improvised with the use of suitable reflectors, positioned in ultrasound conducting media e.g. liquid, gel or a solid block. Professional test objects guarantee specific acoustic parameters that have to be periodically tested by the responsible authority for their stability. Such authority may be the test object's manufacturer, National metrology laboratory (e.g. Czech metrology institute or National Physic Laboratory in Great Britain etc.) or a commercial laboratory accredited by another responsible authority.

Standard manual measuring procedure using the test object starts with positioning the transducer onto an acoustic window of the phantom to obtain a sonogram of its inner structures. Then the measured sonograph must be adjusted well enough to obtain optimum quality of the picture. After that an operator evaluates the observed picture and records all reported data along with: the measured sonograph and transducer

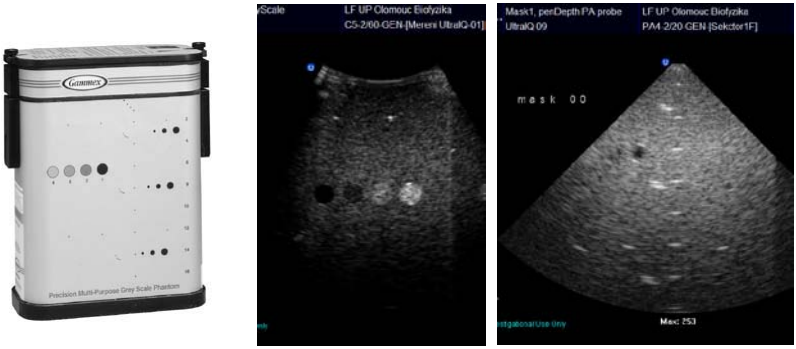

Figure 4 One of commercially available tissue mimicking objects with samples of its scans. The left picture was made by a convex transducer and evaluates gray resolution targets, the right one was scanned by a phased array sector transducer to check spatial resolution and the accuracy of depth penetration distance measurements. Scanner: Sonix RP.

identification, the sonograph working parameters setting, ambient conditions and observed results.

Most of the test object methods suffer from results dependent on the adjustment of sonograph working parameters such as: gain, dynamic range, look-up table, dynamic focussing, non-linear post-processing etc. for a particular measurement. Another remarkable and noteworthy difficulty is a subjective evaluation of the resulting sonogram by the operator. Some software tools evaluating the digitalized sonograms of professional test objects have been designed over the years to eliminate or decrease the influence of the operator subjectiveness. The computer assisted picture analysis mostly eliminates subjective misinterpretations of the sonogram details such as brightness assessment but still has the subjective factor of sonograph parameters adjustment for a particular measurement.

With computer assisted measuring methods, two methods may be mentioned. The first is from Zagzebski and Satrapa; the work of whom is very interesting, as it applies a test object method which has been developed utilizing spatial analysis of the signal-to-noise ratio in a three-dimensional image of a special voids containing test object. The analysis results in imager & transducer set characterization by using the parameter Voids Detectability Ratio (VDR) that is derived from small amplitude signals generated by low reflectance structures, similar to the signal obtained from real tissue, such as the kidney or liver. This method is suitable for reviewing measurements quickly and is substantially more objective than the methods referred to previously. Its main disadvantage is in displaying a depth dependent integral parameter derived from a specified plane in a lateral and transversal direction; resulting in the fact that one cannot determine the lateral details of the image defects. Also, the analysis of a spatial image distortion and characterization of the system for high amplitude reflected signals is not possible. More detail is available in another chapter of this book, where Überle describes his experiences he achieved with the method for which he uses an alternative term Signal to Noise Ratio (SNR) method.

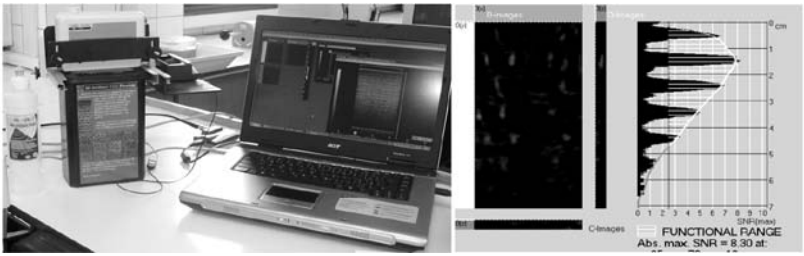

Figure 5 The test to detect the presence of voids is shown together with transducer and test object. The measured linear transducer is fixed on top of the test object and the notebook is running the evaluation program to apply the Voids Detectability Ratio method (left picture)**.** A scan of the test object (voids are visible as light spots on a dark background) and the characteristic VDR (marked as SNR) versus depth in cm are in the picture on the right side.

Professional software UltraIQ based on Thijssen's method [22] is commercially available as a test kit including frame-grabber to digitalize, store and analyse the test object sonograms. The program considers both the grabbed video and or copied digital pictures. This tool is designed to serve as a fast but easy to use system, operated to measure a rather wide range of basic quality parameters. An additional chapter in this book is included describing the UltraIQ test pack capability.

All these methods that employ different test-objects are primarily suitable for in-situ screening studies. They are not time consuming which is important where there is heavy equipment workload. Due to the high influence of operator individuality, a skilled person is needed and even so these methods are rather limited in producing detailed objective information.

2.2.4 First Call aPerio

The FirstCall aPerio™ (formerly called The FirstCall 2000™) is a unique portable, high-speed testing device designed to measure the relevant acoustic and electrical parameters of most electronic array transducers. It measures transducers only, that is, without the scanners. [1]

The test device will reveal the source of transducer performance and safety problems such as:

1. The number and location of dead acoustic elements across an array
2. Elements that have reduced sensitivity which can contribute to poor imaging quality as well as lower colour flow or Doppler sensitivity
3. Acoustic lens delamination, a condition which often results in image drop-out, potential electrical safety issues and long term destruction of the array
4. Broken signal wires or cable termination issues within the transducer, cable, or connector
5. For each element the following electrical characteristic parameters are specified:
    a. Capacitance on connector pin end
    b. 20dB Pulse Width
    c. Center Frequency
    d. Fractional Bandwidth.

The FirstCall aPerio™ data is reported in a format that allows clear tracking of performance changes while documenting the key indicators of probe related problems, even before the user can see changes in image or Doppler performance and often while the probe can still be cost-effectively repaired. FirstCall pulses each element within an array to test for: Element Sensitivity (volts p-p), Capacitance (pF), Pulse Width (ns), Pulse Shape, Centre Frequency (MHz) and Fractional Bandwidth (%).

The test is very fast; it takes about 10 minutes to adjust and measure any pre-programmed transducer. The measured protocols are arranged in a database with capacity to compare results obtained by periodical testing of the identical transducer to follow up its possible time degradation.

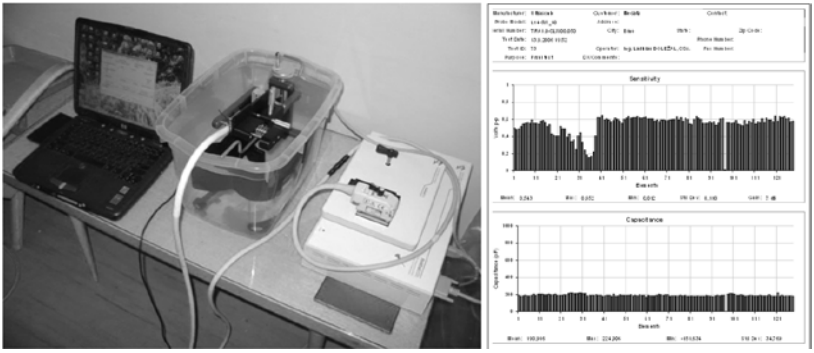

Figure 6 The FirstCall 2000™ system just evaluating a special linear transducer from Aloka dedicated for peroperative use. From left to right – notebook running the program, tank filled with water in which the transducer holder with reflector is immersed and box containing hardware plus transducers connecting interface on the top. The second picture shows part of the measuring results protocol, where element effectivity in the top graph and channel capacitance on the bottom graph are displayed. The result may be interpreted as delamination of the elements 1 till 38 and disconnected element 98.

2.2.5 Irradiated acoustic pressure determination by use of hydrophone

Ultrasound field characteristics could be measured as another type of data for sonograph qualitative parameter analysis. This however does not evaluate the image quality but determines whether parameters of the actuating ultrasound signal and data obtained is suitable for the radiated ultrasound intensity checking or possibly its space and time stagger, which is significant for maintaining allowed limits and for assessment of the effects of ultrasound energy at various types of tissue borderlines. Additionally, there are mathematical models of the ultrasound field radiated by certain types of probes and its heat effects. Comparison of calculated and measured values of acoustic pressure distribution may determine the model's accuracy and definition. The method and equipment needed is described in a separate chapter of this book.

2.2.6 Point Spread Function (PSF) method

The PSF method is referred to in IEC standards [23] and [24] where PSF measurement is specified as the characteristic response of the imaging system to a high contrast point target. For most optical systems, the PSF is a singular, symmetrical and isotropic function. Thus, the measurement of the PSF is normally sufficient to characterize the system's impulse response and all the parameters derivable from this function.

The PSF measuring system generates a measured signal by use of a spherical target of diameter D inside an ultrasound conducting medium. The target diameter D depends on the frequency of ultrasound used. See Attachment A4, [23].

The PSF function may be analysed from both – a RF signal or video output signals digitalised by an appropriate A/D converter. Because an output of the RF signal is not the property of a standard scanner in the main, and in general practice the more the digitalised video signal is analysed, by special software, to derive various objective parameters of the imager, the more numeric data can be obtained for precise analysis.

Two kinds of PSF measuring systems may be used. The first consists of a **fixed** spherical target and the second more sophisticated method maps

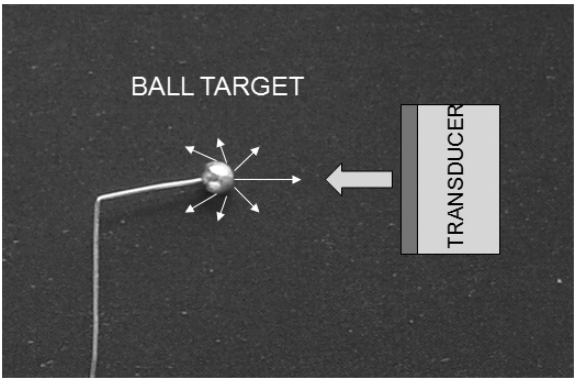

Figure 7 Ball target as a point reflector.

the PSF over an ultrasonographic image by scanning a **moving** spherical target. See Fig. 7. The target is moved in a measuring bath filled by degassed water over a specified scanned volume via a 3D computer controlled positioning system. The PSF function may be analysed from scanner output signals digitalised by a proper A/D converter and analysed by special software to derive various objective parameters of the imager. Exact numeric data is obtained as a measurement result for precise analysis. More details concerning the PSF mapping system are available in the literature [25].

The moving target PSF measurement gives the following outcomes for an ultrasound scanning system derived from both the Region of Interest (ROI) and the target position dependent PSF data analysis over the scanning area:

- The ROI digital image stored for scanned plane axis in each point of the measuring grid.
- The echo signal amplitude distribution over the measured area.
- Distribution of the parameter Full Width in Half of the Maximum (FWHM) of the PSF in an azimuth direction over the measured area.
- The peak echo amplitude at each step of the target position in the elevation (transversal) direction.

The method has the capability to derive from the data following ultrasound scanner parameters and functions over the scanning areas:

1. Focal areas in both the azimuth and the elevation directions
2. Ultrasound scanning lines visualisation
3. Manufacturer preloaded TGC function
4. Depth dependence of the scanning plane width
5. Side lobe levels
6. Amplification uniformity in the azimuth direction.

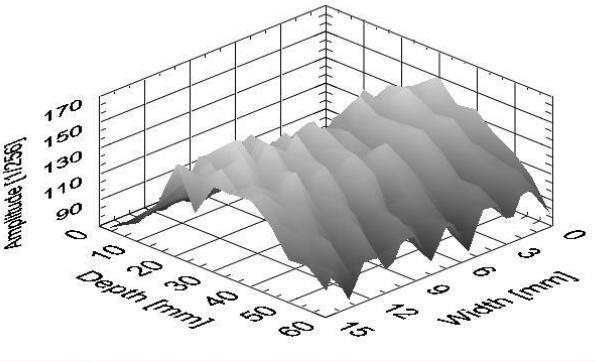

Figure 8 Separate scanning lines imaged in a scanned area. The graph is derived from an amplitude plot of the signal reflected by the point reflector moving over the area.

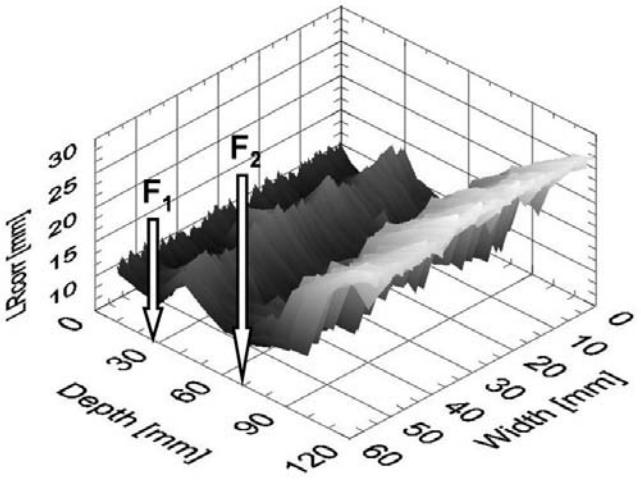

Figure 9 Focal length derived from the FWHM distribution over the scanned area. (FWHM is scaled on the y axis marked as LRcorr).

Such a set of parameters declares specific and comprehensive QA data concerning the particular sonograph and transducer(s) measured. The measured data contains information over the whole imaging system, beginning at the transmitter and continuing with the transducer, receiver and picture elaborating system. Data evaluation and the final measurement report need skilled staff in both; the measuring methods and the data interpretation. Measurement over thousands of points in a scanned volume is time consuming. Therefore this method is dedicated more to specialized laboratories than quality inspectors in hospitals. The application might be very useful for the expediency and conclusion of a final inspection on both new systems being manufactured or some used but refurbished scanners for sale.

2.2.7 The methods comparison

For a better overview a table comparing particular measuring methods in six basic parameters is enclosed. The compared parameters are as follows:

1. Results obtained by measurements
2. Data evaluated by measuring method
3. Operation
4. Evaluating method – the basic method used for measurements
5. Measuring duration – the time is needed to obtain the results
6. Price – approximate price as available at the middle of the year 2010.

Table 4 Comparison of the measuring methods.

Method	Results	Data evaluated	Operation	Evaluating Method(s)	Measuring duration (estimated)	Approx Price kEUR
Estimation - from background noise	Basic information, may detect dead elements and/or receiver malfunction.	On screen picture. Noise level and its homogenity over the picture	Simple; Skilled; The sonograph and monitor adjustment	Subjective picture analysis	Short = from 1 till 5 min. per transducer	0
Estimation - metal rod (coin) reflections	US lines; Dead elements; Aperture size; Dynam. focussing	On screen picture. Multiple reflections inside the metal generate comet tail like picture.	Simple; Skilled The sonograph adjustment	Objective picture analysis	Short = from 1 till 5 min. per transducer	0
AUStrian Test kit®	Picture quality parameters; The imager status; Image documentation. Report.	On screen picture. Printed pictures. Imager and transducers inspection.	Moderate; Skilled The sonograph adjustment Inspection	Picture analysis Some objective Some subjective. Status evaluation Questionary	Short = from 5 till 20 min. per transducer	0.8
Nickel®	US lines; Aperture; Dynam. Focussing; Received frequency range.	On screen picture of the Nickel generated pattern signal, received by one transducer element.	Moderate; Skilled The sonograph adjustment + Nickel operation	Picture analysis by observer: Objective	Short = cca 5 min. per transducer	1

Method	Results	Data evaluated	Operation	Evaluating Method(s)	Measuring duration (estimated)	Approx Price kEUR
Tissue mimicking test objects	Spatial & Contrast resolution Sensitivity Geom. Measuring accuracy	On screen picture.	Moderate; Skilled The sonograph adjustment; Positioning the transducer on the test object	Picture analysis Observer: Subjective Analyzing software: Objective	Short = from 5 till 10min. per scan	2 till 5 (per test object)
Ultra IQ®	Spatial & Contrast resolution Sensitivity Geom. Measuring accuracy Long term stability	On screen picture.	Moderate; Skilled The sonograph adjustment; Positioning the transducer on the test object	Digital picture analysis Analyzing software: Objective	Short = from 5 till 15min. per transducer	4
Hydrophone 3D scanning	Acoustic pressure distribution Intensity calculation	RF signal generated by hydrophone US beam mapping by scanning the US field	Difficult; High skilled	RF signal analysis Accurate Objective	Measured volume depended From minutes till hours	20 till 80
First Call™	The particular element's sensitivity, frequency bandwidth, capacity	Reflected signal generated and received by each particular element is analysed	Moderate; Skilled Results interpretation is more difficult than measurement	Received RF signal Accurate Objective	Short = from 10 till 15 min. per transducer	20 till 40 (according to # of adaptors)

Method	Results	Data evaluated	Operation	Evaluating Method(s)	Measuring duration (estimated)	Approx Price kEUR
Signal to noise ratio	Reccommended range of imaging depth is specified, long term stability	Digitalised video signal 3D evaluation of signal-to-noise ratio	Moderate; Skilled Moving transducer over 3D test object	Video signal analysis Accurate Objective	Short = from 10 till 15 min. per transducer	5
Point Spread Function	Azimuth and elevation focal area; Scanning lines visualisation; TGC function over depth; Scanning plane width profile; Side lobe levels; Amplification uniformity	Digitalised video signal Sophisticated interpretation	Difficult; High Skilled Moving a metal sphere over scanned volume	Video signal analysis Accurate Objective	Time - consuming Measured volume depended, may be even hours	Not commerc. available yet 40 (guessed)

Methods for Ultrasound Scanners Performance Evaluation

A number of the measuring methods are available to support maintenance care for diagnostic ultrasound equipment. They have a capability of accepting different kinds of data, from primitive or crude detection of failure, actually on site in the examination room, to obtaining precise values, directly in a laboratory. A supporting system of standards and guidelines is available. There are tools used by equipment manufacturers and maintenance bodies that specifically examine the resulting quality. What is needed, is a sonograph Quality Control (QC) periodical testing/checking schedule which may be applied during the application's lifetime in the health care system. With both health insurance requirements from official authorities and from financial inducement, the QC standard maintenance schedules can be introduced into the healthcare system.

2.3 References

[1] WEIGANG, B.; MOORE, G.W.; GESSERT, J. et all. *The Methods and Effects of Transducer Degradation on Image Quality and the Clinical Efficacy of Diagnostic Sonography* [Online]. Sonora Medical Systems, Inc. [Cited: 5.6.2010]. WWW: <http://www.4sonora.com/ultrasound/Transducer%20Degradation%20on%20Image.pdf>.

[2] AIUM. *Methods for measuring performance of Pulse-Echo Ultrasound Equipment - part II: digital methods (stage 1)*. s.l. : American Institute of Ultrasound in Medicine, 1995.

[3] AIUM. *Quality Assurance Manual for Gray-Scale Ultrasound Scanners (stage 2)*. s.l. : American Institute of Ultrasound in Medicine, 1995.

[4] KOLLMANN, C. Ergebnisse einer Studie zur Qualitätskontrolle von diagnostischen Ultraschall-Geräten. *Ultraschall in Medizine*. 1995, 16, pp. 206 - 209.

[5] *WFUMB Homepage* [Online]. World federation for Ultrasound in Medicine and Biology. [Cited: 21.3.2010]. WWW: <http://www.wfumb.org/>.

[6] *IEC Homepage* [Online]. International Electrotechnical Commission. [Cited: 5.8.2010]. WWW: <http://www.iec.ch>.

[7] *About FDA* [Online]. U. S. Food and Drug Administration. [Cited: 21.3. 2010]. WWW: <http://www.fda.gov/AboutFDA/CentersOffices/default.htm>.

[8] *FDA bodies* [Online]. U. S. Food and Drug Administration. [Cited: 5.8.2010]. WWW: <http://www.fda.gov/Radiation-EmittingProducts/RadiationEmittingProductsandProcedures/MedicalImaging/ucm115357.htm#lrps>.

[9] *EFSUMB Homepage* [Online]. European Federation of Societies for Ultrasound in Medicine and Biology. [Cited: 5.8.2010]. WWW: <http://www.efsumb.org>.

[10] *EFSUMB history* [Online]. EFSUMB. [Cited: 10.5.2010]. WWW: <http://www.efsumb.org/governance/history.asp>.

[11] *ECMUS Micro Site* [Online]. EFSUMB. [Cited: 20.3.2010]. WWW: <http://www.efsumb.org/ecmus/index.asp>.

[12] *ECMUS Tutorial Papers* [Online]. ECMUS. [Cited: 15.5.2010]. WWW: <http://www.efsumb.org/ecmus/ecmus-tut-uk.asp>.

[13] *ISUOG Homepage* [Online]. International Society of Ultrasound in Obstetics and Gynecology. [Cited: 5.8.2010]. WWW: <http://www.isuog.org>.

[14] *ISCU Homepage* [Online]. International Society of Cardiovascular Ultrasound. [Cited: 25.7.2010]. WWW: <http://www.iscu.org/default.htm>.

[15] *ACR Homepage* [Online]. American College of Radiology. [Cited: 15.7.2010]. WWW: <http://www.acr.org/default.htm>.

[16] *AAPM Homepage* [Online]. American Association of Physicists in Medicine. [Cited: 16.4.2010]. WWW: <http://www.aapm.org/default.htm>.

[17] *NEMA Homepage* [Online]. The Association of Electrical and Medical Imaging Equipment Manufacturers. [Cited: 16.9.2010]. WWW: <http://www.nema.org/about/>.

[18] *NCRP Homepage* [Online]. National Council of Radiation Protection & Measurements. [Cited: 21.4.2010]. WWW: <http://www.ncrponline.org/>.

[19] *ICRU Homepage* [Online]. International Commission on Radiation Units and Measurements. [Cited: 21.5.2010]. WWW: <http://www.icru.org/>.

[20] KOLLMANN, C. *Apparative Quality Assurance of Ultrasound Imaging Equipment* [Online]. Medizinische Universität Wien - Zentrum für Medizinische Physik und Biomedizinische Technik. [Cited: 22.7.2010]. WWW:

<http://www.zbmtp.meduniwien.ac.at/fileadmin/zbmtp/uploads/ultrasound/science/austr_testkit_basic_v1engl.pdf>.

[21] Sonora Medical Systems, Inc. *The Nickel Ultrasound Probe and System Testing Device - Operator's Manual* [Online]. Sonora Medical Systems. [Cited: 22.7.2010]. WWW: <http://www.sonora-nickel.com/technical_info/nickel_operators_manual_revb.pdf>.

[22] THIJSSEN, J.M.; WEIJERS, G.; DE KORTE, C.L. Objective performance testing and quality assurance of medical ultrasound equipment. *Ultrasound in Med. & Biol*. 2007, 33, 3, pp. 460 - 471.

[23] IEC 60854. *Methods of measuring the performance of ultrasonic pulse echo diagnostic equipment*. Geneva, Schwitzerland : International Electrotechnical Commission, 1986, pp. 12 - 13.

[24] IEC 61391-1. *Ultrasonics - Pulse-echoscanners - Part 1: Techniques for calibrating spatial measurement systems and measurement of system point spread function response.* Ed 1.0. Geneva, Schwitzerland : International Electrotechnical Commission, 2006, p. chapter 8.

[25] DOLEŽAL, L.; MAZURA, J.; TESAŘÍK, J.; KOLÁŘOVÁ, H.; KORPAS, D.; BINDER, S.; HÁLEK, J. Derivation of sonograph quality parameters by the use of Point Spread Function analysis. *Physiological research*. 2007, 56, Suppl. 1, pp. 69-76.

3 Ultrasound Image Quality Assurance Using a Signal-to-Noise Measurement Method

Friedrich Überle

Since the first appearance of real-time ultrasound imaging systems (US imagers) around 1970, constant technical improvement of the machines and transducers lead to major advancement in image quality and therefore diagnostic significance. Some of the most important steps in the process of development were:

- Increasing the number of steps in the gray scale resolution from 4...16 to 256 and more in recent imagers. As human vision in an adapted environment has a limited resolution of gray scale of about 50…100 steps [1], the increase in gray scale resolution results in smooth images and close-to-optimum detectability of very low-contrast structural changes in tissue.
- Development of electronic multi-channel transducers, enabling the implementation of multiple focus zones, electronic beam steering and optimization of the beam pattern by fine-tuning of the send – and receive parameters of each single array element. At the same time, the array transducers do not contain mechanically moving parts and therefore usually are less susceptible to damage by mechanical stress, e.g. dropping or long hours of service than mechanical scanners.

In the doctor's practice and in hospitals a wide spectrum of sonography devices from many manufacturers can be found. Usually, each device is equipped with multiple transducers, each serving specialized diagnostic tasks. Today an increasing number of diagnoses are based on US images. Therefore the number of sonographic diagnoses to be reimbursed by the health insurance system increases; in 2006 57.9 Million US diagnoses were made [17]. In turn the pressure on the ultrasound practitioners to proof

that their equipment is working properly increases in order to guarantee diagnostic quality.

3.1 Efforts towards increasing US image quality assurance

In contrast to the long established constancy control of X-ray machines, only since April 1st, 2009 an arrangement based on new regulations in the Sozialgesetzbuch § 135 Abs. 2 SGB V was set in action in Germany enforcing the regular check of the image consistency of the ultrasound imaging devices during their life cycle. In order to perform the constancy check, the doctors are required to send a set of diagnostic images including documentation every four years to experts of the health insurance association (KV), which then confirms the image quality. The use of diagnostic images instead of phantom images was chosen as the experts who created the rules did not identify a validated test phantom up to now. Triggered by the health insurance system as well as by concerned physicians, recently the Bavarian Kassenärztliche Vereinigung (KVB) gave birth to the "Sono Baby" quality program for prenatal ultrasonic examinations [2].

In some other countries similar efforts are underway. In 2008, the NPL published a report on ultrasound image quality, which was based on an international questionnaire [5], [9]. A Dutch paper from 2006 by Thijssen et al. describes the evaluation of US image quality using different phantoms and a dedicated software [3]. A Czech group currently looks for the usefulness of methods for US image quality [11]. Their research also includes the creation of a database for the tracking of US devices and transducers over their service life. The Technical Committee TC87, Working group 9 of the IEC (International Electrotechnical Commission) is working on technical standards and reports describing methods of US image quality and its control [4, 7].

A range of commercial products is available which can mainly be used for US device testing for repair and servicing purposes [8]. Some of these devices are using electrical signals to measure the impedances of transducers or to mimic acoustic echoes. And finally, even a simple paper clip may show defective US transducer elements, simply by sliding the clip

over the surface of a transducer and watching for a homogeneous image of the multiple reflections between transducer surface and metal.

Scope

The scope of this chapter is to discuss ways to evaluate the needs and specifications of appropriate image quality testing methods and to present first results using one of the methods with a special test phantom.

For the purposes of quality consistency, it is NOT necessary to focus on methods, which would compare different US devices of several types and brands, BUT it is vital to track the consistency of the image quality over the life cycle of each individual imaging device. This approach guarantees the independence of the physicians to use their choice of US device which suits their needs best.

Consequently, the information and continuous education of physicians using the US devices must be the "second arm" of a broad initiative towards increasing US image quality.

3.2 Ultrasound Image Parameters

The main parameters determining image quality are:

- Contrast
- Signal – to Noise ratio (SNR)
- Resolution (Axial / lateral / elevation)
- Dynamic range

The contrast of adjacent areas in the image is defined as the difference between the gray values of the pixels. As the ultrasound images from real objects represent textures of the objects (tissues), areas of the same gray value cannot be found. Instead, it is useful to define the gray value of an area by the mean value of the image pixels inside the area. Thus the contrast of two tissue structures is given by the difference of the mean gray values μ_i.

Noise in ultrasound devices includes electronic noise, external interferences and speckle noise. The first two noise sources mainly are of

electrical nature, whereas the speckle noise is an acoustic phenomenon which is caused by interferences of the US signals from the fine structure of the tissue. In the current context, noise coming from inadequate coupling of the US transducer to the tissue and from strong reflecting boundaries (e.g. bones, large gas bubbles) can be neglected, if the quality test devices are set up properly.

Although these are significantly different sources of noise, in practice we may simply look at the appearance of an image area and determine an overall noise figure by measuring the variance of the gray levels σ_i^2 inside this area. Thus the signal-to-noise ratio (SNR) of two regions of an ultrasound image is defined [3] as:

$$\mathrm{SNR} = \frac{|\mu_1 - \mu_2|}{\sqrt{\sigma_1^2 + \sigma_2^2}} \tag{1}$$

where the values of μ_i are linear and thus have to be computed by an inverse log operation from the (dB) gray scale values of the image.

The resolution of an ultrasound image is mainly determined by the ultrasonic wavelength and thus by the frequency of the ultrasound beam. In modern ultrasound devices the applied frequency may automatically be adjusted depending on the penetration depth of the tissue. Then resolution may be finer in the areas of the image closer to the transducer.

The dynamic range is determined by the number of gray scale values and by the maximum and minimum echo amplitude which can be displayed. Local dynamic range may be determined for each pixel, whereas the global dynamic range represents the ratio of maximum to minimum echo level a US device can measure [4, 6].

3.3 Sources of failures and degradation of ultrasound imagers

In 2007 a statistical evaluation including 1500 doctors revealed that 34% had severe problems to deliver appropriate US diagnoses [17]. Inappropriate device settings, mainly from the contrast/brightness and TGC controls were criticized as well as flaws in the documentation of the cases. The components of an US imager which are most endangered to degrade image quality are the US transducer and the video screen.

3.3.1 US transducer failures

The US transducer is the most fragile part, as it is used free-hand and it has to be put away frequently between different applications. Additionally, it must be cleaned, disinfected and even (sometimes) sterilized after each patient. So the main sources of damage are dropping, scratching of critical parts, penetrating of fluids and degradation of electrical and mechanical contacts by heat, chemicals etc.

The heart of a modern US transducer is composed of a multi-layer: The acoustic backing material, the piezo-electric crystals, the impedance – matching layer(s) and an acoustic lens to keep the ultrasonic beams narrow in the elevation direction. The piezo-electric crystals are the active elements for transmission and reception of the acoustic signals; usually 64 to 256 crystals are used to form the US beams. These crystals have electrical contacts at the front and rear side. They are arranged side-by-side, separated by insulation. For electrical connection, each element has to be connected to the electronic circuits of transmitter and receiver by shielded wires.

Often, a transducer does not fail completely, but quality is sneakily degraded. This degradation influences the pattern of the acoustic beam field both in transmission and in receive mode: The sensitivity in the main direction (Central beam lobe) is reduced, whereas the sensitivity in the direction of side lobes increases. As the final image is composed of the overlay numerous US beams, the homogeneity of the image is degraded. There are various reasons for the degradation of the beam pattern:

- Damage of single Piezo crystals or of their electrodes
- Degradation of the polarization of the elements by mechanical stress, excess temperatures or ageing
- Degradation of electrical contacts like plugs and soldering points
- Sneaking degradation of the specifications of electronic components due to ageing or failure of single electrical modules
- Delaminating of the acoustic lens, the matching acoustic layers or backing layer, reducing the sensitivity of adjacent of the transducer elements
- Breaking of cables

Delaminating is the major source of defects in US imagers, as reported in [8]: 39.8% of 676 transducers from 7 manufacturers at 32 showed defects. Delaminating was detected in 26.5% and break in the cable was detected in 8.4% of the tested transducers. In contrast, defective piezoelectric elements seemed not to create a significant number of defects.

3.3.2 Standard Tests for US imagers

Any test method for US imager quality constancy should be:

- Quick (Should suffice with few tests, day-to-day basis)
- Easy and intuitive (Must be doable by laymen)
- Reliable (Minimal false results, hard to cheat)
- Reproducible
- Easy to document
- Economic

+ In the case of service / repair the test method should also:

- Show problem sources
- Document / track the status (Before / After)

Table 1 describes the methods which may give a complete set of technical information about an US imager. Unfortunately, the efforts to do all the measurements in terms of time consumption and the amount of materials, e.g. different phantoms, are too demanding for routine checks. On the other hand, as described in [15] the correlations between clinical quality (Correlations are cited in the discussion chapter in this paper) and most of these technical parameters seem not good enough to justify the necessary amount of technical measurements for a routine check of every US imager.

Table 1 Inspection methods for U/S imagers according to ACR [10].

	What to do	When	Equipment	Who should do it
1	Physical and mechanical inspection	Daily	None	Medical personnel
2	Display and/or work station monitor fidelity	Daily	None	Medical personnel
3	Calliper distance accuracy	Regular	Phantom	Technician/ trained person
3a	Vertical	Regular	Phantom	Technician/ trained person
3b	Horizontal	Regular	Phantom	Technician/ trained person
4	Depth of penetration/visualization	Regular	Phantom	Technician/ trained person
5	Dead-zone depth	Regular	Phantom	Technician/ trained person
6	Image uniformity	Regular	Phantom	Technician/ trained person
7	Axial resolution	Regular	Phantom	Technician/ trained person
8	Lateral resolution	Regular	Phantom	Technician/ trained person
9	Elevation resolution	Regular	Elevation phantom	Technician/ trained person
10	Anechoic object imaging	Regular	Phantom or human	Medical Personnel
11	Film processor quality control (QC)	Regular	Test images	Technician/ trained person
12	Hard-copy fidelity	Regular	Test Images	Technician/ trained person

3.4 Materials and Methods

We tested a method, which is presently under development in the form of a Technical Report by the IEC Technical Committee TC87/WG9. The measurement equipment (Figure 1) for the SNR (or VDR) measurements consists of:

- Phantom
- Transducer positioning slider
- Connection cable for tv signal from US imager
- Video digitizer
- Mobile PC including software for image recording and analysis

3.4.1 Construction of the test phantom

For the measurement of the SNR a special ultrasound phantom made of polyurethane (PU) foam is used [7]. The foam is layered in slices of 5 mm thickness (Figure 2A). Every second layer contains artificial cylindrical voids, which are cut into the foam (Figure 2B). Both foam and voids are soaked with degassed 7% saline water. The saline in combination with the foam is adjusted to a speed of sound of 1540 ± 10 $m/s_{@20°C}$.

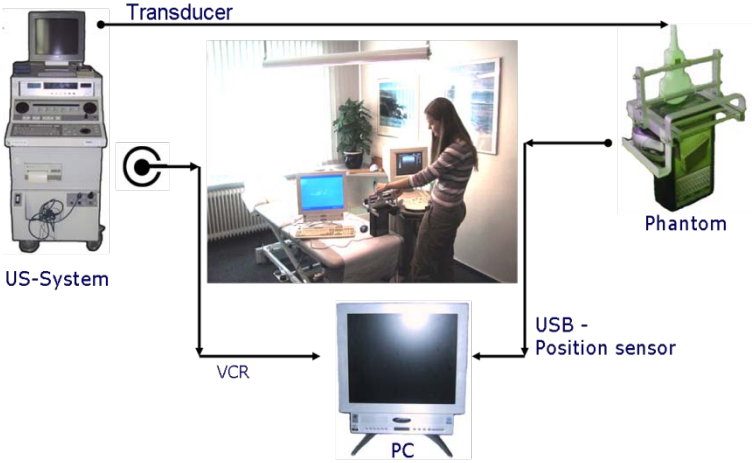

Figure 1 Measurement setup in a practice.

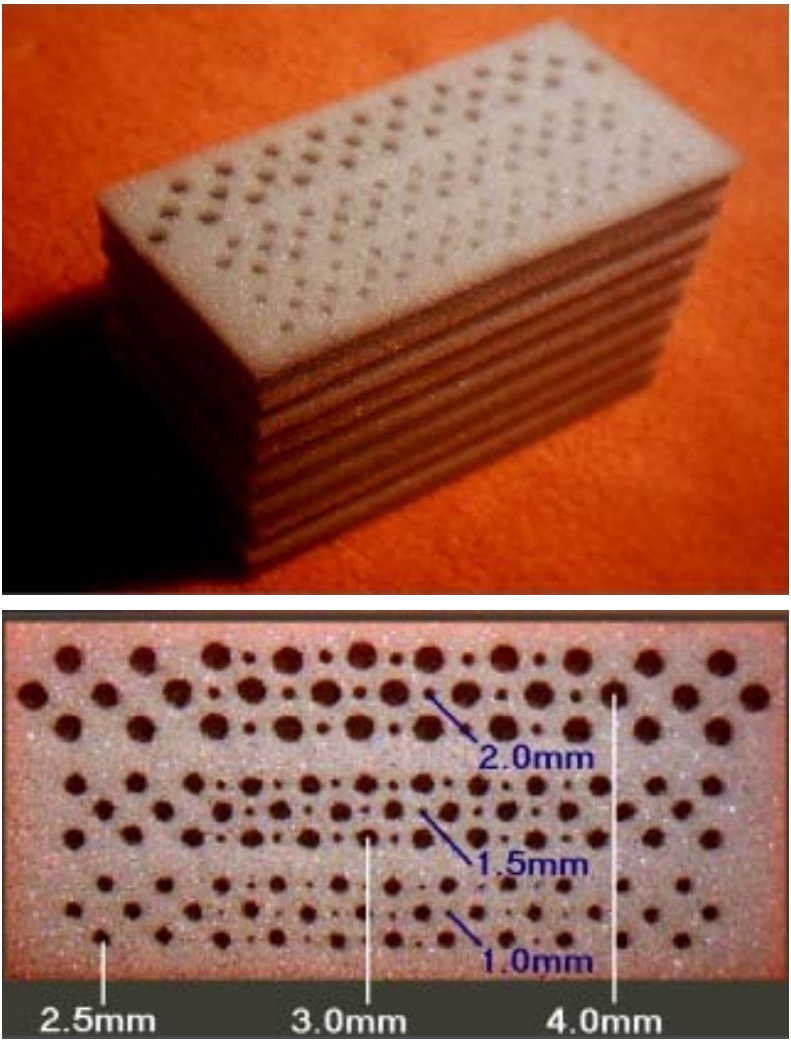

Figure 2 A: Stack of alternating 5 mm PU foam layers, which forms the tissue mimicking contents of the phantom. B: Holes of different diameters in the void layers allow the use of the phantom with different US frequencies (2 – 15 MHz) [7].

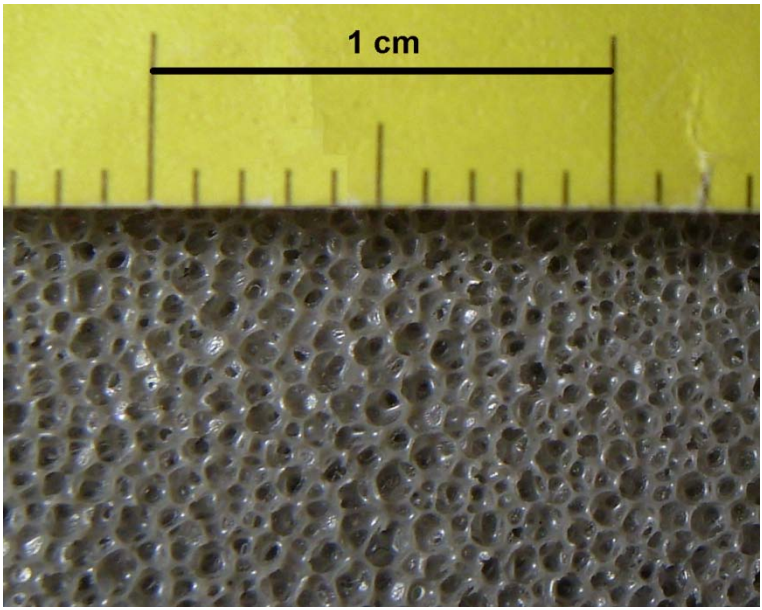

Figure 3 Typical pores of the PU foam of the phantom. Left: attenuating slice material, right: void slice material. The pore walls are 0.1 mm to 0.25 mm thick. The pores must be open in order to allow complete soaking with saline.

The foam density of the attenuating slices is 120 – 130 kg/m³, that of the void slices is 20 – 30 kg/m². The pore size of the PU foam shall distributed smaller or equal to the acoustic wavelength to allow for scattering of the waves (Figure 3). In the present phantom, open pore walls of 0.1 to 0.25mm diameter are used. The foam has attenuating properties; the mean overall attenuation is 0.45 dB/cmMHz. Attenuation in the foam layers containing the artificial voids is ≈ 0.2 dB/cmMHz, whereas the attenuation in the other layers is ≈ 0.7 dB/ cmMHz. The overall properties of the PU foam make the images appear like those of human liver, including speckles. The voids represent artificial cysts or vessels inside the liver tissue. As they are filled with pure saline, they should appear as anechoic areas inside the tissue-mimicking foam. The size of the voids varies from 1 mm to 4 mm. This variation allows choosing voids of

Figure 4 Complete setup of the phantom with attached transducer sledge [7].

appropriate size for the images depending on the frequency of the US transducer. The void diameter should be wider than the expected elevation extension of the ultrasonic beam in order to avoid noise inside the voids which results from slice thickness artefacts.

The phantom is housed in a tight plastic cube. It is covered by a 0.25 mm polyurethane foil.

At the top side of the phantom the transducers are placed inside a sledge, which is either moved by hand or by a stepper motor drive (Figure 4). During the measurement, the transducer slides over the coupling surface of the phantom. In order to provide good acoustic contact between the transducer and the phantom, a sufficient amount of ultrasound coupling gel has to be administered between transducer and coupling PU foil.

3.4.2 Measurement procedure

The measurement process is fully automatic, it comprises

1. Fixation of the US transducer on top of the phantom, ensuring proper coupling.
2. Proper adjustment of the ultrasound imager (Brightness, contrast, image size, preprocessing and postprocessing controls).
3. Connection of the image output to the digitizer input of the PC.
4. Adjustment of the digitizer and adjustment of the image recording window of the software.
5. Start of scanning (Manual or motorized).

The whole measurement procedure usually takes less than 20 minutes per transducer. Evaluation of the data can be made off line from the stored data. The US images are analyzed with dedicated software. The first step in this analysis is to open a measurement series in a digitizer window on the screen and to manually identify the proper region of interest (ROI) inside the digitizer window (Figure 5). Then an electronic ruler has to be adjusted to fit to the size of the US image in order to display the measurement results in the right scale. As the different foam layers are easy to identify inside the images, the marks of the ruler can be properly adjusted in 1 cm steps for each two foam layers. After inputting the hospital, department, device and transducer data in a special screen mask the automatic rendering of the measured images starts.

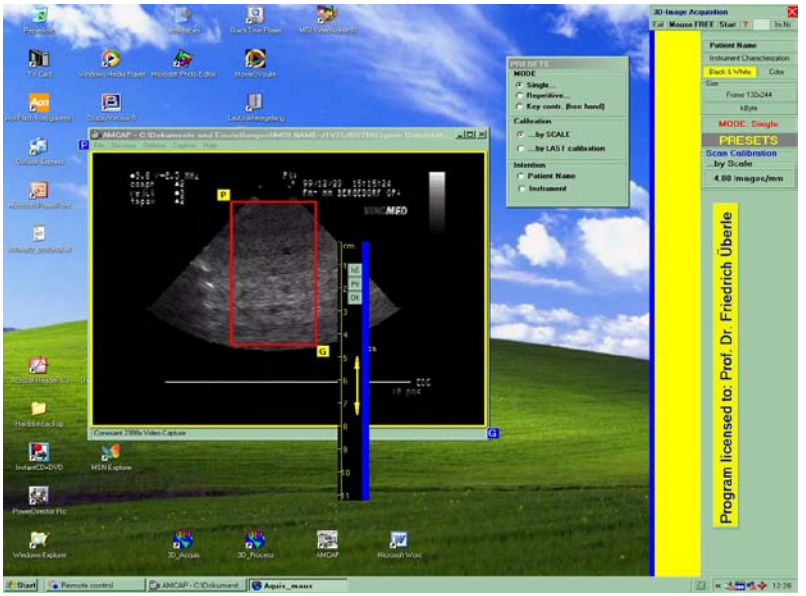

Figure 5 Measurement software screen with window markers and adjustable scale.

3.4.3 Automated evaluation of the measurement results

During the measurement process, a number of US image slices have been stored. These image slices are now arranged in a 3D image matrix side by side. From this matrix, both C-plane and D-plane images are calculated (Figure 6). The C-planes are parallel to the scanning surface, the D-planes are perpendicular to the C-plane and the scanned images plane. Therefore, some of the C-planes also contain areas inside the voids, which should be circular. The D-planes are automatically adjusted to include square cuts of the cylindrical voids in their longitudinal direction.

In the next step, the gray values of the images are inverted. This procedure is not necessary for the SNR calculation, but it results in clearer images of the voids, which now are in bright colours. The final step of the calculation is the calculation of the SNR in each of the C-planes of the image [7, 12]: The software calculates a depth dependent “3D mean value”

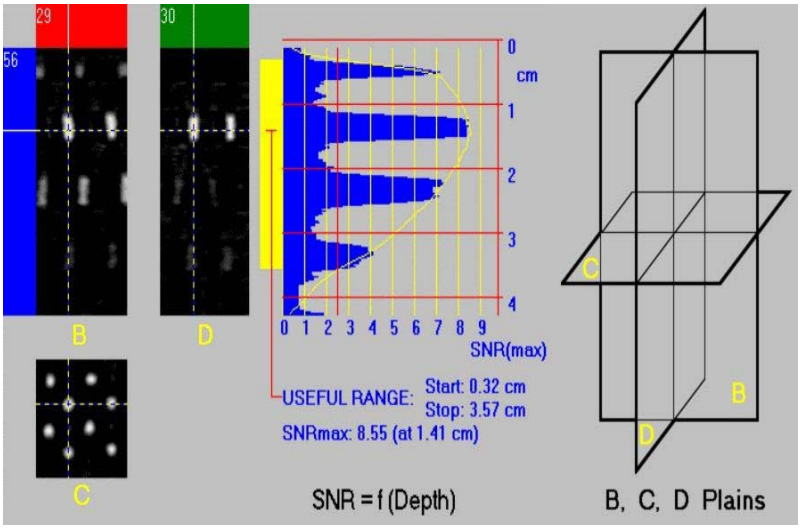

Figure 6 Measured data after 3D rendering, description of B-, C- and D- plains: B-plane is the actual scan plane of the US images, C is parallel to the transducer surface, cutting the cylindrical voids and D is parallel to the US beam propagation and perpendicular to the B-scan planes [7].

and subtracts it from the inverted 3D data matrix (Figure 7). The remaining gray values at each spot of the image then represent the noisy signal (Which strictly spoken is the inverted gray level inside the voids, which ideally should be maximum white). All matrix values which are larger than the “3D mean value” are “Signal”, all other matrix values are “Noise”. The resulting SNR versus depth is then displayed.

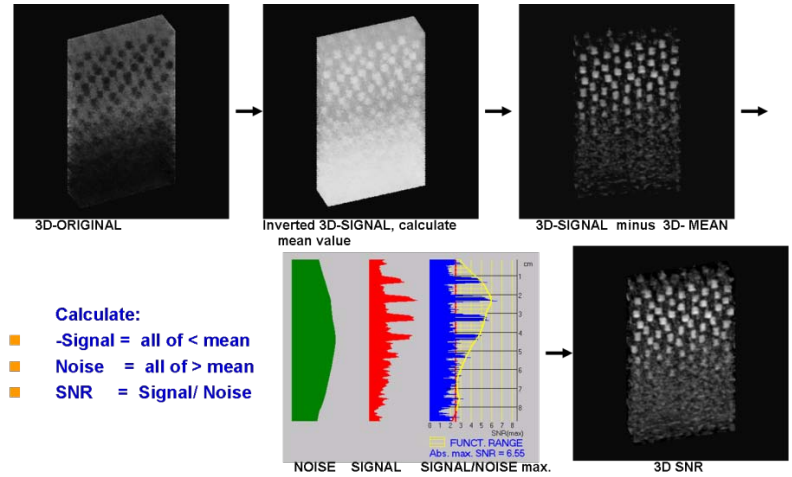

Figure 7 Evaluation of the 3D SNR from the rendered data [7, 12].

3.4.4 Interpretation of the measurement results

With this algorithm the Signal-to-Noise-ratio (SNR) inside the voids is calculated from the ultrasound images. The artificial voids are anechoic, as they contain pure saline. Therefore in the ideal case the signal level inside the voids should be zero, no echoes should occur. All signals from these areas are always related to „noise“. This noise has various causes, mainly

a. Side lobes of the transducer in lateral direction
b. Side lobes (grating lobes) of the transducer in the elevation direction perpendicular to the scan plane
c. Elevation width of the US beams, when these beam portions hit tissue mimicking material areas outside the voids (Slice thickness artefacts).
d. In areas far from the transducer, electronic noise may increase significantly due to the growing amount of acoustic attenuation of the tissue, which requires increasing amplification by use of the TGC (Time-gain-compensation) controls.

While the side lobes of modern US transducers are optimized to a minimum by proper design, they increase rapidly when damage to the crystals or the cables occurs or the transducer starts to delaminate. These side lobes generally hit tissue mimicking areas and thus produce additional echoes, which also occur inside the voids. In the image, they appear as “clouds” or “fog” overlaying anechoic areas as well as other structures. When comparing images from the same transducer in a healthy state and damaged, the increase of noise inside the voids is an indicator of the damage. The same “clouding” of anechoic areas and other structures also will occur in patient images, resulting in deterioration of fine contrasts and the detection of small parts and small lesions.

If the beam width of the US beam is larger than the diameter of a cyst, then layer thickness artefacts inside the voids occur. These artefacts also reduce the SNR. They may occur in regions of the US beam outside the adjusted (electronic transmit and receive) focus areas (usually close to and far from the transducer). They also occur in less focused areas in the elevation direction (Slice thickness), which are determined by the lens. Slice thickness varies e.g. from 0.9 mm in the focus area to 2.5 mm close to the transducer [4, Figure 4b]. In practical measurements, the maximum SNR is found in the regions of the beam where the elevation dimension is minimal, namely the focus of the lens. As the design of the lens is a design property of the transducer depending on its intended use, the maximum SNR is not a valid measure of the transducer quality. Nevertheless, additional image degradation by side lobes leads to increasing “clouding” in the areas outside the elevation focus. This effect then degrades SNR in the farther image area and thus reduces the maximum usable penetration of the transducer.

The most significant measure for transducer quality is the extension of the region, where the SNR exceeds a certain minimum threshold. This SNR threshold was empirically determined as 2.5 [12]. In the regions, where SNR exceeds 2.5, the structures inside the US image can be used for diagnosis. In regions where SNR is less than 2.5, the structures and particular the voids fade into noise, which results in the loss of diagnostic information. A SNR > 4 usually yields good visibility of anechoic voids inside tissue [3].

From these descriptions of the algorithm and the evaluation process it can be seen, that for the quality control of an US transducer only the

maximum SNR (Which gives a figure of the lens quality) and the usable range where SNR exceeds 2.5 need to be measured and compared to historical data of the ***same*** transducer and machine (or at least of the same type of transducer, e.g. in a manufacturers specification).

On the other hand, a comparison of the maximum SNR figures of different transducers or different brands of imagers is not sufficient to compare their image qualities and may be even misleading, because all other design parameters and the intended use of the transducers have to be taken into account for this purpose.

3.5 Pilot Study

3.5.1 Materials and Methods

We did a pilot study with 15 US imagers (built 1990 – 2005) including 29 transducers. The imagers were clinically used in private practices and hospitals in Hamburg. The study comprised 13 linear array transducers and 16 convex array transducers. Repeat measurements were possible in 5 cases. In one case, we could track the enhancement of image quality after imager repair.

Average measurement time per transducer was 20 minutes. A phantom (TCC, Timmelkam, Austria) and software from the same manufacturer was used. The phantom had to be serviced once in the last 3 years due to the loss of saline, no other problems occurred.

Images were digitized from the analog screen outputs of the ultrasound imagers, using the built-in video digitizer of a commercial laptop computer (Gericom). The software to digitize and display the images on the computer screen was AmCap, which is supplied by Microsoft®.

Before the start of the measurements, the imagers were set to typical clinical settings according to the instructions of their users. Care was taken to optimize brightness and contrast of the monitors [3].

3.5.2 Results

4% of all transducers reached a maximum SNR of 1 – 3, 57% reached SNR of 3 – 6, 32% reached a SNR of 6 – 9 and 7% reached SNR of 9 – 12. Linear Array transducers had better SNR values (Mean SNR 8.2) than curved array transducers (Mean SNR 5.3), see Figure 9.

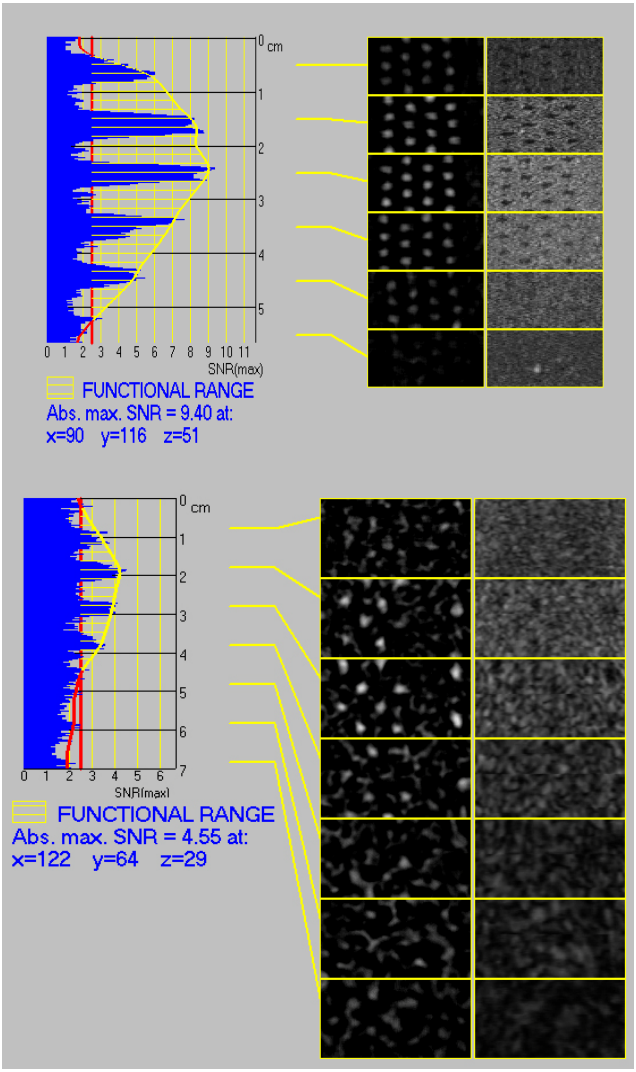

Figure 8 Measurement result of a modern high resolution US linear array (top) and an older imager with linear array (built 1980) with weak resolution.

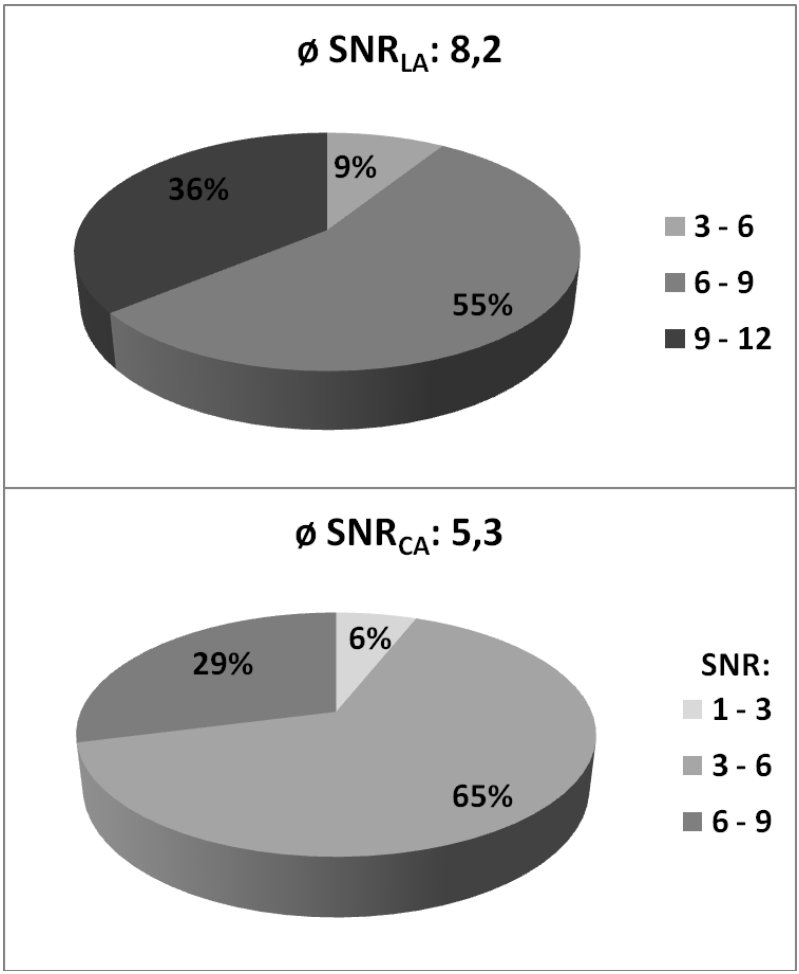

Figure 9 SNR results a. Linear transducers (N=13), b. Convex transducers (N=16).

The higher the working frequency of the transducers, the better mean SNR values were found (Figure 10).

The older the US imagers, the lower SNR values were found (Figure 11).

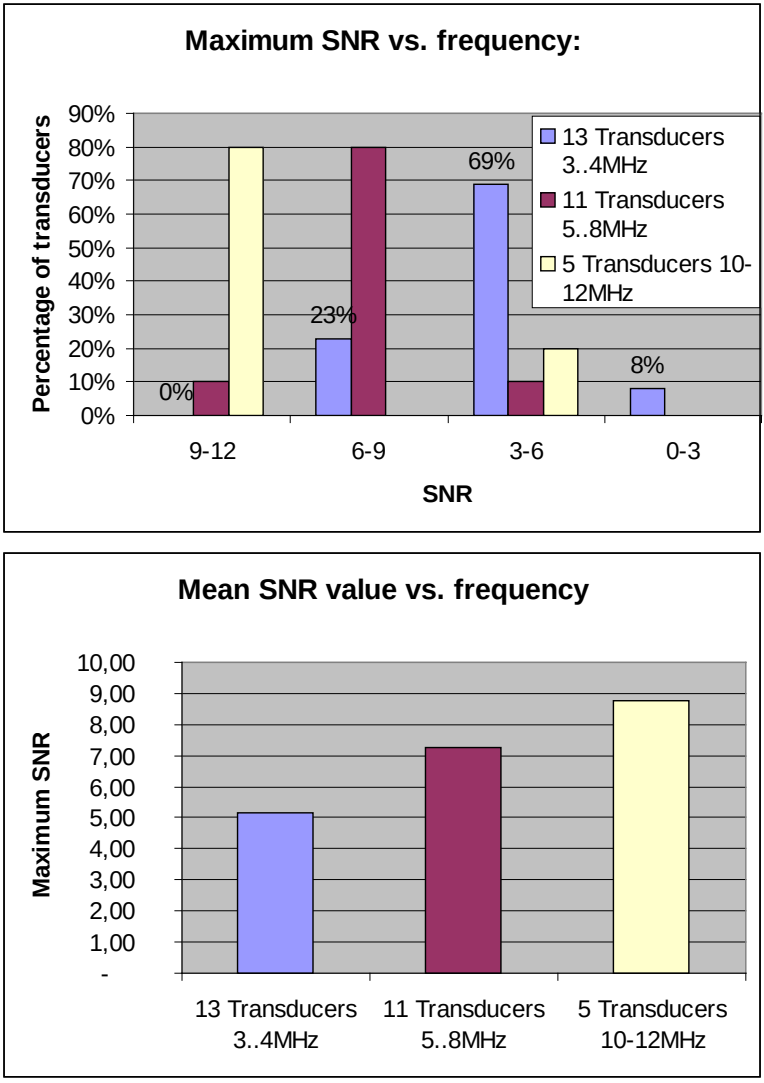

Figure 10 SNR results vs. transducer frequency.

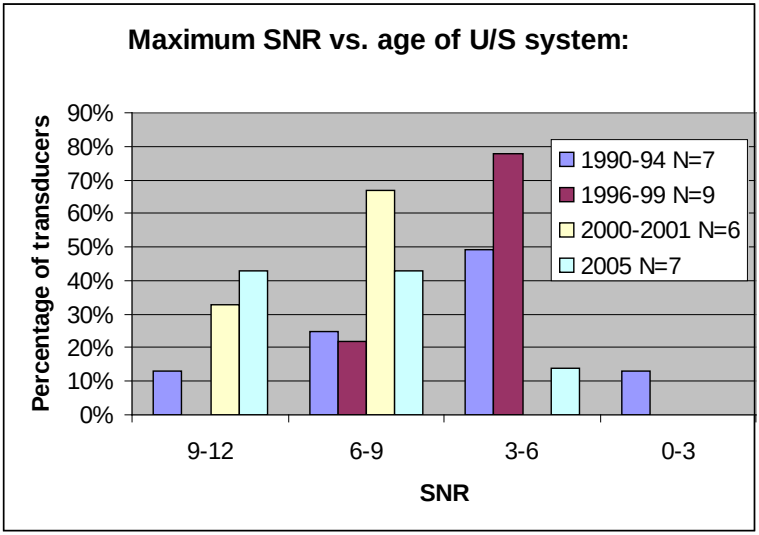

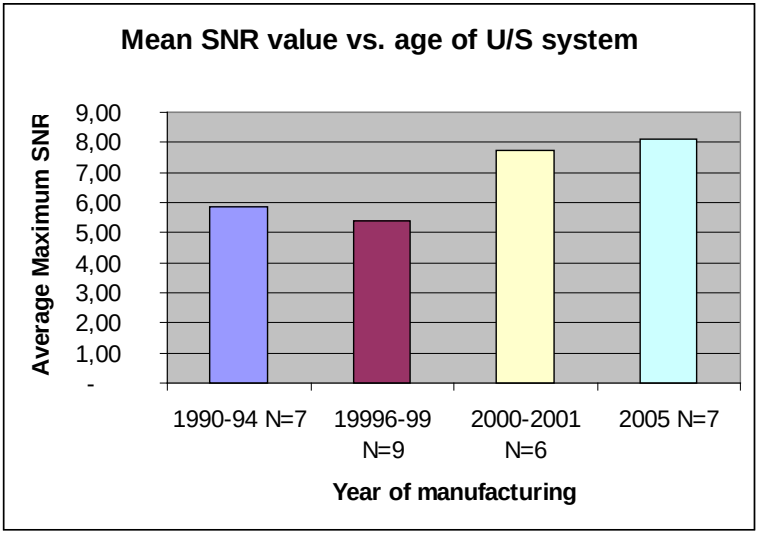

Figure 11 SNR results vs. age of the imager.

When repeating the measurements at the same transducer, the maximum SNR varied by 0.1 … 0.9.

After repair of one US imager, the maximum SNR of two transducers of this imager increased by 1.6 (Linear Array) and 0.85 (Curved Array) respectively (Figure 12).

3.6 Discussion

The complete testing of ultrasonic transducers and imagers requires a large amount of technical measurements. Unfortunately, easy-to-measure technical parameters like axial / lateral resolution etc. often are not significant for the determination of the clinical image quality and usability of a specific device. Browne et al. [15] found moderate correlation between B-mode test parameters and clinical parameters (lateral resolution vs. clinical resolution: r = -0.69*, anechoic target detection vs. clinical noise: r = 0.5 (p = 0.14) and penetration depth vs. clinically useful penetration depth: r = 0.56* (* statistically significant values). Correlations

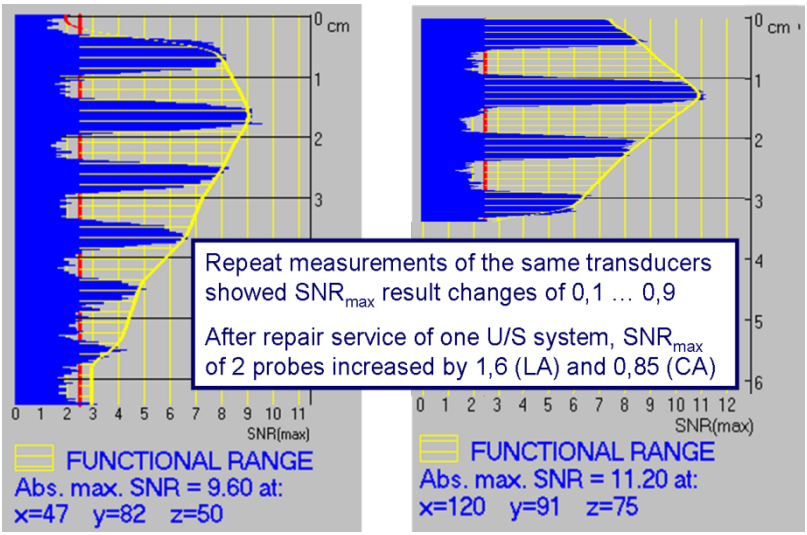

Figure 12 Repeat measurements before and after repair of an imager demonstrate the success of the repair action.

of axial resolution vs. tissue texture variation, slice thickness vs. overall clinical image quality and contrast resolution vs. clinically useful dynamic range were poor. Therefore, important "homework" still needs to be done: It is important to continue studies which show the correlation between technical test results of different electronic testers, phantoms etc. and the clinical opinions about the image quality of the tested transducers.

The pilot study using the tissue mimicking phantom with cylindrical voids revealed some interesting results.

It confirmed that the image quality of newer devices is better than that of older generation imagers (ca. > 8 years). 46 ± 8% of the US imagers in German practices are at least 10 years old and 24 ± 6% are older than 15 years [17], thus diagnostic quality is obviously suboptimal in many cases.

It was also possible to demonstrate the enhancement of image quality after repair. The SNR results revealed that 6% of the curved array transducers should be replaced or repaired. Both literature results [8] as other users of the SNR method reported higher numbers of failed transducers in several discussions, so the results of this pilot study may not be typical for larger numbers of test specimen.

The axial distributions of the SNR are most strongly influenced by the elevation focussing. As this focussing mainly depends on the acoustic lens on top of the crystals, the amount of maximum SNR alone is not important. But the maximum SNR value and the axial position of it can be used to identify incorrect lens repair.

The lower SNR limit of 2.5 is an empirical estimation, but it was communicated from a number of users of the same phantom that they get satisfying quality results when using this value. Nevertheless, scientific proof is still to be established. Using this limit, the clinically useful range of the transducer can be estimated. The tracking of this range is an important criterion for the deterioration of a specific transducer or a failed lens repair.

During the pilot study, some technically important issues showed up:

– It is important to control the impedance of the video cabling between imager and digitizer. Mismatching impedance or excess cable length results in shaded images or increased noise, which reduces the measured SNR value. Moreover, it seems that the video

outputs of some US imagers give inferior image quality as compared to the monitor images, as they are electrically isolated from the imager in order to fulfil the requirements of medical device standards (e.g. IEC 601 series).

– The specification of the video digitizer has an influence on the outcome of the measurements. Digitizers of different brands can have limited gray scale resolutions, and the adjustment of the digitizers has to be optimized individually. This process should be done using standard video test images before starting the US imager tests. It is most desirable to supply a standard protocol for the digitizer setup of the test device. When it is possible to use the same digitizer and settings for each test, these influences can be minimized.
– In future versions of the software, the import of DICOM images and other image formats should be supported. Then it would be possible to store the complete phantom scan in a “cine loop” and transfer the data electronically, e.g. by USB stick.
– Before starting the SNR measurements, it is advisable to test the uniformity of the US transducer in order to detect dead elements. Such uniformity tests can be made with specialized phantoms, but it is also sufficient to use a uniform tissue area like the tester’s forearm or the “paper clip test” mentioned in the introduction. In both cases, dead elements are detected by a significant change in the brightness level along single image lines perpendicular to the transducer surface [12].

The pilot study also leaves some open questions. From our preliminary results, there seems to be a significant difference in the maximum SNR of linear and curved array transducers. One possible explanation is that the voids, which lie apart from the centre beam of the US transducer, are not penetrated parallel to the cylinder axis. Therefore, partial volume artefacts occur which increase the noise inside the more lateral voids.

Another possible source of problems with concave transducers may be the coupling to the flat coupling window. An elevated rim on top of the phantom allows large amounts of coupling gel to be used; or even filling with water, which guarantees a bubble-free acoustic coupling of the complete transducer surface. Nevertheless, the path between transducer

and phantom has a position-dependent distance which is bridged by a medium with (slightly) different acoustic properties than the phantom's. This might result in reverberation phenomena, which can cause noise signals inside voids.

In the IEC, the shape and orientation of the voids is still under discussion. Spherical voids or cylindrical voids which are orientated parallel to the US beam axes might help to solve the disparity between linear and curved array transducer results, although this approach would require very large or multiple phantoms.

3.7 Conclusions

The SNR measurement method delivers quality figures for the transducers and the imager electronics. The goal of this method is not the comparison of various devices, but the tracking of quality of individual US imagers over time.

The expense of time per transducer is ca. 20 minutes, which may be reduced with increasing routine. Most other procedures require more time for measurement, so the SNR method is a great step towards routine quality constancy tests of US imagers. The most practical method for regular quality constancy tests may be the combination of the SNR measurement method with a simple electronic check and a protocol for visual inspection of the transducer, the imager and the video screen.

Care should be taken that the development of complicated test methods will not lead to more public acceptance of the quality control measures – the ultimate goal should be a simple procedure and device, which gives quick response to the question of image quality degradation. Other, more sophisticated methods should be reserved for R&D, production QA and service purposes.

Finally, the maximum allowed degradation in terms of SNR loss over time may not be the same for every type of imager and/or transducer. It strongly depends on the intended use, if degradation is still acceptable for the doctor or if it is not.

The results are encouraging to continue the development of simple quality test phantoms and simplified methods of applying them. Before they can be introduced in regulatory practices, it is necessary to validate the methods by doing comparisons of the phantom test results with independently reviewed clinical images.

Acknowledgement

Many thanks to Birte Blichenberg and Christian Hamann for doing the measurements, and to the experts Schultz, Satrapa, Doležal and all the colleagues of TC87 for the enlightening discussions.

3.8 References

[1] OPPELT, A. (ed.). *Imaging Systems for Medical Diagnostics*. Erlangen : Publicis Corporate Publishing , 2005, pp. 28.

[2] GUTER, S. „Sono Baby“ geboren!. *Bayerisches Ärzteblatt*. 2008, 10, pp. 612.

[3] THIJSSEN, J.M. et al. Objective performance of medical ultrasound equipment. *Ultrasound Med. Biol.* 2007, 33, 3, pp. 460-471.

[4] IEC 87/400/CDV. *Ultrasonics – Pulse-Echo-Scanners – Part 2: Measurement of maximum depth of penetration and local dynamic range.* Geneva, Switzerland : International Electrotechnical Commission, 2008.

[5] SHAW, A.; HEKKENBERG, R. *NPL REPORT DQL/Acoustics XXX: Standards to support performance evaluation for diagnostic ultrasound imaging equipment*. NPL, August 2007.

[6] SCORZA, A. A novel method for automatic evaluation of the effective dynamic range of ultrasound scanners. In ECIFMBE 2008. *IFMBE Proceedings.* 2008, 22, pp. 1607-1611.

[7] IEC 62558-TS. *Ultrasonics – Real-time pulse-echo scanners - Phantom and Method for Automated Evaluation and Periodic Testing of 3-D Distributions of Signal – to – Noise Ratio Using Anechoic Voids.* Geneva, Switzerland : International Electrotechnical Commission TC 87 WG9, 2009.

[8] MÅRTENSSON, M.; OLSSON, M.; SEGALL, B.; FRASER, A.G.; WINTER, R. and BRODIN, L.A. High incidence of defective ultrasound transducers in use in routine clinical practice. *European Journal of Echocardiography*. 2009, 10(3), pp. 389-394.

[9] NPL. *NPL Ultrasound Survey Results* [online]. 2008. [downloaded 22.6.2008]. WWW: <http://www.surveymonkey.com/Report.asp?U=371771779502>.

[10] ACR Standards. *ACR Standard for Diagnostic Medical Physics Performance Monitoring of Real Time B-Mode Ultrasound Equipment*

[online]. 1999. WWW: <http://intranet.alemana.cl/lac_intraclinica/Mbe/GPC/Guidelines/Radiologia/physics_monitoring_us_equip.pdf>.

[11] DOLEŽAL, L.; MAZURA, J.; TESAŘÍK, J.; HÁLEK, J.; KOLÁŘOVÁ, H. *A New Approach to an Ultrasound Imaging System Evaluation Using the Point Spread Function*. Prague : The 3rd European Medical and Biological Engineering Conference November 20 – 25, 2005.

[12] SATRAPA, J. *Private communication to IEC TC 87, WG9*. Prague, 2008.

[13] DGBMT/DEGUM/DRG. *Ultraschall in der Medizin – Grundlegende Aspekte zur sicheren Anwendung von Ultraschall in der Diagnostik*. DGBMT Deutsche Gesellschaft für Biomedizinische Technik (ed.), 2004. Available from Deutsche Gesellschaft für Biomedizinische Technik in VDE, Stresemannallee 15, 60596 Frankfurt, service@vde.com.

[14] Fachverband elektromedizinische Technik ZVEI. *Qualitätssicherung an Bildwiedergabegeräten* [online]. Januar 2004. WWW: <www.zvei.org/medtech>.

[15] BROWNE, J.E.; WATSON, A.; MUIR, C.; HOSKINS, P.; ELLIOTT, A. An Investigation of the Relationship between in Vitro and in Vivo Ultrasound Image Quality Parameters. *Ultrasound*. 2004, 12, 4.

[16] IEC 61391-1. *Ultrasonic - Pulse-Echo Scanners - Part 1: Techniques for calibrating spatial measurement systems and measurement of systems point-spread function response.* Geneva, Switzerland : International Electrotechnical Commission, 2006.

[17] PFANDZELTER, R.; SPIRO, T.C. Strengere Qualitätskontrollen in den Praxen. *Deutsches Ärzteblatt*. 2008, 105(48).

4 Quality control of ultrasound equipment with UltraIQ software

Wendy Berkers

To check the performance of Ultrasound equipment there are various phantoms commercially available. Those phantoms are designed with multiple structures with different characterizations. By measuring those characterizations you are provided with specific information about the accuracy of your ultrasound machine. When you measure with the same phantom and identical settings of the ultrasound system you will get relative results. With UltraIQ it is possible to compare these results to define the variety in time. This is known as the trend analysis. Quality control only based on visual qualifications is labor intensive and time consuming. But more important the human interpretation makes the tests very subjective combined with the interpretation of the large number of results it is more likely to make mistakes. To exclude all these disadvantages by the use of just a phantom UltraIQ has been developed.

4.1 History

UltraIQ was initially developed by the Canadian company Ramsoft, founded in 1994. Early 2000 Cablon Medical, Dutch company specialized in QA applications and software development, obtained the rights of UltraIQ. Cablon Medical B.V. converted it into a Windows application with additional features and possibilities.

4.2 General information

By developing and optimizing UltraIQ there were several goals. The main objectives of UltraIQ;

- Efficient and reliable
- Easy to use
- Compatible to all multipurpose ultrasound QA phantoms
- Applicable for all ultrasound equipment
- Adjustable and flexible

There is a variety of people who execute quality assurance for example clinical physicist, sonographers and medical technicians. The application has to be easy to use and understandable for a divergent group of people. To make UltraIQ compatible to all quality assurance ultrasound phantoms there has to be the possibility to integrate the structures and their characterization in UltraIQ.

The performance measurements in phantoms as well as in UltraIQ are:

- Axial and lateral resolution; Curvatures or linear placed nylon fibers in a phantom are used to give a visual impression of resolution of an ultrasound machine. To exclude the visual aspect UltraIQ analyses the vertical pin target group and measures the width and high of those nylons which indicates the lateral and axial resolution as a point spread function.
- Contrast; Grey targets are provided for monitoring contrast, grey scale processing and range capabilities of the ultrasound system. Measuring grey values and steps per dB indicates the numeric values.
- Penetration depth; either measuring cyst disappearing in speckle or weeping the transducer on the surface of the phantom are two ways for visual interpreting the penetration depth of your ultrasound machine. Because of the vagueness and inaccuracy of the visual measurement UltraIQ calculates the minus 6 dB value in relation to the background and gives a numeral value to this depth.
- Dead zone; superficial nylon fibers are places to indicate the capability of the ultrasound machine in the near field.
- Distance; Nylon fibers with fixed distances in the vertical and horizontal plane can be measured to check if the measured distance at the ultrasound machine correspondence to the fixed distance in the phantom.
- Cysts; cyst targets can visual be used to measure the distortion and can be used for penetration depth interpretation. In UltraIQ the width and high of the cysts will be measured numerical.

4.3 Image import

There is a large variety in ultrasound equipment. Most of the manufacturers of ultrasound systems combined that last for several years using new techniques. To have access to either older systems as well as the latest models we need to export images in different formats. For video images we capture the signal by using a frame grabber. For the newer ultrasound machines we use either CD or USB and store images in BMP or DICOM.

4.4 Usability with commercial test objects

UltraIQ supports all multipurpose phantoms of the 4 major companies who develop ultrasound phantoms. Cablon Medical works close with these manufacturers to be impartial. Over the years there will be new machines and new phantoms and UltraIQ will be developed to insure compatibility. At least to not get asphyxiated UltraIQ is flexible at those points. If you have designed and manufactured your own ultrasound phantom you have a possibility to specify the size and characterizations of the earlier mentioned performance measurements.

4.5 Actual developments and advantages

The first version of UltraIQ by Cablon Medical is commercially available since 2004. During the years there were several improvements and new developments. In 2008 there was a desire list that they decide to make another new modern version know as UltraIQ version 2. To meet the needs of the users there were new conditions. Conditions for version 2 added to the main objectives to UltraIQ 1 are:

- DICOM interface
- Less clicking to get results
- Average calculations
- Export possibilities (PDF. CSV)
- Linearity compensation
- Report designer

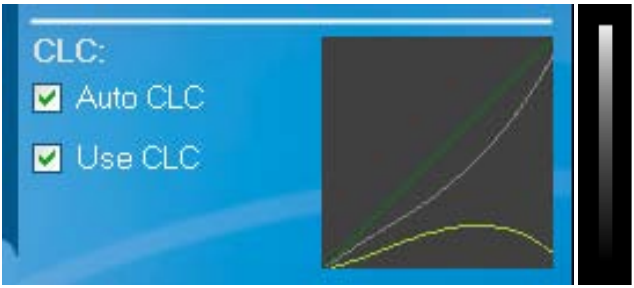

Figure 1 CLC figure and grey level bar.

Improving the software UltraIQ was possible by using DICOM images. DICOM is the standard if we talk about digital imaging and communication. DICOM has the feature to have different "tags" we can display and use during the QA measurements. By using DICOM images we improved UltraIQ to be even more objective and faster. To accomplish less handling our software engineers developed sliding windows so we have access to all different sections without clicking. Due to pixel size and scanning swerves there were little changes in results. To measure a certain parameter more often and get the average of those results we will increase the accuracy of the measurements. All the data will be stored in a report in the UltraIQ program. To have the results in a back up there is the possibility to export the results. There are two different ways. The first one is exporting the report in a PDF or exporting the results using a CSV. Even calculations afterwards are possible using the CSV in other statistic or mathematic programs.

Further we discovered the often non linearity of the grey scale steps in ultrasound UltraIQ interprets the non linearity using the grey level bar displayed in the ultrasound image and correct it into a linear scale by using the CLC button.

Last but not least there is the possibility to create your own report. You're free to decide which graphs, images and numbers will be displayed in the report and you can add a logo.

4.6 How to perform a QA check

Make, according to a protocol, images of an ultrasound phantom. Than export the required images and integrate them in the software UltraIQ. Analyze and measure all images and get the temporary results (Figure 2) of all performance measurements. By editing the results to an ultrasound machine - transducer combination you can save the results in your self designed report.

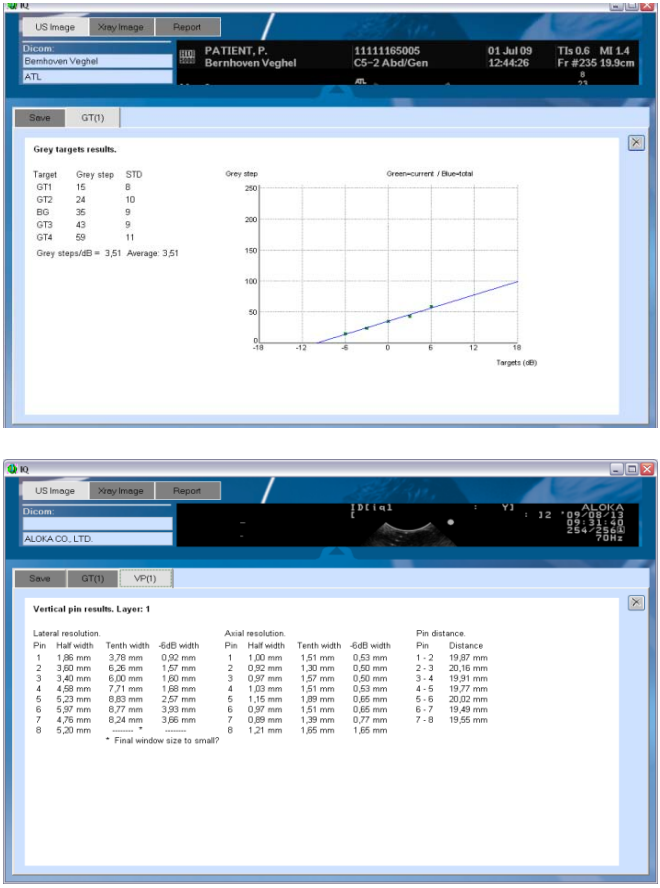

Figure 2 Two examples of temporary results. Result of the grey

target measurement is on the top and vertical pin measurement with lateral, axial and distance information on the bottom table.

4.7 Summary

As quality control gets more and more important we succeed in launching a new product named UltraIQ 2. With UltraIQ 2 it is possible to analyze, measure and store all results of a quality control performance check. Parameters that can be measured are: resolution, contrast, -6 dB penetration depth, dead zone and distortion of an ultrasound system. UltraIQ 2 had several improvements and is able to easily work with DICOM images, has average calculations, contrast linearity, intuitive workflow and a report designer.

5 Automated measurements for ultrasonic QA

Andrew Hurrell

When attempting to characterise ultrasonic fields, there are many features that will be of concern to the QA investigator. Total ultrasonic power can be readily quantified with a radiation force balance, but power takes no account of spatial variations of the field. In order to provide a more comprehensive assessment of patient exposure to ultrasound it is important to find, and measure, the spatial maxima of a field. However there could be various spatial maxima to consider. The region of largest rarefaction pressure will be of most interest for the assessment of potential cavitation activity. In contrast, the region of highest temporal average intensity will be where most ultrasonic energy is deposited, and is thus likely to be the area of greatest temperature rise. Field quantification is not restricted to find maxima. Once a spatial peak has been located, the beam widths at a given threshold level (e.g. -3 dB, -6 dB) can be quantified. Furthermore, if the field is focussed, the depth of field (i.e. beam width in the axial direction) is often of interest.

Measurement of acoustic quantities at specific locations within a field requires the use of a hydrophone. Ultrasonic hydrophones can take many forms, for example: needle, membrane and fibre-optic hydrophones. However all hydrophones have a common set of performance requirements; they should all:

- have a broad bandwidth to allow accurate assessment of both high and low frequency content within a waveform
- have a small acoustically active area (to minimise spatial averaging and provide a less directional response)
- be either physically small or acoustically transparent (to minimise perturbations of the field being measured)
- have an acoustic output that is stable over a long time scale (so that the frequency response of the hydrophone can evaluated, via a calibration process, and subsequently used to convert hydrophone voltage to acoustic pressure)

– have sufficient signal to noise to measure the smallest signals of interest.

The complexity of acoustic fields produced by modern ultrasonic equipment is such that field mapping by manual movement of a hydrophone would be so time consuming as to render it impractical. The solution is therefore to use a measurement system that automates the hydrophone motion, data acquisition and data processing functions. This chapter begins by presenting a fully automated measurement tank solution and considers how it can be used in the quantification of various ultrasonic fields. The discussion then moves on to examine the various hydrophone types and their suitability for ultrasonic QA measurement. Finally the calculation of ultrasonic output parameters is reviewed in the context of the automated data processing offered by the measurement system.

5.1 Measurement tank

5.1.1 Scanning rig

As can be seen in Figure 1, the measurement system comprises a 300 litre PMMA (Perspex/plexiglass) water tank surrounded by a high strength, extruded aluminium frame. Mounted on the frame are three, high resolution mutually orthogonal, linear motion stages. These actuators incorporate load-mounted, linear, magnetic encoders that ensure the system is capable of a positional repeatability of 5 μm. This distance corresponding to half a wavelength at 148 MHz in water – far above than the current highest frequency in used in medical ultrasound.

An ultrasonic source transducer is mounted in a fixture at one end of the measurement tank. A hydrophone holder is then attached to the motion stages to allow a hydrophone to be positioned anywhere within the ultrasonic field of the ultrasonic source.

The movement of these stages is conducted over a USB interface by a controller PC running a custom software package. The software synchronizes the movement and data acquisition processes to ensure that spatial mapping of an acoustic field becomes a simple task. Furthermore, to minimise the effect of electro-magnetic interference on measurements,

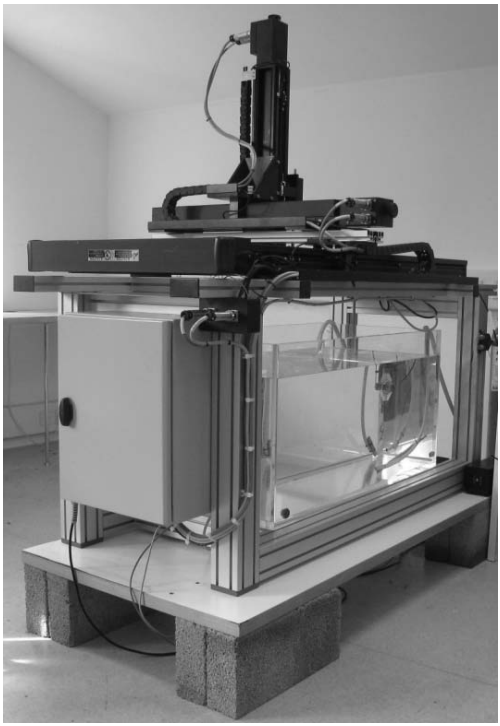

Figure 1 Fully automated 3-axis scanning gantry.

the host PC de-energises the stepper motor drives during signal acquisition.

5.1.2 Data acquisition

All data acquisition is conducted with a high sample rate digital storage oscilloscope (DSO). Many modern scopes are based around personal computer (PC) technology and can therefore exploit current communications protocols including Gigabit Ethernet and Hi-speed USB, as well as more traditional interfaces like RS-232 and GPIB. Any of these interfaces can be used to transfer acquired waveforms back to the host PC, although Ethernet connection is recommended for optimum data rates. Most DSOs are capable of using averaging techniques to improve

signal-to-noise ratio whenever a stable trigger signal is present. The custom software that controls the automated measurement system has DSO driver modules that can exploit this functionality.

The software continually checks the status of the DSO and can provide Automatic Gain Control (AGC). AGC is a function that dynamically adjusts the DSO amplifier settings to ensure that both very large and very small signals are sampled with sufficient resolution. The system is also capable of providing Time Delay Compensation (TDC). This means that the triggering delay of the DSO is automatically adjusted to compensate for the altered time of flight when the hydrophone is moved along the acoustic axis.

Fully synchronised movement and data acquisition offers considerable advantages for the ultrasonic researcher. The process of mapping an ultrasonic field now becomes a comparatively simple task of aligning the hydrophone with the acoustic beam and then specifying the scan parameters (*e.g.* number of points and scan increment) over which the scan is to be conducted. The system will then automatically acquire data, storing each waveform to disk, thereby releasing the researcher to carry on alternative tasks. The automated scanning has a further application; if a hydrophone is placed within an ultrasonic beam, the system can be set to automatically re-position the hydrophone at the beam maximum. This further simplifies the measurement process.

5.1.3 Tank lining

When measuring short duration acoustic signals (*e.g.* the short pulses produced by diagnostic ultrasound machines) spurious reflections from measurement tank walls can easily be isolated by appropriate time gating. However when measuring a continuous wave ultrasonic signal (*e.g.* from a physiotherapy machine or from a HIFU source) it is not possible to temporally separate direct signal from any reflections. This can lead to standing wave patterns cause by the interaction of direct acoustic signals with reflections from the walls and bottom of the measurement tank.

The solution to this problem is to coat the walls and base of the measurement vessel with an ultrasonically absorbent rubber material. Clearly lower frequencies are of most concern since they have a longer wavelength and have less attenuation than higher frequencies. Ideally a lining material should also be sufficiently compact to prevent large volumes of the tanks be occupied by anechoic coatings. Fortunately

acoustic materials capable of more than 15 dB echo reduction (in the range 1-6 MHz) in a thickness of only 10 mm are readily available.

5.1.4 Water treatment

Whilst tap water is a readily available medium in which to make ultrasonic measurements, it does have some limitations. Foremost of these is that tap-water is super-saturated with dissolved gases (*e.g.* oxygen, nitrogen, carbon dioxide). These gases have the tendency to leave their dissolved state and form small bubbles on the surface of any hard surface within the water of the measurement tank. Given their high acoustic impedance mismatch with water, small bubbles tend to act as point reflectors/scatterers. Clearly, formation of a point reflector on the surface of either a source transducer or receiving hydrophone can have detrimental effect on measurements. The measurement system in Figure 1 addresses this by having a water treatment system that incorporates reduced pressure degassing. This system is capable of reducing the dissolved oxygen content of a 150 litre body of water to below 3 ppm in about 3 hours.

The water treatment system also incorporates a de-ionisation cylinder that provides water with a conductivity that is less than the 5 μS limit recommended by IEC 62127 - Part 1 [1]. Static bodies of water are also prone to two other inter-related issues. Firstly particulate matter (either airborne or introduced on the surface of objects placed within the water) can contaminate the water. This particulate matter can then become a food source for biological growth. This second issue (biological activity) not only produces an unpleasant, odorous film, but can be a source of bacterial health hazard to the users of the measurement facility. These two problems are addressed with a series of filters included within the water treatment system. A two-stage particulate filter (one at 5 μm, one at <1μm) removes any suspended particulate matter. Similarly a UV-filter ensures that bacterial growth is effectively suppressed without the need to add anti-bacterial chemicals to the water that would compromise the low conductivity achieved by de-ionisation.

5.2 Hydrophones

The term hydrophone is used to refer to any underwater transducer intended purely to receive acoustic signals. In underwater acoustics generally there are a wide range of different types of hydrophones. However for the frequency range typical of medical applications there are only three commonly found hydrophone types; membrane, needle and fibre-optic.

5.2.1 Membrane hydrophones

Membrane hydrophones are considered the "gold-standard" hydrophone due to their smoothly frequency response over a very broad frequency range. This response has been accurately modelled by Gélat et al [2]. These hydrophones are constructed of a very thin layer of the piezo-polymer PVDF. The PVDF has been carefully prepared so that only a small region in the middle of the film is piezo-electrically active.

Membrane hydrophones are excellent for characterising the broadband short pulses that are produced by ultrasonic imaging systems. However these hydrophones are less suited to the measurement of continuous wave (CW) signals due to the possibility of flexural standing waves modes developing on the membrane.

Figure 2 Membrane hydrophone.

5.2.2 Needle hydrophones

Needle hydrophones are good general purpose measurement device and are constructed from a small disc of a piezo-electric material mounted on the end of a co-axial conductor. They are commercially available in a wide range of sizes as small as 40 μm. Needle hydrophones have greater sensitivity and lower cost than a comparable sized membrane hydrophone. The frequency response of a needle hydrophone shows more variation due to radial interference effects that occur when an incident acoustic wave diffracts around the needle tip.

However, needle hydrophones have been shown by both Hurrell [3] and Wilkens and Koch [4] to yield an accurate representation of broadband acoustic signals if the whole frequency response is used to calculate the pressure waveform using a method such as that of IEC 62127-1 [1].

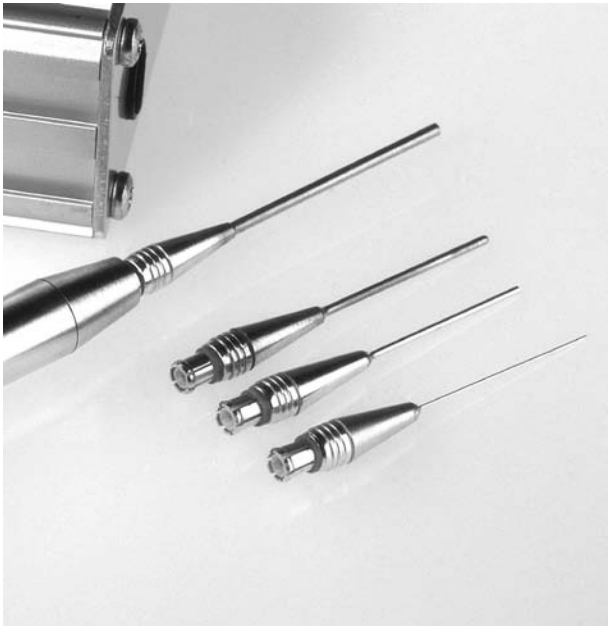

Figure 3 Selection of needle hydrophones.

5.2.3 Fibre-optic hydrophones

Fibre-optic hydrophones are the latest development in hydrophone technology. Some fibre-optic sensors are based upon a measurement of the change in refractive index of water due to ultrasonic pressure [5]. Alternatively a sensor based upon a Fabry-Perot interferometer built on the end of the optical fibre was proposed by Beard et al [6]. Fibre optic hydrophones can exhibit the same radial mode interference effect as needle hydrophones, but as before these can easily be corrected for.

In contrast to either needle or membrane hydrophones, fibre-optic devices are based solely on an optical transduction method and are thus immune to electro-magnetic inference. The Fabry-Perot interferometer hydrophone has also been shown by Morris et al [7] to be capable of simultaneous measurement of temperature and pressure. This, coupled with the ability to withstand high amplitude acoustic fields, makes this latter type of fibre-optic sensor ideal for characterising the fields produced by therapeutic (e.g. HIFU) fields.

Figure 4 Fibre-optic hydrophone.

5.3 Data processing

Hydrophone data acquired with the automated measurement system is commonly stored on the controller PC, but requires processing to yield results relevant to ultrasonic QA.

5.3.1 Voltage-to-pressure conversion

Waveforms acquired from a DSO are the raw voltage output from the hydrophone. However assessment of ultrasonic output requires an acoustic pressure waveform or a measure of acoustic intensity derived from it. IEC 62127-1 [1] specifies two possible methods to convert hydrophone voltage to acoustic pressure, depending on the frequency response of the hydrophone used. If the hydrophone complies with the narrowband approximation identified in IEC 62127-1, then it is sufficient to calculate acoustic pressure from the ratio of the voltage waveform and the sensitivity of the hydrophone at the acoustic working frequency. This can be done with a simple spreadsheet application. If however the full hydrophone response needs to be included (*i.e.* when using a needle hydrophone to measure a broadband source) dedicated software capable of conducting a full hydrophone deconvolution is required.

5.3.2 Acoustic output parameters

International standards relating to ultrasonic output (*e.g.* IEC 61157 [8], IEC 62127-1 [1], IEC 62359 [9]) specify a range of different parameters that may be of interest to the ultrasonic QA professional. Whenever a pressure waveform is calculated a number of parameters should also be computed including:

Pressure parameters	P_c	Peak compressional pressure
	P_r	Peak rarefactional pressure
	P_{RMS}	RMS pressure
	PPSI	Pulse pressure squared integral

Derived intensity parameters	I_{ta}	Temporal average intensity
	I_{pa}	Pulse average intensity
	I_{tp}	Temporal peak intensity
	PII	Pulse intensity integral
Other parameters	F_{awf}	Acoustic working frequency
	t_d	Pulse duration
	MI	Mechanical Index

The software used to drive the system in Figure 1, calculates these parameters automatically and is also capable of applying in-tissue de-rating to derive attenuated parameters consistent with those of IEC 62359.

5.3.3 Quantifying spatial variation

An ultrasonic QA measurement is rarely a single waveform. In practice the ultrasonic field will have been systematically mapped by scanning a hydrophone around the field. Processing software should also be able to automatically calculate the acoustic output parameters (above) for every point in a scan and then display a spatial map to the user. If the measurement was a simple linear scan then various beamwidths (e.g. -3, -6, -10, -20 dB) should also be displayed as well as centre and peak values. For planar scans, this is extended to include the beam areas (at -3, -6, -10, -20 dB). The system shown above also calculates the spatial average and spatial peak values for each of the derived intensity parameter.

5.3.4 Reporting

The form of data processing above dramatically simplifies the process of quantifying output from medical ultrasonic equipment. The final stage of the ultrasonic QA process is reporting of data, and the automated system described in this chapter includes the option to export data to a PDF formatted report file. The advantage of PDF files are that they are less prone to accidental editing and therefore provide a more reliable and secure audit trail. All reports also include a record of the operator, date and equipment used in the measurement. This ensures that if a piece of equipment has been found to be out of calibration, tracing all potentially affected measurements is much easier.

5.4 References

[1] IEC 62127-1. *Ultrasonics – Hydrophones – Part 1: Measurement and characterisation of medical ultrasonic fields up to 40 MHz*. Geneva, Switzerland : International Electrotechnical Commission, 2007.

[2] GÉLAT, P.N.; PRESTON, R.C. and HURRELL, A.M. A theoretical model describing the transfer characteristics of a membrane hydrophone and validation. *Ultrasonics*. 2005, 43, pp. 331–341.

[3] HURRELL, A.M. Voltage to Pressure Conversion: Are You Getting "Phased" by the problem? *J. Phys: Conf. Ser*. 2004, 1, pp. 57-62.

[4] WILKENS, V. and KOCH, C. Improvement of hydrophone measurements on diagnostic ultrasound machines using broadband complex-valued calibration data. *J. Phys: Conf. Ser.* 2004, 1, pp. 50-55.

[5] STAUDENRAUS, J. and EISENMENGER, W. Fibre-optic probe hydrophone for ultrasonic and shock-wave measurements in water. *Ultrasonics*. 1993, 31 (4), pp. 267-273.

[6] BEARD, P.C.; HURRELL, A.M. and MILLS, T.N. Characterization of a Polymer Film Optical Fiber Hydrophone for Use in the Range 1 to 20 MHz: A Comparison with PVDF Needle and Membrane Hydrophones. *IEEE Trans UFFC*. 2000, 47 (1), pp. 256-264.

[7] MORRIS, P.; HURRELL, A.; SHAW, A.; ZHANG, E. and BEARD, P. A Fabry–Pérot fiber-optic ultrasonic hydrophone for the simultaneous measurement of temperature and acoustic pressure. *J. Acoust. Soc. Am.* 2009, 125 (6), pp. 3611-3622.

[8] IEC 61157. *Standard means for the reporting of the acoustic output of medical diagnostic ultrasound equipment*. Geneva, Switzerland : International Electrotechnical Commission, 2007.

[9] IEC 62359. *Ultrasonics – Field characterization – Test methods for the determination of thermal and mechanical indices related to medical diagnostic ultrasonic fields*. Geneva, Switzerland : International Electrotechnical Commission, 2010.

6 Doppler Performance Testing: Is it hitting the mark?

Jacinta E. Browne

Diagnostic ultrasound techniques have been shown, since their inception into modern medicine in the 1960's, to be powerful and versatile imaging technique. Ultrasound is used as a means of obtaining information about the structure of organs and the cardiovascular function of the body. One of the most important applications of ultrasound is to obtain blood flow information from the cardiovascular system within the body. Blood flow throughout the body is studied extensively by non-invasive ultrasonic continuous wave (CW) and pulsed wave (PW) Doppler, as well as colour and power Doppler methods [1]. Indeed, the use of ultrasound has become more widespread over the last decade, largely due to advances in transducer technology and digital electronics [2]. These developments are extending the availability of ultrasound to new users, through reduced cost and improved performance and reliability [2, 3]. With the widespread and ever-increasing use of medical ultrasound techniques, it is necessary that ultrasound scanners meet the requirements of each of the different clinical applications, and in order to ascertain whether these requirements are achieved, performance tests are carried out. The product of a Doppler Ultrasound Examination is often a measurement of a physiological quantity such as Peak Systolic velocity, furthermore; Doppler examinations are frequently directed toward a well-defined question concerning blood flow. Therefore, the accuracy of the Doppler parameters being measured (maximum velocity) need to be known as well as the detection limits (penetration depth, lowest detectable velocity) of the Doppler system.

Due to the rapid rate at which the performance and imaging capabilities of ultrasound scanners are being improved, designing performance test procedures and test phantoms which will challenge state-of-the art, top-of-the range ultrasound scanners represents a growing challenge. Furthermore, the inherent value of these recommended test parameters and test procedures is questionable, since limited evidence has been presented which demonstrates their usefulness, and in addition, some studies have found that the tests are not reflective

of clinical performance [4, 5]. It is imperative that these performance and quality control (QC) test protocols and test devices keep pace with developments in medical ultrasound technology – one only has to look at the plethora of new imaging and Doppler modes appearing on modern-day ultrasound scanners to gain an appreciation of how far the test protocols and devices are falling behind what should be considered a minimum standard.

This paper will provide a review of the current technical standards and test procedures for Doppler ultrasound performance published by the different professional organisations from around the world, as well as a review of commercial and laboratory test objects currently available and in use for Doppler performance testing.

6.1 Review of current Doppler Performance Test Procedures

Doppler ultrasound quality assurance (QA) and performance techniques have been recommended for several years by several professional bodies including the American Institute for Ultrasound in Medicine [6], the International Electrotechnical Commission [7, 8, 9], and the Institute of Physics and Engineering in Medicine [10]. Despite these test protocols being periodically updated, they do not include recommended test protocols for newer Doppler techniques such as Tissue Doppler and contrast specific imaging. The following is a review of the recommendations made by these different professional bodies.

6.1.1 Continuous Wave and Pulsed Wave Doppler Performance Test Protocols

Continuous wave (CW) and pulsed wave (PW) Spectral and Duplex Doppler modes have been tested adequately for a number of years with well established test protocols and test phantoms [11, 12, 13, 14, 15, 16, 17]. Furthermore, these tests have been found in some cases to be reflective of clinical performance [4]. The spectral Doppler performance tests usually include measurements of the following parameters: (i) velocity direction accuracy; (ii) range gate accuracy; (iii) sample volume dimensions; (iv) direction discrimination; (v) penetration depth; (vi) maximum velocity estimation accuracy; (vii) waveform index

estimation accuracy; and (viii) volume flow estimation accuracy and this range of parameters have been successfully evaluated for the last fifteen to twenty years [11, 18, 19, 20, 10].

(i) Velocity Direction Accuracy

This test is an assessment of the directional accuracy of the Doppler system, if the scatterer moves towards the Doppler beam it is registered as a negative Doppler shift whereas if the scatterer moves away from the Doppler beam it is registered as a positive Doppler shift. If pathology is present in organs such as the heart or the liver, the flow direction may be reversed and it is important that this is correctly identified by the Doppler system. Velocity directional accuracy has been successfully measured using a string phantom and flow phantom [11, 18, 20, 10].

(ii) Range Gate Accuracy

This test is an assessment of the accuracy of the range gate marker at indicating the location of the range gate. Doppler examinations require acquisition of Doppler information from the correct spatial location. Range gate registration has been successfully measured using a string phantom [20, 10].

(iii) Sample Volume Dimensions

This test assesses the accuracy of the sample volume dimension. The acquired Doppler information is critically related to the interaction of the sample volume with the blood flow field. If the sample volume is too large then it may not be possible to obtain signals without contamination from other vessels or from vessel wall motion. Sample volume dimension has been successfully measured using a string phantom [18, 20, 10].

(iv) Directional Discrimination

This test provides a measure of the amount of cross-talk present in the Doppler ultrasound system. Many arterial flow signals have bi- or tri-phasic signals present, exhibiting forward and reverse flow at different times in the cardiac cycle. Analysis of the shape of the waveform is used to detect the presence of pathology in these organs. In these circumstances it is

important that spectral trace of the arterial waveform is not affected by mirror image signals from the opposite channel. Directional discrimination has been successfully measured using a string phantom and flow phantom [11, 18, 20, 10].

(v) Penetration Depth

This is the maximum depth of a vessel in tissue from which a Doppler signal free of extraneous noise can be obtained. In clinical practice it is often desirable to obtain signals from major vessels within the body, and also from small vessels for assessment of perfusion. Pulsed Wave Spectral Doppler penetration depth has been successfully measured using a flow phantom [11, 10].

(vi) Maximum Velocity Estimation Accuracy

Maximum velocity estimation accuracy provides an assessment of the accuracy of the Doppler system's estimate of the maximum scatterer velocity. This is one of the most common measurements made using Doppler ultrasound and provides information concerning the degree of arterial stenosis, or of the pressure drop across cardiac valves in a patient. Maximum velocity accuracy has been successfully measured using a string phantom and a flow phantom [11, 18, 19, 20, 10].

(vii) Waveform Index Estimation Accuracy

This test provides an estimation of the Doppler systems ability to estimate the flow waveform index. This assessment is carried out using a simulated physiological waveform similar to those found *in-vivo*. Measurements of percentage error in the waveform index estimation are carried out, (100 (R-1) where R is the ratio of the estimated value of the index to the true value of the index), and the co-efficient of variation of the estimated index is also determined. Waveform Index Estimation accuracy has been successfully measured using a string phantom and a flow phantom [11, 18, 19, 20, 10].

(viii) Volume Flow Estimation Accuracy

This test provides an estimate of the accuracy of the Doppler system's ability to estimate flow rate. This assessment is carried out using a simulated physiological waveform similar to those found *in-vivo*. Volume flow rate in arteries and veins may change as a result of the presence of pathology and this can be used as a diagnostic tool and therefore, the accuracy of the system should be evaluated. Volume Flow Estimation accuracy has been successfully measured using a flow phantom [11, 18, 19, 20, 10, 21].

6.1.2 Colour and Power Doppler Performance Test Protocols

Despite the existence of recommended performance test protocols for colour and power Doppler imaging, very few test devices exist [22, 18, 23, 24, 25, 20, 26]. As a consequence, the implementation of colour and power Doppler performance testing has been limited. The colour Doppler performance tests include measurements of the following parameters: (i) lowest detectable velocity; (ii) highest detectable velocity; (iii) sensitivity; (iv) spatial resolution; (v) temporal resolution; (vi) velocity resolution; (vii) clutter filter performance; (viii) penetration depth; and (ix) tissue movement artefact suppression however, only a handful have been successfully evaluated.

(i) Lowest detectable velocity

Lowest detectable velocity is the lowest velocity which it is possible to display unambiguously on the colour image. Visualisation of low velocities is important in venous flow detection and in very tight stenoses to distinguish between vessel occlusion and vessel patency. Colour Doppler lowest detectable velocity has been measured using a string phantom; however, the usefulness of this measurement is limited in the absence of attenuation [19, 10].

(ii) Highest detectable velocity

Highest detectable velocity is the highest velocity which it is possible to display unambiguously on the colour image. Velocities in the presence of an arterial stenosis or a cardiac valvular narrowing can reach up to

5 – 6 ms^{-1} and it is desirable for the colour flow system to display these velocities without aliasing. Colour Doppler highest detectable velocity has been successfully measured using a flow phantom and a string phantom [11, 20, 10].

(iii) Sensitivity

Sensitivity is the minimum signal strength (from different diameter vessels and from different depths) for the lowest detectable velocity that can be detected unambiguously. The distinction between slow flow and no flow is of great clinical importance. Sensitivity is closely linked with the parameter lowest detectable velocity. Attempts have been made to evaluate colour Doppler sensitivity by Wang et al [26] using a vibrating disk, which allowed them to precisely control the frequency output and the signal amplitude. However, due to the bi-directional symmetrical side bands, ambiguity was produced for colour Doppler systems and, consequently, reliable measurements of colour / power Doppler sensitivity could not be made using this test object. An alternative method has been described by Browne et al, this involves the use of a flow phantom with small vessels (inner diameter 1.6 mm, 3.2 mm and 4.8 mm) at varying depth within the flow phantom. The pump system was capable of producing low velocities (1 cms^{-1}) and from this information a sensitivity performance index was determined [27].

(iv) Spatial resolution

This is the minimum separation in space for which two separate point or line targets can be resolved or the point spread function of a point source. Visualisation of small areas of flow is required, for example for small vessels, or for regions near to minor degrees of atheroma. Colour Doppler lateral spatial resolution has been measured in separate experiments using an acoustic grid in one instance and a modified string phantom with two strings with adjustable separation in another [23, 24]. The acoustic grid approach provided a measure of lateral spatial resolution with separation sizes between 0.5 mm and 10 mm [24]; however, the arrangement of the acoustic grids may have caused diffraction of the ultrasound beam, which may have affected the spatial resolution measurements. The approach using the modified string phantom also

provided a measure of spatial resolution with separation sizes between 0.5 mm and 10 mm [23]. However, the measurements were carried out using O-ring rubber, which has a significantly higher backscatter value than blood, and to further compound this problem the measurements were carried out in water. Therefore, the resulting colour Doppler signal was significantly stronger than typical blood signals. Furthermore, string phantoms are not particularly suitable for measuring colour Doppler spatial resolution because, instead of producing a volume of flow, they produce a narrow line of flow. Two alternative methods of measuring spatial resolution are described by Browne et al: the first involves the use of a flow phantom with two vessels of varying separation, while the second involves the use of a flow phantom with a series of line pair vessels of different separations [28].

(v) Temporal resolution

This is the minimum separation in time for which two separate events can be identified. Flow events may change very rapidly, particularly for flow in the heart, and a high frame rate is needed to follow these changes. To date, no test device has been developed to evaluate temporal resolution however; Browne [29] describes a protocol for determining colour Doppler temporal resolution using a string phantom. A square wave is produced by the string phantom and imaged using colour Doppler. A cine loop is captured and analysed off-line to produce a plot of velocity as a function of time from which the temporal resolution of the colour Doppler system can be determined.

(vi) Velocity resolution

This is the minimum discernible velocity difference of a colour flow image. Quantitative and semi-quantitative analysis of flow in vessels is being used more frequently in the clinical setting, therefore, which necessitates a high accuracy of velocity estimation. Colour Doppler velocity resolution has been successfully measured using a rotating rubber disk phantom [30].

(vii) Clutter filter performance

This is the ability of the clutter filter to remove strong signals from the vessel wall movement, while still preserving the low velocity content of the colour flow signal. Colour flow signals associated with wall movement effect the velocity content of the colour flow signal and are generally considered to be undesirable. Colour Doppler clutter filter performance has been successfully measured using a modified belt phantom (clutter phantom) [25].

(viii) Penetration depth

This is the maximum depth of a vessel in tissue from which a Doppler signal free of extraneous noise can be obtained. In clinical practice it is often desirable to obtain signals from major vessels within the body, and also from small vessels for assessment of perfusion. For both large and small vessels, it is desirable to obtain noise-free Doppler signals from all sizes of patients. Colour Doppler penetration depth has been successfully measured using a flow phantom [11, 10].

(ix) Tissue movement artefact suppression

This is the degree of colouring in the tissue region compared to that in a vessel. Colour flow signals may arise from tissue motion as well as from moving blood. Colour flow signals associated with tissue motion are generally considered to be undesirable and the ability of the machine to suppress tissue motion signals is a very important feature. Colour Doppler tissue movement artefact suppression performance has been successfully measured using a modified flow phantom [29] which contains two vessels of equal dimensions through which blood mimicking fluid and tissue mimicking fluid are separately pumped.

(x) Velocity Accuracy

This is the accuracy of the colour Doppler estimate of the mean scatterer velocity. Quantitative and semi-quantitative analysis of flow in vessels is being used more frequently in the clinical setting, therefore, this requires high accuracy of velocity estimation. Colour Doppler velocity accuracy is the most frequently evaluated performance parameter and has

been measured using either a belt phantom, a rotating rubber disk or a torus phantom, together with computer analysis programs which determined the mean velocity in each case [30, 19, 31]. Measurement of this parameter does not require tissue equivalence of the test object, although it is very important to have an accurate and precisely controlled velocity source. Thus all of the above mentioned test devices are suitable for measuring velocity accuracy.

6.2 Colour and Power Doppler Tissue Mimicking Phantoms and Test Objects

There are several types of test devices of varying complexity available for CW Doppler, PW Doppler, colour and power Doppler testing. The majority of these test devices have facilitated complete evaluation of CW and PW Doppler; they usually measure only mean velocity accuracy in the case of colour Doppler, although spatial resolution and clutter filter response have also been measured. The test devices can be divided into two main groups similar to B-mode test devices: tissue mimicking phantoms and test objects.

Flow phantoms are an example of tissue mimicking phantoms and consist of TMM surrounding a vessel through which blood-mimicking fluid (BMF) is pumped [32, 33, 34, 35, 36, 37]. The flow through the flow phantom can be steady or pulsatile [38]. The TMMs used in flow phantoms have similar requirements to the TMMs used in B-mode phantoms, speed of sound of 1540 m s^{-1} and attenuation coefficient of between 0.3 – 0.7 $dBcm^{-1}MHz^{-1}$. However, the vessels used in the flow phantoms are usually made of latex rubber, which is known to cause distortion of the ultrasound wave as it propagates through it [39]. To overcome this problem some researchers have used human vessels removed during either autopsy or endarterectomy, or alternatively used wall-less vessels [40, 41, 36, 42] or vessel mimicking materials such as polyvinyl alcohol cryogel [43, 44].

An alternative approach to using these simplistic design flow phantoms, which have only been used in research laboratories, is to use a phantom which is closely representative of that part of the body for which the ultrasound scanner is used to image routinely. There has been limited research in this area of phantom development apart from the production

of an carotid artery bifurcation phantom, which mimics the human carotid artery bifurcation with respect to both anatomy and flow perfusion [45, 46]. A particularly important aspect of this carotid bifurcation phantom is that it can be used to produce both normal and stenosised lumen geometry, and thus the effect of factors such as stenosised geometry and flow rate on the observed Doppler ultrasound spectra and haemodynamic patterns can be studied. Several types of blood mimicking fluid have been developed [11, 47]; however, the BMF which most closely matches real blood was developed as part of an European Commission project [48, 35, 49]. The Doppler test parameters which have been evaluated using a flow phantom are the following: maximum velocity accuracy; penetration depth; range gate registration; directional discrimination; spatial resolution; lowest detectable velocity; mean velocity accuracy; sensitivity; and flow rate [11, 50, 24, 51, 18, 27]. Flow phantoms are commercially available from Gammex-RMI (www.gammex.com), ATS Laboratories (www.atslabs.com), Shelly Medical Imaging Technologies (www.simutec.com) and Dansk Phantom Services (www.fantom.suite.dk) however, they have a number of limitations associated with them: usually only one vessel size is available; they have a limited velocity range; and some produce air bubbles as a result of cavitation in the pump head, even at low velocities.

Despite the major research interest in the development of flow phantoms, a number of non tissue mimicking Doppler test objects have been developed. The most common test device is the string phantom, which consists of a filament attached to a series of pulley wheels and a drive wheel contained within a water tank [19, 10, 20]. The drive wheel is driven by a motor, which can be controlled directly by an electronic controller or via a computer, to produce steady or pulsatile movement of the filament. The Doppler test parameters which have been evaluated using a string phantom are maximum velocity accuracy, intrinsic spectral broadening, range gate accuracy, directional discrimination and the lowest and highest detectable velocities [19, 20, 15, 21]. A modified version of the string phantom, which consisted of two filaments with adjustable spacing, has been used to evaluate the spatial resolution of colour Doppler [23]. Only one type of string phantom is commercially available from CIRS Tissue Simulations & Phantom Technology (www.cirsinc.com); however, this too has a number of limitations associated with them, including: the filament

passing out of the water and air bubbles are left on the filament; it has a limited depth range; and the motor can produces strong vibrations which effects the Doppler measurements.

Another type of Doppler test object is the belt phantom, which consists of a layer of reticulated foam stitched onto a rubber belt. It can provide a 2-D representation of flow and has been used to determine the mean velocity accuracy of colour Doppler [19]. A modified version of the belt phantom, consisting of an acoustic beam splitter which allowed simulated flow and simulated clutter to be interrogated by the transducer simultaneously, was used in a later study to evaluate colour clutter filters [25]. However, due to the complexity of the belt phantom, only one such research test object exists and consequently there has been a limited amount of research conducted using it. The rotating phantom is a variant of the belt phantom. It consists of a circular disk of reticulated foam which is rotated around a central axis [30]. This phantom is technically easier to build than the belt phantom and is available commercially; it has been used to measure velocity resolution and to validate velocity measurement techniques such as colour vector Doppler or Doppler tissue imaging [30].

The vibrating target is a commercially available test object and consists of a diffusely scattering circular plate, 15 cm in diameter, which can be set to vibrate at a set audio frequency and is used to determine colour Doppler sensitivity [26]. A rotating torus phantom was a research test object developed by Stewart to evaluate mean velocity accuracy of colour Doppler [52]. Phillips et al have described a laboratory - constructed oscillating thin film test object, consisting of a number of precisely deposited sub-resolvable scatters for making spatial resolution and sensitivity measurements in colour Doppler [53].

Another type of Doppler research test object is an electronic injection device, there is currently one such test device available, the Sonora Nickel™ (www.4sonora.com). This device has no moving parts, but instead synthesises the Doppler signal electronically and injects it into the Doppler system in the ultrasound scanner. There are two approaches used in electronic injection of the Doppler signal: direct injection, in which the signal is directly injected at some point in the signal processing chain, and acoustic injection, in which the acoustic signal is produced by a separate transducer which is then detected by the Doppler instrument under test [54, 55, 56, 57, 58]. Electronic injection test objects have been used to

measure colour Doppler directional accuracy, high-pass filter response and frequency response linearity.

As can be seen from above, the majority of test devices capable of evaluating the individual Doppler test parameters in particular the colour and power Doppler test parameters are not available commercially. Therefore, there is a need for test devices which will reliably and accurately determine the full range of colour and power Doppler test parameters. When choosing or designing a test device for colour and power Doppler performance testing, the degree of tissue equivalence of the test phantom is the most important factor to be considered, and a flow phantom is the most tissue equivalent test device available. However, it should also be considered that the flow phantom may not be capable of carrying out all of the desired tests, and therefore the suitability of other test objects should be considered for measuring the colour and power Doppler test parameters.

6.3 New Technology

As mentioned in the introduction, ultrasound technology continues to evolve at a rapid rate with the introduction of new and exciting Doppler ultrasound techniques being implemented into clinical practice. However, no independent evaluation of these techniques can be carried out as there are firstly no recommended test parameters nor test objects capable of testing this new technology. There is currently no consensus reached in the ultrasound community over the precise clinical application of the use of contrast agents, therefore it is difficult to define performance criteria for this new technology. Furthermore, all new technology need to have performance criteria established for them in other for it to be possible to define important test parameters for evaluating the performance of this new technology. This produces a particularly severe challenge to the design of test objects for these new technologies.

6.4 Conclusions

In conclusion, it is imperative that the current Doppler performance guidelines [10, 6, 7, 8, 9] are updated to take into account new Doppler technology such as Tissue Doppler and Contrast Agents as well as the need for further research to be carried out in the area of Doppler test object

development. The current Doppler technical standards and test procedures are sufficient for CW and PW Doppler testing, as well as Colour and Power Doppler testing with regard to Doppler shift accuracy and detection limitation performance testing.

6.5 References

[1] ALLAN, P.L.; DUBBINS, P.A.; POZNIAK, M.A. and MCDICKEN, W.N. *Clinical Doppler Ultrasound*. 2000, pp. 123-190.

[2] WELLS, P.N.T. Ultrasound Imaging. *Physics in Medicine and Biology*. 2006, 51(13), pp. R83-R98.

[3] WHITTINGHAM, T.A. New developments in ultrasound. *Reflections*. 2000, 5, pp. 9-13.

[4] Common Services Agency. *Comparative evaluation of imaging and Doppler ultrasound systems for examination of the heart.* EEV/91/3. 1991, pp. 1-38.

[5] BROWNE, J.E.; WATSON, A.J.; MUIR, C.; HOSKINS, P.R. and ELLIOTT, A.T. An Investigation of the Relationship Between In-Vitro and In-Vivo Ultrasound Image Quality Parameters. *Ultrasound*. 2004a, 12 (4), pp. 202-210.

[6] AIUM. *Performance criteria and measurements for Doppler ultrasound devices.* American Institute of Ultrasound in Medicine Standards Committee. 1993.

[7] IEC 1206. *Ultrasonics - Continuous-wave Doppler systems - Test Procedures.* Geneva, Switzerland : International Electrotechnical Commission, 1993.

[8] IEC 61895. *Ultrasonics – Pulsed Doppler diagnostic systems: Test Procedures to determine performance.* Geneva, Switzerland : International Electrotechnical Commission, 2001.

[9] IEC 61685. *Ultrasonics – Flow measurement systems: Flow test Object.* Geneva, Switzerland : International Electrotechnical Commission, 2001.

[10] HOSKINS, P.R.; SHERRIFF, S.B.; EVANS, J.A. (eds.). *IPEM. Report no 70 : Testing of Doppler ultrasound equipment.* York : IPEM, 1994.

[11] BOOTE, E.J. and ZAGZEBSKI, J. Performance tests of Doppler ultrasound equipment with a tissue and blood mimicking phantom. *Journal of Ultrasound in Medicine.* 1988, 7, pp. 137-147.

[12] DAIGLE, R.J.; STAVROS, A.T.; LEE, R.M. Overestimation of velocity and frequency values by multi-element linear array Dopplers. *J Vasc Technol*. 1990, 14, pp. 206-213.

[13] KIMME-SMITH, C.; HUSSAIN, R.; DUERINCKX, A.; TESSLER, F.; GRANT, E. Assurance of consistent peak-velocity measurements with a variety of duplex Doppler instruments. *Radiology*. 1990, 177, pp. 265-272.

[14] HOSKINS, P.R.; LI, S.L.; MCDICKEN, W.N. Velocity estimation using duplex scanners. *Ultrasound in Medicine and Biology*. 1991, 17, pp. 195-199.

[15] EICKE, B.M.; KREMKAU, F.W.; HINSON, H.; TEGELER C.H. Peak Velocity overestimation and liner-array spectral Doppler. *J Neuroimag*. 1995, 5, pp. 115-121.

[16] HOSKINS, P.R. Accuracy of maximum velocity estimates made using Doppler ultrasound systems. *Br J Radiol.* 1996, 69, pp. 172-177.

[17] STEINMANN, A.H.; TAVAKKOLI, J.; MYERS, J.G.; COBBOLD, R.S.C.; JOHNSTON, K.W. Sources of error in maximum velocity estimation using linear phased-array Doppler systems with steady flow. *Ultrasound Medicine and Biology*. 2001, 27, pp. 655-664.

[18] GOLDSTEIN, A. Performance Tests of Doppler Ultrasound Equipment with A String Phantom. *Journal of Ultrasound in Medicine*. 1991, 10, pp. 125-139.

[19] RICKEY, D.W.; RANKIN, R. and FENSTER, A. A Velocity Evaluation Phantom for Color and Pulsed Doppler Instruments. *Ultrasound in Medicine and Biology.* 1992, 18, pp. 479-494.

[20] RUSSELL, S.V.; MCHUGH, D. and MOREMAN, B.R. A Programmable Doppler String Test Object. *Physics in Medicine and Biology*. 1993, 38, pp. 1623-1630.

[21] WALKER, A.; OLSSON, E.; WRANNE, B.; RINGQVIST, I.; ASK, P. Accuracy of spectral Doppler flow and tissue velocity measurements in ultrasound systems. *Ultrasound in Medicine and Biology*. 2004, 30, pp. 127-132.

[22] DEANE, C.R.; FORSBERG, F.; THOMAS, N. and ROBERTS, V.C. Accuracy of Color Doppler Ultrasound Velocity-Measurements in Small Vessels. *Journal of Biomedical Engineering*. 1991, 13, pp. 249-254.

[23] LANGE, G.J. and LOUPAS, T. Spectral and color Doppler sonographic applications of a new test object with adjustable moving target spacing. *Journal of Ultrasound in Medicine*. 1996, 15, pp. 775-784.

[24] LI, S.; HOSKINS, P.R. and MCDICKEN, W.N. Rapid measurement of the spatial resolution of colour flow scanners. *Ultrasound in Medicine and Biology*. 1997, 23, pp. 591-596.

[25] RICKEY, D.W. and FENSTER, A. A Doppler ultrasound clutter phantom. *Ultrasound in Medicine and Biology*. 1996, 22, pp. 747-766.

[26] WANG, K.Y.; BONE, S.N. and HOSSACK, J.M. A tool for evaluating Doppler sensitivity. *The Journal of Vascular Technology*. 1992, 16, pp. 87-94.

[27] BROWNE, J.E.; WATSON, A.J.; HOSKINS, P.R. and ELLIOTT, A.T. Validation of a sensitivity performance index test protocol and evaluation of colour Doppler sensitivity for a range of ultrasound scanners. *Ultrasound in Medicine and Biology*. 2004, 30, pp. 1475-1483.

[28] BROWNE, J.E.; BROWN, I.; HOSKINS, P.R.; WATSON, A.J. and ELLIOTT, A.T. Colour Doppler Spatial Resolution Performance Testing. *Ultrasound*. 2007, 15 (3), pp. 162-166.

[29] BROWNE, J.E. *Diagnostic Ultrasound Real-time and Colour Doppler Imaging Assessed by In-Vivo and In-Vitro Methods*. 2002. PhD Thesis. University of Glasgow.

[30] FLEMING, A.D.; MCDICKEN, W.N.; SUTHERLAND, G.R. and HOSKINS, P.R. Assessment of Color Doppler Tissue Imaging Using Test-Phantoms. *Ultrasound in Medicine and Biology*. 1994, 20, pp. 937-951.

[31] STEWART, S.F.C. Effects of transducer, velocity, Doppler angle, and instrument settings on the accuracy of color Doppler ultrasound. *Ultrasound in Medicine and Biology*. 2001, 27, pp. 551-564.

[32] HOSKINS, P.R.; ANDERSON, T. and MCDICKEN, W.N. A Computer-Controlled Flow Phantom for Generation of Physiological Doppler Waveforms. *Physics in Medicine and Biology*. 1989, 34, pp. 1709-1717.

[33] LAW, Y.F.; JOHNSTON, K.W.; ROUTH, H.F. and COBBOLD, R.S.C. On the design and evaluation of a steady flow model for Doppler ultrasound studies. *Ultrasound in Medicine and Biology*. 1989, 15, pp. 505-516.

[34] PETERSEN, J.N. Digitally Controlled System for Reproducing Blood-Flow Waveforms Invitro. *Medical & Biological Engineering & Computing*. 1984, 22, pp. 277-280.

[35] RAMNARINE, K.V.; NASSIRI, D.K.; HOSKINS, P.R. and LUBBERS, J. Validation of a new blood-mimicking fluid for use in Doppler flow test objects. *Ultrasound in Medicine and Biology*. 1998, 24, pp. 451-459.

[36] RAMNARINE, K.V.; ANDERSON, T. and HOSKINS, P.R. Construction and geometric stability of physiological flow rate wall-less stenosis phantoms. *Ultrasound in Medicine and Biology*. 2001, 27, pp. 245-250.

[37] HOSKINS, P.R. Simulation and validation of arterial ultrasound imaging and blood flow. *Ultrasound in Medicine and Biology*. 2008, 34(5), pp. 693-717.

[38] SHORTLAND, A.P. and COCHRANE, T. Doppler Spectral Waveform Generation Invitro - An Aid to Diagnosis of Vascular-Disease. *Ultrasound in Medicine and Biology*. 1989, 15, pp. 737-748.

[39] THOMPSON, R.S.; TORTOLI, P. and ALDIS, G.K. Selective transmission of a focused Doppler ultrasound beam through a plastic layer. *Ultrasound in Medicine and Biology.* 2000, 26, pp. 1333-1346.

[40] DABROWSKI, W.; DUNMORE-BUYZE, J.; RANKIN, R.N.; HOLDSWORTH, D.W. and FENSTER, A. A real vessel phantom for imaging experimentation. *Medical Physics*. 1997, 24, pp. 687-693.

[41] DABROWSKI, W.; DUNMORE-BUYZE, J.; CARDINAL, H.N. and FENSTER, A. A real vessel phantom for flow imaging: 3-D Doppler ultrasound of steady flow. *Ultrasound in Medicine and Biology*. 2001, 27, pp. 135-141.

[42] RICKEY, D.W.; PICOT, P.A.; CHRISTOPHER, D.A. and FENSTER, A. A Wall-Less Vessel Phantom for Doppler Ultrasound Studies. *Ultrasound in Medicine and Biology.* 1995, 21, pp. 1163-1176.

[43] SURRY, K.J.M.; AUSTIN, H.J.B.; FENSTER, A.; PETERS, T.M. Poly (vinyl alcohol) cryogel phantoms for use in ultrasound and MR imaging. *Physics in Medicine and Biology*. 2004, 49, pp. 5529-5546.

[44] DINELEY, J.; MEAGHER, S.; POEPPING, T.L.; MCDICKEN, W.N.; HOSKINS, P.R. Design and characterisation of a wall motion phantom. *Ultrasound in Medicine and Biology*. 2006, 32, pp. 1349 – 1357.

[45] POEPPING, T.L.; NIKOLOV, H.N.; RANKIN, R.N.; LEE, M. and HOLDSWORTH, D.W. An in vitro system for Doppler ultrasound flow studies in the stenosed carotid artery bifurcation. *Ultrasound in Medicine and Biology*. 2002, 28, pp. 495-506.

[46] POEPPING, T.L.; NIKOLOV, H.N.; THORNE, M.L. and HOLDSWORTH, D.W. A thin-walled carotid vessel phantom for Doppler ultrasound flow systems. *Ultrasound in Medicine and Biology*. 2004, 30, pp. 1067-1078.

[47] HOSKINS, P.R.; LOUPAS, T. and MCDICKEN, W.N. A Comparison of the Doppler Spectra from Human Blood and Artificial Blood Used in a Flow Phantom. *Ultrasound in Medicine and Biology*. 1990, 16, pp. 141-147.

[48] LUBBERS, J. Application of a new blood-mimicking fliud in a flow Doppler test object. *European Journal of Ultrasound*. 1999, 9, pp. 267-276.

[49] RAMNARINE, K.V.; HOSKINS, P.R.; ROUTH, H.F. and DAVIDSON, F. Doppler backscatter properties of a blood-mimicking fluid for Doppler performance assessment. *Ultrasound in Medicine and Biology*. 1999, 25, pp. 105-110.

[50] DI NALLO; STRIGARI, L. and BENASSI, M. A Possible Quality Control Protocol for Doppler Ultrasound for Organizational Time Optimisation. *J. Exp. Clin. Cancer Res*. 2006, 25(3), pp. 373 – 381.

[51] TEIRLINCK, C.J.P.M.; BEZEMER, R.A.; KOLLMANN, C.; LUBBERS, J.; HOSKINS, P.R.; FISH, P.; FREDFELDT, K.E. and SCHAARSCHMIDT, U.G. Development of an example flow test object and comparison of five of these test objects, constructed in various laboratories. *Ultrasonics*. 1998, 36, pp. 653-660.

[52] STEWART, S.F.C. A rotating torus phantom for assessing color Doppler accuracy. *Ultrasound in Medicine and Biology*. 1999, 25, pp. 1251-1264.

[53] PHILLIPS, D.; MCALEAVEY, S. and PARKER, K. Colour Doppler Spatial Resolution Measurements with an Oscillating Thin Film Test Object. *IEEE Ultrasonics Symposium*. 1997, pp. 1517-1520.

[54] BASTOS, C.A.C. and FISH, P.J. A Doppler Signal Simulator. *Clinical Physics and Physiological Measurement*. 1991, 12, pp. 177-183.

[55] EVANS, J.A.; PRICE, R. and LUHANA, F. A Novel Testing Device for Doppler Ultrasound Equipment. *Physics in Medicine and Biology*. 1989, 34, pp. 1701-1707.

[56] LUNT, M.J. and ANDERSON, R. Measurement of Doppler Gate Length Using Signal Reinjection. *Physics in Medicine and Biology*. 1993, 38, pp. 1631-1636.

[57] POTTER, D.J. Wave-Form Index Evaluation Using An Electronic Injection Phantom. *IEEE Engineering in Medicine and Biology Magazine*. 1995, 14, pp. 91.

[58] WALLACE, J.J.A.; MARTIN, K. AND WHITTINGHAM, T.A. An Experimental Single-Side-Band Acoustical Reinjection Test Method for Doppler Systems. *Physiological Measurement*. 1993, 14, pp. 479-484.

7 Ecological competence of yeast suspensions in acoustic filters

Stefan Radel, Cosima Koch

The first description of the concentration of particles suspended in a fluid in certain regions of an acoustic standing wave dates back more than a century. Kundt and Lehmann reported the phenomenon already in 1874 when using it for the visualisation of an ultrasonic field [1]. The effect obviously arises from forces acting on the particles when a dispersion is irradiated within a resonator by an ultrasonic wave. A somewhat detailed explanation of these so-called radiation forces will be given in chapter 7.1, in short words particles in a fluid are concentrated in the pressure regions[1] of the standing wave [2].

This technique of ultrasonic particle manipulation has been used to design retention systems able to immobilise particles for instance against a streaming liquid, hence called acoustic filters. One application of utmost interest is the flow filtration of bio-suspensions [3], which is by now established from an industrial point of view as well [4]. Other important exploitations are the reliable sample concentration systems for (medical) sensor applications [5].

Potential filtration applications employing this separation principle to biological material have been identified for animal cells [6, 7], hybridoma [8, 9], plant cells [10], red blood cells [11] and even DNA [12]. Beside the micro-organisms the process of building up of the aggregates [13, 14] and their inner structure [15] have been investigated. The assessment of the inner structure was made possible by a novel protocol of “freezing” the spatial distribution allowing for the use of light and scanning electron microscopy [16].

Recent exploitations include micro-fluidic and lab-on-the-chip applications like specific concentration [17], sorting by size [18] and cell washing [19]. Reports throughout the time showed the exertion of acoustic

[1] In literature sometimes “loop” or “displacement/velocity anti-node” are found to denote the region of vanishing acoustic pressure in a standing wave.

radiation forces on various cell lines to be gentle and not decreasing viability as long as the cells are kept in the pressure nodes of a standing wave. This has been holding true for the mentioned micro-fluidic systems [20].

The work presented here shall be a report of results with biological cells in acoustic filters employing the principles of ultrasonic particle manipulation. We will present data about the viability of cell cultures and the integrity of the cells after exposure to well-controlled ultrasonic fields in such devices. Furthermore we will deliver results about certain changes of the cells' internal morphology when kept in certain regions of an ultrasonic standing wave field and of damages to them on leaving these protecting whereabouts. Our report will as well briefly include data of the separation efficiency, i.e. the fraction of particles removed.

We have used two different acoustic filters, i.e. two set-ups employing the principles of ultrasonic particle manipulation for removing particles from a suspension [21]. One is the Ultrasonically Enhanced Settler (see chapter 7.1.3) based on the accelerated sedimentation brought about by the increased diameter of ultrasound induced aggregates. The other one is the so-called h-shape separator (see chapter 7.1.4) which utilises the radiation forces exerted on particles very much like rails to guide them to one of two outlets. Subsequently an enriched suspension can be retrieved from one outlet and the cleared fluid from the other.

Both devices are continuous throughput filters. The former one is already successfully applied in industrial environments, especially in biotech [22]. The latter excels itself by its independence of gravity, thus being a candidate for the sophisticated handling of suspensions in micro-gravity environments.

We used yeast as the live biological model like others before in the regime of ultrasonic particle manipulation [23, 24] and different (hydro)dynamical environments [25, 26]. This micro-organism with a diameter in the range of 4-10 µm is of advantage for such studies for a couple of reasons. Firstly, it is of spherical shape and therefore close to the ideal spheres used in the mathematical theory of ultrasonic particle manipulation. Yeasts are eukaryotes, hence results can deliver some insight in the reaction of a number of cell types to similar stresses. Moreover yeasts are important in many fields of biotechnological environments themselves, e.g. for the production of enzymes and proteins

in the pharmaceutical industry. Finally yeast is easy to cultivate and save to handle. The particulate strain used in the experiments presented here was *Saccharomyces cerevisiae*, brewer's yeast.

7.1 Ultrasonic particle manipulation

7.1.1 Ultrasonic resonator

Most of the applications employing the principle of particle concentration in the nodal regions of a standing wave use a set-up where the cavity of an acoustic resonator contains a suspension. When the volume is irradiated with ultrasound the initially homogeneously distributed particles are driven into the nodal regions of the standing wave field. The formation of a standing wave in a resonator is shown in Figure 1. A wave is emitted by a sound source, the transducer, in the direction towards a reflector (a). The incoming and reflected waves are both progressing but their superposition is stationary (b), i.e. does not change its location over time and therefore is called a *standing* wave. The amplitude distribution or the *envelope* describes the maximum of displacement or pressure for a given location (c). Under certain boundary conditions - very simplified when an integer number of half-wavelengths fits between the two terminating surfaces transducer and reflector - resonance is observed, meaning the amplitude of the sound field becomes large (d). If the transducer emits a plane wave, i.e. the locations of equal phase are on a plane in space, the pressure nodes of the resulting standing wave will be planes as well.

7.1.2 Radiation forces

The source of the mentioned radiation forces is the spatial gradient of the sound waves' acoustic pressure. Hence the relation between the sound wavelength and the particle diameter is of great importance, the phenomenon is size-dependent. The direction and strength of the forces is influenced by the compressibility – which itself is a function of the material properties speed of sound and mass density - of both components of the dispersion. The coefficient representing this dependency is called acoustic contrast. Solid particles in water travel into the pressure nodes whilst gas bubbles or oil droplets are concentrated in the displacement nodes.

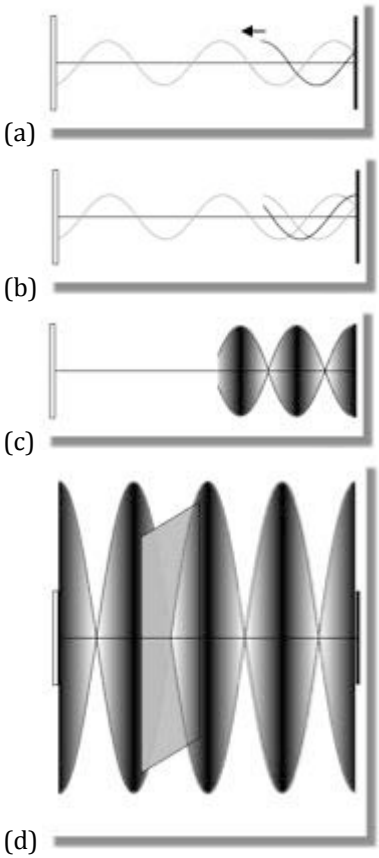

Figure 1 A standing (radiation pressure) wave composed as the superposition of a progressive wave and its reflection (a), the superposition is stationary (b). The amplitude distribution is called envelope (c). When resonance (d) occurs i.e. when a frequency is used at which a whole number of wavelengths 'fit' into the given space between transducer and reflector high amplitudes are the result of constrictive interference.

The principle has been shown to work with all combinations of liquid or gaseous carrier fluids and solid, liquid and gaseous "particles" [27, 28] – for

obvious reasons with the exception of gas-gas systems. Thereby *suspensions* are dispersions of solid particles in liquids, while a liquid-liquid system is called *emulsion*, an important example is oil in water. The nomenclature for gaseous carriers is *smoke* if solid particles are dispersed and *fog* or *mist* when liquid droplets are present in the gas (air). Of the greatest practical importance are *hydrosols*, i.e. dispersions based on water, and *aerosols* with air as the carrier medium.

The explanation for the observed effects was 1934 delivered by King [29]. He integrated the radiation pressure exerted by a plane standing acoustic wave over the surface of a rigid sphere in an ideal, i.e. non-viscous fluid. This derivation taking second order effects from the scattered sound field into consideration led to a nonvanishing time-averaged force displacing the particle. This effect is called the *axial primary radiation force* to express that it is originating from direct (primary) interactions of the particle and the initial sound field in direction of sound propagation (axial).

Please see Figure 2 for an overview of this and the forces mentioned in the following. The *transverse primary radiation force* emerges from uneven distributions of the amplitude over the surface of a transducer[2], i.e. the sound source. These deviations arise from the boundaries of real resonators and lead to a force exerted perpendicular (transverse) to the direction of sound propagation.

The so-called *secondary radiation forces* are brought about by additional (secondary) sound sources, e.g. an excited particle. They therefore surface as particle-particle interactions. In other words, they describe the effect on one particle in the sound field emitted or scattered by another particle and vice versa. Because of their early investigations in 1871 and 1909, respectively, these forces are sometimes also called after König [30] or Bjerknes [31].

For a situation where both the distance between two soft particles, e.g. biological cells and their radii are small in comparison to the wavelength, like in the pressure node of a standing wave, a repulsing force between them can be calculated [32].

[2] It has to be emphasized that nevertheless one deals with a plane wave, i.e. the phase of the wave is unaffected and therefore the surface of equal phase is flat!

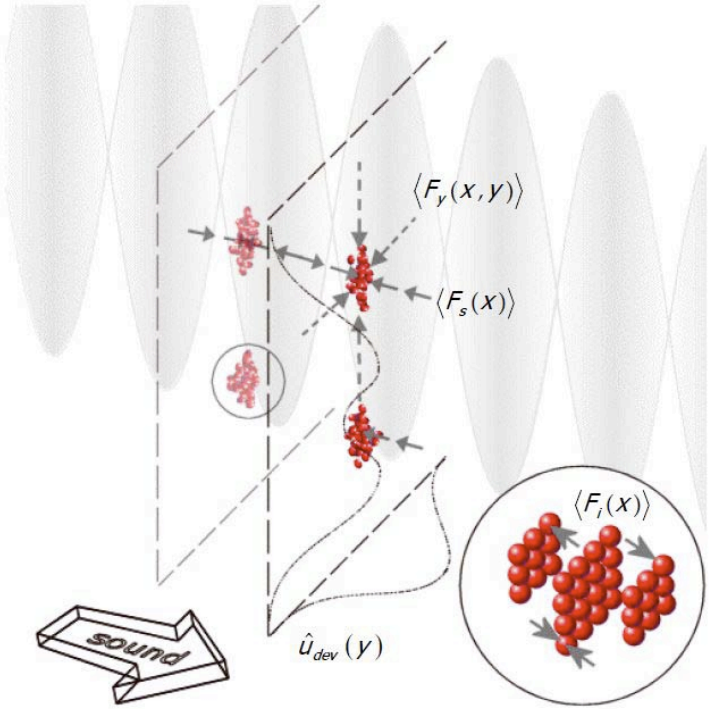

Figure 2 Acoustic radiation forces exerted on a particle in a separation system.

7.1.3 Ultrasonically Enhanced Settling

One utilisation of particle manipulation by ultrasonic radiation which has been developed during the last decade up to successful application in industrial environments is the Ultrasonically Enhanced Settling (UES) [22, 33, 34]. The principle here is it to locally increase the particle concentration by a standing ultrasonic field, which results in loose aggregates stabilised by the ultrasound within certain regions. Due to the increased diameter of this “super-particle” the ratio of surface friction and gravitational force decreases leading to an increase of the terminal sedimentation velocity.

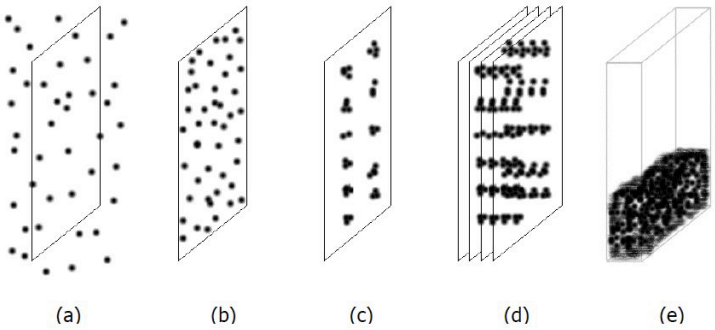

Figure 3 Stages of Ultrasonically Enhanced Settling; homogeneously dispersed particles (a) get accumulated in planes (b) and further concentrated within the planes (c) by the ultrasound, columns are formed in multi-wavelength resonators (d). The aggregates finally settle at the bottom of the vessel (e).

This subsequently delivers an increase of sediment per time. Thus the build up of aggregates by *ultrasound enhances* the *settling*.

Figure 3 shows the stages of the UES process: in the beginning the particles are freely distributed in the liquid (a). After the ultrasonic field has built up the axial primary radiation force drives them into nodal planes (b), which appear periodically in the direction of sound propagation. Typically it does not take more than a couple of seconds until such a spatial distribution is reached.

It depends on the mentioned acoustic contrast between particle and liquid if this force points towards the pressure nodes or towards the displacement nodes for a given suspension, cells however are driven into the pressure nodes.

The transverse primary radiation force further concentrates the particles within these planes (c). This force perpendicular to the sound propagation direction is a result of the mentioned uneven amplitude distribution over the transducer's surface. The transverse primary radiation force is weaker, as it takes some tens of seconds until the concentration within the planes is finished.

In case of multi-wavelength resonators, as used throughout this work, columns of aggregated particles in the direction of the sound propagation

are forming (d). This arrangement is as well referred to as “banding”. Finally these aggregates settle at the bottom of the vessel (e) due to their increased “effective” density in consequence to the decrease of the surface-to-volume ratio.

Figure 4 shows the pilot series UES system (USSD-05, Anton Paar GmbH, Austria) used for the experiments in this work in a batch set-up (left-hand side) and in flow-through mode (right-hand side) on the top of a reservoir holding the suspension, e.g. a bio-reactor. In both cases the ultrasound is emitted by the transducer (Trd) at the left in horizontal direction to the reflector (Ref). Between the transducer and the reflector a cooling volume (C) and the active volume (AV) filled with the suspension are located. The cooling water circulation avoids the transducer to heat the suspension in the active volume.

In case of the flow-through set-up (Figure 4, right-hand side) as used as filters for perfusion reactors the clarified liquid is harvested at the top (out). The suspension is pumped into the system from the side at the

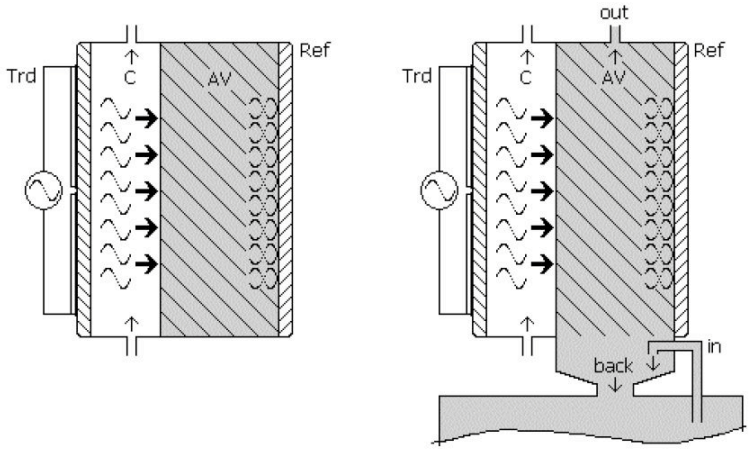

Figure 4 UES Separation system in batch mode (left) and in flow-through set-up (right) on top of a reservoir, e.g. a bio-reactor. The ultrasound is emitted from the transducer (Trd), passing a cooling volume (C) and the active volume (AV) holding the suspension and finally reflected at a reflector (Ref).

bottom (in) and together with the bottom outlet (back) this builds up a re-circulation loop by which the settled particles are immediately fed back into the reservoir. For obvious reasons the sound propagation direction in UES systems is oriented horizontally as the consequently vertical nodal planes allow an upward streaming of the clarified liquid between the settling aggregates.

The ultrasonic separation technology nowadays is at a stage where applications of practical importance become visible. The main advantages of cell filters based on this technique are the complete absence of moving parts and therefore no filter cakes or filter fouling. The systems can be hot-steam sterilised in-situ, the used materials such as stainless steel and glass are bio-compatible. The scale-up of the technology has progressed, perfusion filtering systems capable of 300 L/d and more are in the market, e.g. 250 L BioSep by AppliSens (Schiedam, The Netherlands).

In a recent paper [35] we have conducted experiments regarding the separation efficiency, i.e. the ability of the filter to remove particles/cells. The study employing an UES system like here was designed to investigate the influence of process parameters like flow through rate, cell concentration and true electric power input on the separation efficiency for the case of yeast/saline suspensions. It was found that up to 99.6 yeast cells can be retained by the acoustic filter. Conditions of not too low cell concentration (5-50 g/L) and not too high throughput (5-20 L/d, in certain cases 46 L/d) were found to be the favourable operation conditions.

7.1.4 The h-shape separator

The h-shape separator uses only the ultrasonic radiation forces and the viscous drag for the separation of particles and the medium they are suspended in. Gravitational forces are not needed for this set-up to work as a filter. Although understandable from a theoretical point of view this has been shown experimentally in a micro-gravity environment during series of parabolic flights as well [36].

In Figure 5 the principle is shown: The filter has an inlet (I) into which the cell suspension is fed and two outlets (O2 or retentate and O1 or filtrate, respectively). In the separation chamber a PZT (lead zirconium titanate) transducer (A) glued (B) to a glass carrier (C) emits an ultrasonic plane wave that is reflected at the opposite glass wall (E) of the chamber.

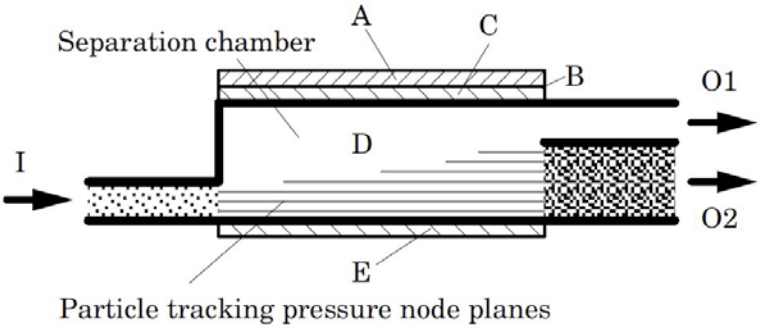

Figure 5 Scheme of the h-shape separator. On the left side the suspension is fed into inlet I of the separator, on the right side the upper outlet O1 is for the separated clean liquid and the lower outlet O2 for the particle enriched suspension.

When a standing wave field is built up in the chamber the cells in suspension entering the chamber are driven into the pressure nodal planes by the primary acoustic radiation force. These planes act as "rails" that guide the cells into the outlet O2. Ideally only clarified liquid exits by outlet O1.

For reasons of efficiency, the volume is split equally between the two outlets resulting in the flow velocity through O1 being about twice that through O2 (the cross-section of O2 is about two times that of O1).

7.2 Methods

7.2.1 Suspensions

When the cells of the strain *Saccharomyces cerevisiae* where cultured, one colony was retrieved from a plate with a loop and seeded in malt extract broth (0.4 g in 40 mL H_2O). This inoculate was left overnight in a 30°C incubator provided with an orbital shaker table (150 rpm). Subsequently, this culture was added to fresh malt extract broth (Fluka, 2 g in 100 mL H_2O) and let grow for approximately 48 hours in the incubator.

The culture was centrifuged at 3800 rpm in a Sorvall centrifuge for 10 minutes and the precipitate was re-suspended in 100 mL saline (0.9 g NaCl in H_2O) or tap water at a concentration between 5E6 and 2E7 cells/mL. Sample preparation was carried out in a sterile environment. Each experiment was conducted with an individually grown population for treated samples and controls.

For separation efficiency assessments in the h-shape separator the cells were bought as wet yeast from the supermarket (Mautner&Markhof, Wien, and Harmer Hefe, Wiener Neustadt). They were either suspended in phosphate buffered saline (PBS; 0.9% NaCl), tap water or two-fold concentrated PBS (PBS 2x, 1.8% NaCl) straight from the package. The final cell concentration was chosen to be around 5E6 cells/mL for the suspension to match the volume/volume ratio used in previous experiments leading to high separation efficiencies [36] and to stay below the upper thresholds suggested by computational fluid dynamic results [37].

7.2.2 Assessment

The performance of filters is measured as

$$\text{Separation efficiency} = (1-C_f/C_i)\cdot 100\%$$

where C_i denotes the initial concentration of the suspension and C_f is the concentration measured in the filtrate. Concentration refers to the number of particles (or cells) per mL. A separation efficiency of 100% corresponds to a perfect filter, whereas an efficiency of 0% means that no filtration at all was taking place - the particles were divided equally between the filtrate and retentate outlet, respectively.

Yeast cell concentration was obtained by haemocytometer counts. The haemocytometer was filled with an aliquot of the sample and placed under a light microscope. Cells within ten squares were counted, the average of two counts times 25,000 gives the concentration, i.e. cells per mL.

Viability was assessed using the methylene blue method (m.b.). Methylene blue is mixed 1 in 2 with a sample of the suspension in question. Under the microscope non-viable cells appear dyed dark blue while viable cells remain un-coloured. The viability is defined as the ratio of blue over non-blue cells, again counted with the haemocytometer.

The cells' integrity/leakage was assessed by measuring the protein content of the supernatant. As protein absorbs ultraviolet light the optical density at 280 nm light wavelength was measured (UV OD). A higher absorbance corresponds to a higher protein content of the sample.

For the growth stimulus experiments in the h-shape separator (chapter 7.3.3) samples of about 15 ml were taken in test tubes (control, sham, retentate and filtrate, respectively) to allow growth after sonication of yeast suspended in malt extract broth. The cell concentration in these samples was assessed one hour and about 18 hours after sonication. The samples were left in a laminar flow at room temperature between the haemocytometer counts.

All experiments were carried out in triplets.

7.2.3 Microscopy

Light microscopy was performed using a standard lab microscope. Horizontal sections of agar gel blocks with thicknesses of 8 to 10 µm were cut at room temperature from a blocks retrieved after sonication from the UES. The sections were mounted on common microscopy slides and photographed.

Scanning electron microscopy was performed according to the principles of biologic applications, as described elsewhere [38]. A block of gel, cut in the desired orientation and of suitable dimensions, was fixed to a specimen holder and snap-frozen in liquid nitrogen slush (-190°C). The specimen was fractured (electron microscope cryopreparation system CT 1500, Oxford Instruments, Oxford, UK), sputter coated with gold (2 mA for 2 min) and examined at an acceleration voltage of 1.6 kV (Jeol 5410).

Transmission electron microscopy (TEM) was performed following standard protocols for preparation of yeast cells. Samples were centrifuged at 3500 rpm for 10 minutes and re-suspended overnight in 2% Glutaraldehyde (Sigma) in 0.1 M phosphate buffer pH 7.4. The suspension was centrifuged again to yield a pellet. The pellet was then treated with a solution of 2% osmium tetroxide (OsO_4) for 1 hour. The samples were washed in phosphate buffer and de-hydrated twice with 70% EtOH for 15 minutes each time, then twice with 90% EtOH for 15 minutes each time and finally three times in absolute EtOH for 20 minutes each time. Propylene oxide was then added twice for 10 minutes each time and subsequently replaced by a 50% solution of propylene oxide and epon for

1 hour at 30°C. The samples were embedded overnight in epon at 60°C. Ultra-thin sections were stained in 6% uranyl acetate for 20 minutes, and 0.4% lead citrate for 10 minutes and then observed using a transmission electron microscope (Jeol 2000) at 80 kV acceleration voltage.

Images for all micrographs were recorded on Kodak film and developed and printed with standard photographic methods.

7.2.4 Handling

For the investigations regarding viability and integrity in the UES the batch set-up (Figure 4, left hand side) and a similar chamber were filled, but a sound field was applied only in the separation system. The sound field was excited by an ultrasonic control system (USCS-05, Anton Paar GmbH, Austria) delivering a true electric power input of 24 W at 2.2 MHz. During irradiation both chambers were thermally connected through the cooling circle, i.e. the output of the cooling circle of the sonicated system was connected to the input of the cooling circle of the sham-treated system to provide both active volumes with the same temperature development. When banding was present, part of the cells sediment at the bottom of the active volume where no sound field exists. Therefore the field was switched off every 15 minutes and the suspension was mixed for 30 seconds. This step was not necessary when the suspension was turbulently driven through the chamber.

For the experiments investigating the h-shape separator Figure 5, a control sample of cell suspension was taken before the system was filled. Then the filter, which was tilted 45° to minimize the influence of gravity, was filled with the suspension using a peristaltic pump set to a through-put of about 14 L/day - special attention was paid to eliminating air bubbles in the separator chamber and the tubes – and a sham-treated sample was taken. Then the ultrasound field was applied driven by a frequency power synthesizer (FPS-2540, PSI, Austria) at around 2.1 MHz with 3 W true electric power input. Once stable conditions and a good separation were established samples were taken from the retentate and filtrate outlet, respectively, every two minutes after the ultrasound was switched on. The last sample was taken 10 minutes after the ultrasound was switched on.

As sterility was of great concern for the growth experiments with cultured yeast, autoclaved test tubes were used for sample collection. The procedure was the same as for the wet yeast, the only difference being

that the sample size was about 15 mL and consequently a sample was taken about 4 minutes after the ultrasound had been switched on from the filtrate and retentate outlet, respectively.

7.3 Experiments

The experiments and measurements in the following chapter were designed to investigate the impacts the application of acoustic filters have on yeast suspensions as a model. Naturally the separation efficiency in the different set-ups will be given. In addition we have closely observed the viability (m.b.) and the leakage of protein (UV OD) of cells due to exposure to ultrasound in the UES and the h-shape separator, respectively. Furthermore we have studied the inner morphology of yeasts by TEM when the cells were kept in the pressure nodes and when a rather unexpected streaming through the UES set in. This was observed first when fermentation end products like ethanol and gas bubbles were present in the suspension, however it could be repeated in absence of those as well.

7.3.1 Influence of US on yeast cells kept in pressure nodes

During sonication in the following experiments the cells were forced into the pressure nodal planes where they experience no or vanishing pressure levels. Mainly this was supposed to simulate the ambient conditions within an acoustic. The duration of sonication in the employed UES system in batch-setup was of course exaggerated here, in the real-life application of such separation systems cells would be exposed to the sound field for one or two minutes at the maximum.

Viability (m.b.) & UV OD

No loss in cell viability or protein leakage was detected for a healthy yeast culture sonicated within the pressure nodes of a standing wave. The viability (m.b.) measurements in Table 1 did not indicate any changes of cells exposed to the ultrasound up to a period of 2 h of sonication when compared to control samples. The measurement of the supernatant‘s protein content (UV OD) did not reveal any changes as well. Both results were not changing over time, not even a trend was picked up. These

findings correlate with previous reports on mammalian cultures where the use of standing waves in retention systems did not affect the physiology of such cells [6].

Table 1 Viability (m.b.) and UV OD of a yeast/water suspension after sonication. Cells were kept within the nodal plane of a standing ultrasonic wave.

Time	Viability (m.b.)		UV OD
	Control	Sonicated	
Start	0.99	0.99	0.01
30′	0.95	0.98	0.03
60′	0.97	0.96	0.11
120′	0.96	0.97	0.0

Ability to grow after ultrasonic arrangement

While gel entrapment was reported to increase the tolerance of cell cultures to external stress factors [39], ultrasonic forces have shown to be capable to manipulate and concentrate yeast cells within a gel [40]. The task in the following experiment was to check for the ability to reproduce of gel-entrapped cells after having been arranged by an ultrasonic standing wave field.

Prior to US treatment, freshly grown yeast cells were suspended in liquid malt extract agar gel at a temperature of 37°C. The suspension was filled into an UES system and ultrasound was used to arrange the randomly distributed cells in the nodal planes. Gel solidification was induced by cooling the suspension to 15°C for a short period of 10 min. It was observed qualitatively, that the final particle arrangement in the standing sound field was not influenced by the use of gel instead of water as host liquid.

Thereafter, the suspension was reheated to 37°C in an incubator to allow further cell growth. This reheating did not cause liquefaction due to the hysteresis effect that characterises the agar gel. Figure 6 left-hand side shows a light microscopy image of a typical yeast cell band, as appeared a few minutes after immobilisation.

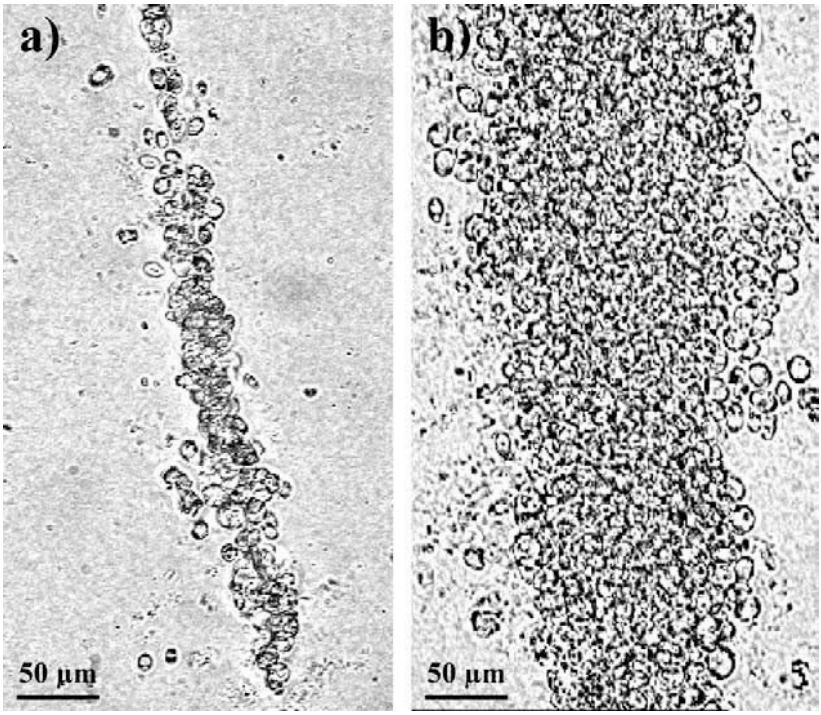

Figure 6 Light microscopy image of yeast cells arranged in an agar gel matrix immediately after US treatment (left) and after 4 days incubation at 37°C (right). The ability of the cells to replicate was not terminated by the US treatment.

It shall be noted that the yeast cells are arranged in a highly organised band by the sound field, whereas the internodal space is virtually free of cells. This arrangement reflects the action of the primary axial radiation force that directed the cells toward the pressure nodal planes during gel solidification. The use of agar requires a significant time as the temperature is brought down for setting the gel. This temperature drop and the phase transition of the gel also influence the sound speed in the gel, thereby changing the resonance conditions in the sonication system. This effect was compensated as the resonance was tracked by the automatic frequency control electronically.

Figure 6 right-hand side shows the image of the same band when the specimen was incubated at 37°C for 4 days after immobilisation. In the latter picture, the number of yeast cells lying in the band is approximately fourfold higher, suggesting that the cells were viable and reproductive.

A qualitative scanning electron micrograph of a cell band (Figure 7) confirmed that the shape of the yeast cells entrapped was preserved after US treatment. Moreover this study showed, that cells arranged by the ultrasonic field might be in touch with each other occasionally, but no tightly packed structure within a band was found. The importance of this is, that the supply of nutrients and oxygen is ensured as the host liquid is still present around the cells in an acoustic filter.

Internal structure investigated by TEM

The internal structure of a yeast cell is dominated by one or more large vacuoles (V) clearly identifiable in the un-sonicated control in Figure 8

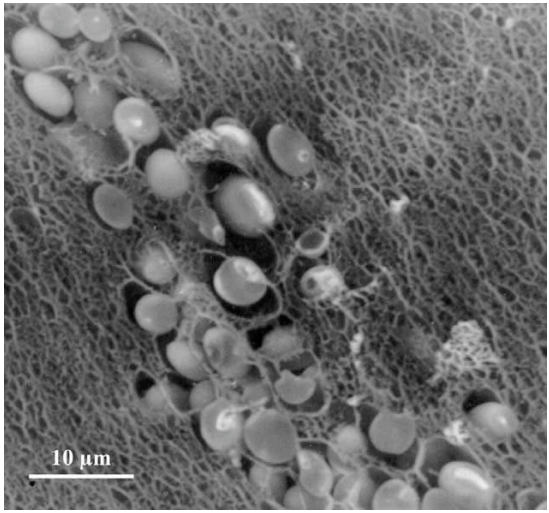

Figure 7 Scanning electron microscopy image of a group of yeast cells arranged within a pressure nodal plane of the UES system. The morphology of the cells does not appear to be compromised by the US treatment.

right-hand side. The spherical cell is delimited by the cell envelope (E). This is comprising the cell wall, in case of yeast reinforced by a calcium cage, and the cell membrane responsible for the exchange of substances with the environment.

One of the possible end-products of a fermentation by yeast is EtOH, which will be of importance when present at low concentrations in the suspension during sonication (see chapter 7.3.2). For now we only mention, that the mere presence of EtOH in the host liquid did not cause alterations of the yeast's morphology. The TEM of cells after having been exposed to 12% (v/v) EtOH in water for half an hour in Figure 8 left-hand side did show the vacuole intact and no changes in the cells' envelope.

However, the TEM image of yeast cells exposed to a 2 MHz standing wave (Figure 9) shows morphological changes when compared to the unexposed cells in Figure 8. In comparison to the very distinct morphology of the control the sonicated cells showed a somewhat differently looking internal composition. The vacuole(s) could not be identified, the cells' internal composition looked mingled. The cells' envelopes (E) however

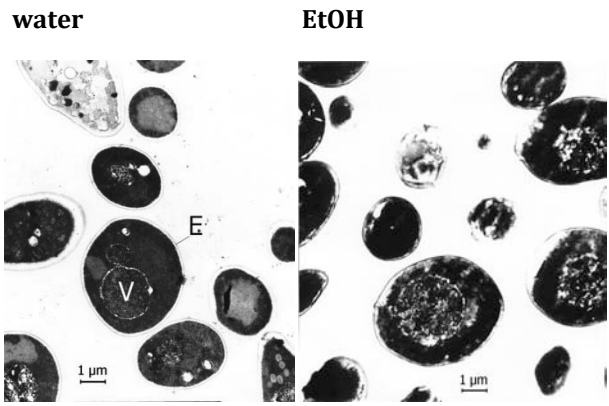

Figure 8 Transmission electron micrograph of non-sonicated yeast cells suspended in water (left) and a water-rich ethanol mixture (right). A typical yeast cell shows the large vacuole (V) and other intracellular organelles. The cell envelope (E) consisting of the cell wall and the cell membrane is also visible.

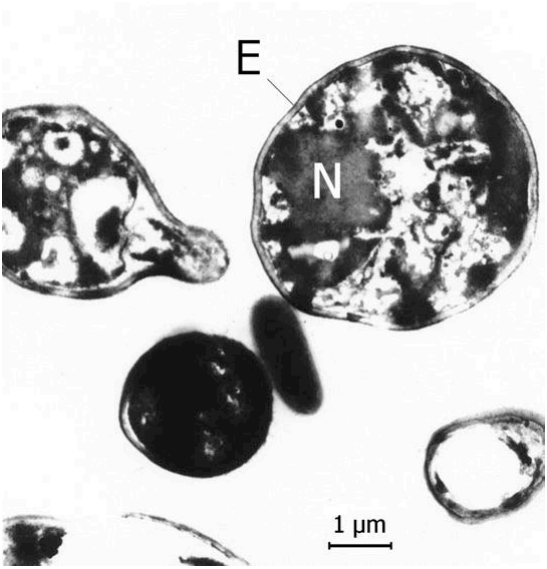

Figure 9 Transmission electron micrograph of yeast cells after sonication with standing ultrasound waves. A re-arrangement of the internal components of the cell was picked up. The nucleus (N) is visible and the envelope (E) seems to remain intact after sonication.

stayed intact and no breakage of the membrane-wall complex was detected. The nucleus (N) was identifiable.

Viability differences between retentate and filtrate in flow-through set-up

In an UES the presented data regarding the cells' viability measured in the batch set-up are valid for a flow-through as well. The gravitational and the drag forces are exerted in vertical direction, therefore no reason exists for the cells to leave the shelter of the pressure nodal plane. However we present additional results on the viability of cells after having been run through the acoustic filter as reports exist of selective retention/filtration of the UES set-up in respect to the viability of cells [41]. This rather surprising fact is explained by changes in the acoustic contrast due to the demise of a cell.

An experiment was conducted to clarify if the ultrasonic field would as well retain viable yeast cells more efficiently than non-viable ones. The UES system in flow-through set-up was used with the inlet closed, as a recycling of the cells by the recycle loop was not desired. Instead the suspension was fed into the back opening (compare Figure 3) to ensure that all cells not kept by the field actually left the system by the top outlet from where the samples were taken.

The resulting percentages of viable cells measured with methylene blue dye did not deviate from the controls, i.e. the viability of the in-going cells did not differ from the cells that left the system by the outlet. Variations of throughput or biomass did not have any effects on the viability of either as shown in Table 2, viability was very high for all measurements. Therefore a selective retention of yeast cells corresponding to their viability was not found, non-viable cells obviously do not differ significantly from viable cells in respect to their acoustic material properties.

Table 2 Viability (m.b.) of yeasts after having left the flow-through set-up by the outlet (Figure 4) for several throughputs and bio-mass levels.

Bio-mass [g/L]	Control	Throughput [L/d]			
		8.9	18.2	27.4	36.7
0.25	0.96	0.96	0.99	0.98	0.97
1.25	1	1	0.98	0.98	0.96
3.75	0.98	0.98	0.99	0.97	0.97
10	0.99	0.99	0.95	0.98	0.97

7.3.2 Damage to yeast cells in inter-nodal space

Originally during investigations, if acoustic filters would be applicable in brewing, we observed an unexpected behaviour when adding fermentation end products. When a small amount of ethanol (EtOH) was present in the suspending phase, the “banding” did not take place anymore. The accustomed arrangement of cell agglomerates was replaced by a vigorous streaming in sound propagation direction, i.e. from the transducer towards the reflector. This type of turbulent behaviour is sometimes called Eckhardt streaming in literature.

The mentioned lack of spatial arrangement of course led to severely impaired separation efficiencies as the UES depends on the radiation forces to build-up agglomerates which then settle more quickly [42]. Instead the cells were next to fed into the up-streaming flow by the mentioned streaming and hence detected in the outlet. A comparison of the retained fraction of the cells when suspended in water with the separation efficiency results when a 12% (v/v) water–EtOH mixture was used as carrier liquid (see Table 3) shows the complete breakdown of retention. There was as well no association with the flow rate for 12% (v/v) water–EtOH detected.

An early assumption, that the presence of EtOH led to some kind of damping and/or a vanishing reflection coefficient and hence the standing wave had disappeared could be rejected. Measurements of the electrical admittance over frequency at electrical power input levels of operation clearly indicated the resonance characteristics of the UES to be intact (data not shown). An increase of damping with rising energy levels suggested the dissipation of acoustic energy into kinetic energy of the suspended particles.

Table 3 Separation efficiency when a 12% (v/v) EtOH-water mixture was used as host liquid (brackets indicate turbulence). The rightmost column gives the means of the similar experiments with water used as a host liquid.

Throughput [L/d]	Single trails of yeast in 12% (v/v) EtOH			Mean, yeast in water
5.6	(-8.3%)	(6.1%)	(-3.6%)	91.7±2.6%
11.3	(-11.4%)	(2.9%)	93.9%	90.2±2.0%
20.1	92.3%	(-23.1%)	(-17.3)	87.0±1.8%
31.7	87.1%	(6.1%)	78.4	84.3±4.0%

Furthermore this breakdown of the spatial order was accompanied by a high number of destroyed cells and a severely decreased viability of the yeast [43]. This result was as well dose related as shown in Figure 10. The longer the cells were exposed to the standing wave field in 12% (v/v) EtOH the higher was the decrease of cell viability (m.b.). The same was recorded for the increase of intracellular material in the supernatant detected by UV

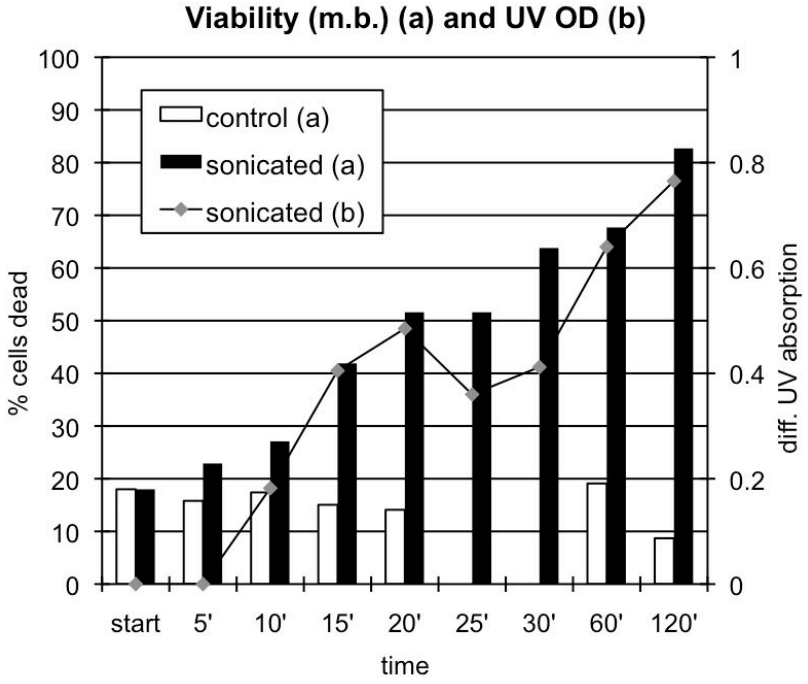

Figure 10 Treatment with standing ultrasonic waves in a 12% (v/v) EtOH-water mixture: the percentage share of dead cells in the sonicated sample (filled bars) and in the non-sonicated control sample (empty bars). The values for the UV absorption due to leakage of intracellular material are also shown (diamond).

O.D. Measurements, protein levels in the supernatant rose with sonication time.

The presence of a more severe damage due to the breakdown of the spatial ordering of the suspended cells caused by the water–EtOH mixture was further documented by TEM images of the cells (see Figure 11). Extensive damage to the envelope of the cell, where the cell wall (W) was found detached from the cell membrane (M) (Figure 11 right-hand side), was characteristic for this type of stress in the internodal space. Consistent with the UV OD data intracellular components were visible in the

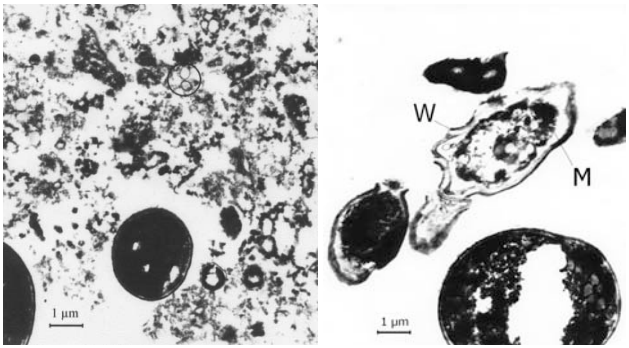

Figure 11 Transmission electron micrographs of yeast cells treated with ultrasonic standing waves in a 12% (v/v) solution of EtOH. (left) Severe leakage suggested by organelles distributed in the supernatant. (right) The cell envelope appears damaged with the cell wall (W) detached from the cell membrane (M). Damage of the vacuole is also visible.

extracellular matrix after sonication in the water–EtOH mixture for 1 h (Figure 11 left-hand side).

When preparing the mentioned water-EtOH mixtures the occurrence of gas bubbles was observed. These were as well present when the water–EtOH based yeast suspensions were sonicated. This was not suppressed when both liquids were boiled and subsequently cooled down in absence of an air interface prior to the preparation of the mixture.

It has been known for a long time that damage can be bubble associated [44]. The basic mechanism is the excitement of the bubble by the ultrasonic field. Subsequently a bubble becomes the source of an additional wave, a phenomenon called cavitation [45]. Especially the so-called transient cavitation, i.e. the occurrence of shock-waves caused by collapsing bubbles and the resulting shear to the cells was held responsible for cell inactivation [46] and cell damage [47] in the past.

Transient cavitation

A theoretical value of the threshold of acoustic pressure below which transient cavitation cannot take place at a given frequency and gas saturation can be derived [48], although the particular circumstances

concerning the liquid and the sound field are of substantial importance [49]. For the UES used in this work the peak pressure of the standing wave was calculated to be 0.6 MPa in the pressure antinodes at the employed true electrical input power of 24 W. It is unlikely for transient cavitation to take place at this pressures at a frequency of around 2MHz [50]. However reports exist that EtOH might provide non-uniform hydrogen bond networks [51] and thus lower the cavitation threshold for alcohol-rich water-EtOH mixtures in comparison to pure water.

One of the most important chemical–physical consequences of the presence of transient cavitation in water during sonication is the generation of free oxygen radicals in the solution volume. A method to detect free radicals was therefore used to confirm/reject the presence of transient cavitation [52]. Briefly the interaction of the free H and OH radicals with KI delivers free iodine, which results in starch as well present in the liquid turning blue. Furthermore this method has the advantage to consider the whole volume of irradiated sample and the full duration of sonication.

To validate the absence of transient cavitation much higher true electrical power inputs than in the presented experiments were employed. The suspensions for the cavitation tests were pure water and 12% (v/v) EtOH-water respectively, both without and with suspended yeast cells at a concentration of 1E7 cells/mL. Each of the four suspension was sonicated for 3 times 10 minutes at rising true electrical power levels.

Neither in the case of clear liquids, water or water-EtOH, nor in the presence of yeast any increase of iodine in the starch indicated by a blue colouring was observed.

Bubbles

However, bubbles can be associated with alterations of the cell membrane in absence of transient cavitation as well [53]. An effect called *Sonoporation*, a transient, unspecific increase of membrane permeability mainly observed in the presence of specially stabilised bubbles is heavily investigated these days [54, 55].

Nevertheless, the results presented next in this study were aiming on clarifying, if the presence or proximity of bubbles was connected to the alterations and damages reported before. We used a small experimental resonator with two transducers glued to opposite walls of a 3 mL cuvette

facing each other. Mainly this was to diminish any asymmetries in reflection or damping, that might have induced the observed streaming.

In a first set of experiments the EtOH concentration was lowered stepwise to find the threshold for the breakdown of the banding. Experiments were conducted at a cell concentration of 4E7 cells/mL. During the 3 minutes of sonication at 2.5 W of troue electrical input power the behaviour of the suspension was observed closely and notes were taken if turbulence was observed. Subsequently a viability (m.b) and UV OD measurement was performed. The findings in Table 4 show that at an EtOH concentration of 4% (v/v) streaming seized to set in. Moreover no significant changes of viability (m.b.) or UV OD were detected at this EtOH concentration, whereas the results obtained at 5% (v/v), EtOH where the turbulent behaviour was observed, showed a tremendous decrease of viability (m.b.) and an increase of extra-cellullar protein by the UV OD.

Bubbles were observed in both experiments, however at the lower EtOH concentration they were driven towards the pressure anti-nodes, hence kept at a distance of half a wavelength (approx. 340 µm) from the yeast cells.

Table 4 Effect of turbulence in the presence of EtOH on viability and leakage of yeast cells sonicated for 3 minutes at 2.5 W true electric power input.

EtOH in suspension	Turbolent	Viability (m.b.)		UV OD
		Sonicated	Control	
4% (v/v)	No	0.98	0.96	0.0
5% (v/v)	Yes	0.17	0.97	0.63

No bubbles

To further suppress the occurrence of gas bubbles the suspending phase was additionally degassed after preparation by exposure to an under-pressure of 20 kPa for 10 minutes. This step of refinement of the tests was motivated by the additional stress-factor they may represent to the cells. Although cavitation was not observed the surface of the gas bubbles represented obstacles to the moving yeast.

The suspension used contained 12% (v/v) EtOH in 0.9% (v/v) physiological saline at a cell concentration of some 2E7 cells/mL. Three degassed and three non-degassed samples were sonicated in the experimental resonator at 2.5 W true electric power input for 3 minutes.

During sonication the behaviour of the cells within the resonator was carefully observed over time. Whereas the non-degassed samples did show turbulent streaming for the whole duration of sonication the trials with degassed suspensions displayed a different behaviour because the EtOH concentration was on the threshold of turbulence for this case:

Trial 1 was turbulent from the beginning.
Trial 2 was banding from the beginning until 30 seconds before the end of the sonication, from then turbulence was observed.
Trial 3 was banding for the duration of the experiment, no turbulence occurred.

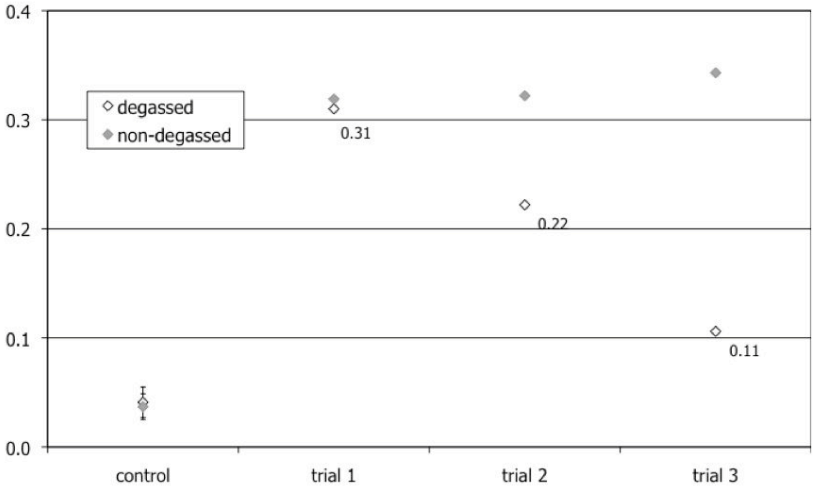

Figure 12 Leakage of intracellular material as delivered by UV OD. The unsonicated control was compared to three trials of sonication at 2.5 W true electric power input. Turbulence was observed for the whole duration of 3 minutes for non-degassed samples (grey markers), but shorter for degasses samples (open markers, see text for further explanation).

The measurement of protein in the supernatant by UV OD in Figure 12 reflected this. During the turbulent treatment (grey markers) the cell leakage was increased in respect to the un-sonicated control to the same level for each experiment. The results for the trials which where only partly turbulent (open markers) indicated a connection between the time it took until turbulence set in and the amount of intracellular material found in the supernatant. The leakage of trial 1 (turbulence during the whole experiment) was not different for degassed and non-degassed samples. No leakage was measured for trial 3, during which no streaming was observed.

Finally we conducted experiments at different true electric power inputs. Clearly an increased power input led to significant higher levels of protein in the supernatant picked up by the UV OD measurements (data not shown).

During all experiments the temperature never rose above 34.5°C, no gas bubbles were observed in the degassed trials.

No EtOH

Our effort to identify the factors playing a role in the generation of the described damages led to the construction of a modified separation chamber (see Figure 13 left-hand side). In this anechoic sonication chamber the resonators reflector was replaced by a water immersed sponge with excellent absorption of the incident ultrasonic wave. The standing wave over travelling wave ratio obtained was better than 0.5% and thus, despite the small sample volume, a free field condition was very well approximated. A weak standing wave with its spatially fixed distribution of pressure and displacement nodes might have been present however the axial primary radiation force was not strong enough to keep the travelling wave from driving the cells through the vessel. The streaming patterns observed were indistinguishable from the cases described earlier, when EtOH was used to induce the streaming.

Treatment within this ‘anechoic chamber’ confirmed the association between the presence of damage and the displacement of the cells from the pressure nodal planes. Figure 13 right-hand side shows a TEM of a cell with a distinct detachment of the cells’ membrane from the wall.

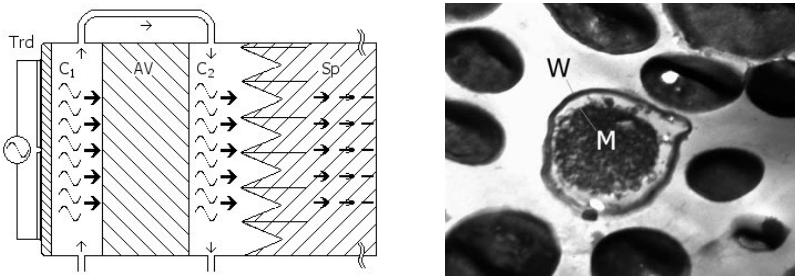

Figure 13 (left) Modified separation system comprising an open-porous sponge (Sp) to impair the reflection coefficient thus leading to an anechoic sonication chamber. (right) TEM of yeast sonicated within the anechoic chamber. Clearly the earlier described damage of the envelope is visible.

Furthermore displayed the cells after this treatment significant loss of viability and increasing amount of intracellular material in the extracellular space, again the significance of which appears to be directly correlated with the duration of the sonication (Figure 14).

7.3.3 Influence of US on yeast cells in h-shape

In the h-shape separator in normal operation particles are guided by the axial primary radiation force to the enriched outlet. However the drag force exerted by the liquid streaming towards the clarified outlet represents a perpendicular component. Therefore certain thresholds for throughput have been calculated previously [37]. Results presented in the following were conducted within the operating limits suggested by these calculations, however partly did not match the outcome delivered by the model.

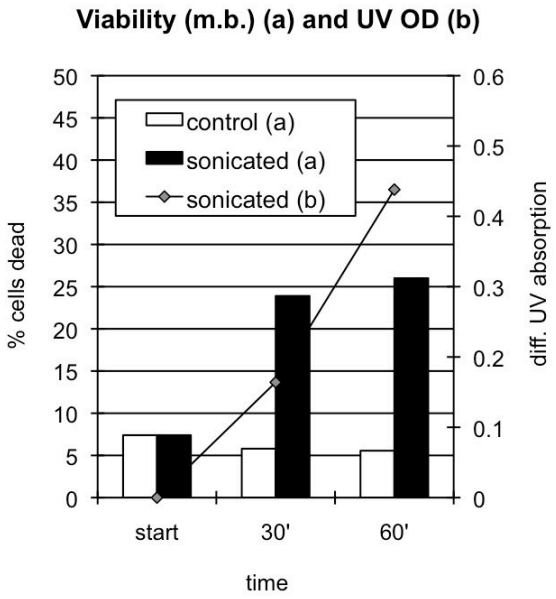

Figure 14 Treatment with propagation ultrasonic waves in water: the percentage share of dead cells in the sonicated sample (filled bars) and in the non-sonicated control sample (empty bars). The values for the UV absorption due to leakage of intracellular material are also shown (diamond).

The experiments with wet yeast suspended in PBS, H_2O tap and PBS 2x showed that the separation process was not very efficient, resulting in an average separation efficiency of about 50%, and rather unstable over time[3]. No significant difference in separation efficiency between the media was detected.

[3] Thus, in contrary to chapter 7.3.1 no time/dose data will be provided here. Results will always be averages of measurements as in an unstable set-up like this every sample taken has to be considered as of a individual experiment.

Viability (m.b.) & UV OD

Cell viabilities as of methylene blue measurements were not significantly altered by the exposure to the ultrasonic standing wave in the h-shape separator as long as the arrangement typical for the forces exerted by the ultrasonic standing wave was observed (see Table 5). For cells suspended in PBS and PBS 2x, respectively, average viability was around 99% for all the samples. Yeast suspended in H_2O tap water showed a slightly lower (but stable) average percentage of viable, non-blue cells of around 89%. No differences were picked up between retentate and filtrate outlet.

Table 5 Average cell viability of control, sham, retentate and filtrate samples for the experiments where wet yeast was suspended in PBS, H_2O and PBS 2x, respectively.

Liquid	Control	Sham	Retentate	Filtrate
PBS	0.99	0.99	0.99	0.98
H_2O tap	0.89	0.89	0.88	0.91
PBS 2x	0.99	0.99	0.98	0.99

No significant difference in UV OD was found between the two outlets (filtrate and retentate) for H_2O tap, PBS and PBS 2x, respectively. PBS-suspensions showed a slightly but significantly higher UV OD for samples exposed to the field in the h-shape separator compared to controls. For H_2O and PBS 2x, however, there was no significant difference between controls and sonicated samples (see Table 6).

Table 6 Average optical density of samples at 280 nm (UV OD) for the detection of protein in the supernatant.

Liquid	Control	Sonicated
PBS	0.05±0.01	0.07±0.02
H_2O tap	0.04±0.03	0.04±0.02
PBS 2x	0.06±0.02	0.06±0.01

Yeast sonicated in culture medium

In the literature reports exist about the concept of “sonobioreactors” [56], i.e. the application of ultrasonic fields to influence the proliferation and/or the metabolism of a culture in a bioreactor. Moreover the immobilisation of yeast cells is said to influence the physiological and metabolic properties of yeast cells [57]. Following this reviews we tested for the hypothesis, that the cell growth could be influenced by exposition to the ultrasonic field in a h-shape separator.

Therefore we conducted the experiment in the h-shape separator like described before, although leaving the culture in the culture medium. This was done to provide proper nutrition, if sonication would have “triggered” additional proliferation despite the fact that the cells had gone into stationary phase, i.e. finished growth, before sonication. To access possible bio-mass alterations the cell concentration was measured before and after sonication.

Firstly, quite surprisingly the separation efficiency was a lot higher for yeast cultured and sonicated in malt extract broth than for wet yeast in the different media mentioned before. Cultured yeast was filtered with a separation efficiency of 87.8 ± 5.7%, while the average separation efficiency for wet yeast was 50.0 ± 19.3%. The separation process also seemed to be a lot more reliable and reproducible for cultured yeast, as suggested by the small standard deviation. Furthermore, cell viability was not influenced by the separation process (data not shown).

However, in one experiment, when the stable alignment of the cells broke down and the separator “fogged up”, cell viability decreased to 0.65 and to 0.67 for retentate and filtrate, respectively. This result was accompanied by an increase of the supernatant’s protein content measure by the UV OD In another case when this happened the loss in cell viability was not that severe, a decreased viability of 0.85 and 0.81 for retentate and filtrate, respectively, was detected. This was supposingly achieved by the re-establishment of the “banding” as the turbulent behaviour could be stopped by turning the field off and on again.

Apart from finding a relatively high separation efficiency, comparison of the cell concentrations found right after the experiment with the concentrations found 18 hours later indicated that only the cells found in the retentate significantly replicated over time.

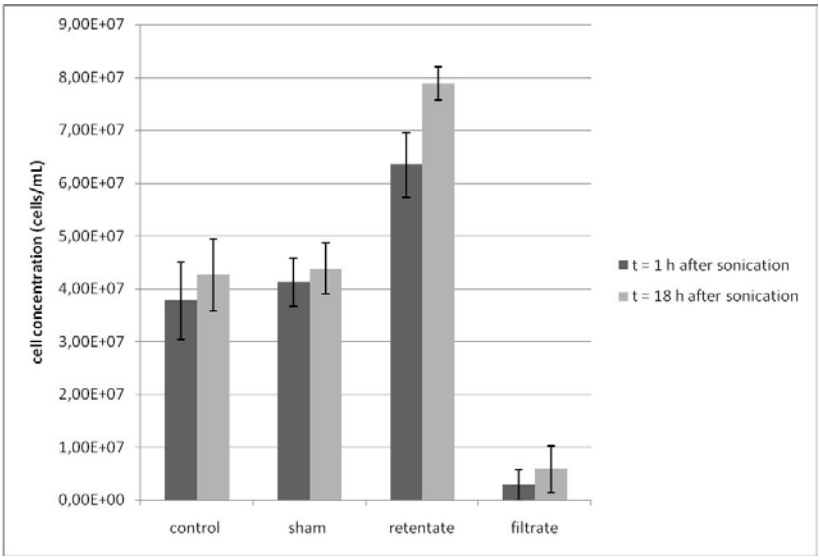

Figure 15 Comparison of average cell concentrations (cells/mL) for the control, sham, retentate and filtrate, respectively, at t_1 = 1 hour after sonication and t_2 = 18 hours after sonication.

Figure 15 shows the cell concentration per mL averaged over four experiments found in the respective samples and their standard deviation. These data suggest a trend towards a higher cell concentration at t_2 = 18 hours after sonication compared to t_1 = 1 hour after sonication, but only the samples taken at the retentate outlet increase at a confidence level of 99% (1-sided t-test).

One might argue that the initial cell concentration is already a lot higher for these samples, so if there was a fraction of the total cells that are still able to divide there would be a greater number of these in the samples. This is not the case as one can see when looking at normalized average cell concentrations number at t_2 in Table 7. The normalized cell number of the retentate samples at t_2 is 1.24, for the controls it is 1.13, for the sham-exposed 1.06 and for the filtrates it is 2.06. That means that the average number of cells in the retentate has increased by 24% during the 17 hours, while the average number of cells in the control and the sham

has only grown by 13% and 6%, respectively. The more than two-fold increase of cells in the filtrate is, although indicating a similar development, due to the small total number of cells and consequently high standard deviations not significant.

Table 7 Cell concentrations at t_2 = 18 hours normalized to the respective average cell number at t_1.

	Control	Sham	Retenate	Filtrate
Ø t_2d/t_1	1.13	1.06	1.24	2.06

7.4 Conclusions

7.4.1 Viable filtration

It was confirmed, that the presented acoustic filters, the UES and h-shape separator are both applicable to suspensions of biological cells. This has been shown in using suspended yeast as a life model. Separation efficiencies have been found to be typically around 90% in UES, a peak of 99.6% was found for optimal conditions.

Lower (50%) and not very stable separation efficiencies for wet yeast were measured in the gravity independent h-shape separator. The results when using suspensions of cultured yeast were higher. Additionally an influence of the used liquids was detected, freshly cultivated yeast cells in malt extract broth were retained at a slightly higher level than suspensions based on PBS (92% vs. 87%). However the reason for this difference is not known.

The exposure to ultrasonic fields exploited in acoustic filtration were, in agreement with the literature, not influencing the yeasts viability as of methylene blue counts. Furthermore the suspensions were checked for protein leaked by the cells and beside the h-shape filtration of yeasts suspended in PBS, where a very small, but significant increase was detected no protein released from the cells due to ultrasonic stress was detected.

All this holds true when the cells are kept in the pressure nodal planes of ultrasonic standing wave, an arrangement referred to as “banding”. Such was observed in the UES in water, saline and up to a certain

concentration of the yeast fermentation end product EtOH. The pressure nodal plane seems to protect the biological material, we will discuss damages brought about by movement through the inter-nodal space in the following chapter.

In the UES by definition no forces perpendicular to the nodal planes exist, hence particles have no reason the leave this shelter. In contrary to that the drag force acting in direction of the axial primary radiation force within h-shape separator could possibly lead to the cells' exposure to the sound field in the inter-nodal space. This was not the case, as long as the "banding" was intact, no decreases have been measured.

It was shown, that the cells' supply with nutrition and oxygen is warranted during their stay in the filter. The aggregate in the pressure nodes turned out to be loose when investigated by scanning electron microscopy. This study revealed as well, that the shape of the cells was unaltered.

Previous reports of the filters' selectivity on the viability of cells could not be confirmed, no experiment with neither of the two set-ups delivered hints of a viability specific retention.

7.4.2 Damaging streaming

Under certain circumstances, amongst which the presence of a small amount of EtOH in the suspending phase, the breakdown of the "banding" was observed. This was not the result of damping or a distortion of the standing wave field, as could be concluded from measurements of the true electric power input spectrum. The reason for the unexpected turbulence in such liquids might be associated with their anomalies in relation to the speed of sound and other acoustical properties over the concentration of EtOH. It was reported that there exists a possibility of micelle-like structures which could be the influencing the material properties in such a way [58].

The lack of spatial distribution (i.e., the fact that the cells are driven through all areas of the sound field), in a water-rich EtOH mixture caused a breakdown of filtration/retention. This was accompanied by severely impaired viability (m.b.) and higher protein levels in the supernatant. This result was found in any employed resonator. The decrease in viability of yeast and increase of protein in the supernatant when sonicated in 12% (v/v) water–EtOH were greater than when cells were exposed to EtOH

alone, where no effect was measured [59]. Thus it can be said that physical damage brought about by sonication was responsible for the decrease in viability of the yeast. Examinations of cells using TEM indicated severe morphological changes resulting from the mixing. Images of sonicated cells showed the disintegration of the cell wall–membrane interface, which consequently might have led to cell disruption. Moreover a significant correlation with duration of exposure to the ultrasound was detected.

Free radicals which would have been indicating transient cavitation were not picked up, so this prominent mechanism was unlikely the reason for the alterations when the cells were sonicated. We started to tailor experiments aiming on stepwise exclusion of factors known to be able to damage cells in the described way. At first the EtOH content was lowered until the streaming would stop. Viability (m.b.) and UV OD indicated damage to the culture in this case again only when the turbulent behaviour was observed.

Bubbles were still present within the sonicated volume during these experiments. As gas bubbles have a negative acoustic contrast they are concentrated in the pressure antinodes. Therefore only when the streaming occurred the cells would come close to the bubbles and possibly suffer because of this proximity. Thus a step of degassing by the use of underpressure was performed additionally. This finally diminished the occurrence of bubbles, nevertheless the streaming could be initiated by addition of EtOH, although at slightly higher levels of EtOH. The threshold concentration of EtOH was chosen, at which the turbulence had a tendency to set in only occasionally and to sometimes seize again. The total duration of streaming was directly correlated to the damages. The longer the cells were driven through the chamber turbulently, the higher the protein level in the supernatant were. No bubbles were observed.

Remarkably we found approximately a linear correlation of the UV OD and the cell concentration for completely turbulent cases, compare Table 4 first row, 0.62@4E7 cells/mL and Figure 12 trial 1, 0.31@2E7 cells/mL. However in the first experiment gas bubbles were present, while in the second degassing suppressed their occurrence. This could be a hint, that bubbles might not have much to do with the damage, as the level of protein seems only to be dependent on the occurrence of turbulence.

The TEM images of yeast cells sonicated in an anechoic chamber in water showed the same type of damage to the cell envelope as found the

experiments in turbulent water-rich EtOH mixtures. However the ultrasonic field in this system is for sure composed of different portions of standing and propagating wave, respectively. The experiments in 12% (v/v) water-EtOH and the anechoic system were conducted at the same true electric power input. However, a much higher maximum value of the spatially varying pressure amplitude of the standing wave in the ordinary system compared to the spatially constant pressure amplitude of the corresponding propagating wave in the anechoic is to be expected.

The findings of stronger influence of the standing wave on viability (m.b.) and UV OD in comparison to the respective results in the anechoic system are supporting the assumption that the damage could be a direct function of the degree of pressure impact on the cells. This is in agreement with previous reports [47, 60, 61].

Speculating about the mechanism of damage one realises, that the yeast cells are distributed in the space between the pressure nodal planes when the described streaming sets in. Therefore they are exposed to the amplitude of ultrasound pressure, which could cause much higher degree of stress than seen when cells are retained in the nodal planes. However the reported pressure of 0.6 MPa would be easily endured by a yeast cell [62] if the pressure increased and decreased slowly. But the acoustic pressure changes two million times per second. This could likely be too fast for the cell to adjust its turgor pressure and furthermore a mass transfer into the cell seems possible [63], the cells would be pumped up and finally burst.

7.4.3 Replication

Some non-lethal alterations in internal morphology were picked up by TEM, the exposure to ultrasound in the nodal plane seems to alter the integrity of the cell vacuole. Although the data on the viability showed that this degree of damage was not lethal, we collected data on cells' ability to reproduce after exposition to the ultrasound as changes in the replicating apparatus could have occurred.

The maintenance of the yeasts' biological competence was shown by cultivation after arrangement by the ultrasonic field in liquid malt extract agar, a nutrient gel for cell culturing. Originally freely suspended cells were then concentrated in the expected manner by the primary radiation forces, i.e. aligned highly ordered in the pressure nodal planes. Subsequently this

arrangement was “frozen” by temperature-induced polymerisation obtain a solid gel-block. After four days of incubation substantial growth had been taking place, as the examination of the immobilised cells under the microscope delivered. Therefore we conclude, that the ability to reproduce of our live model was intact.

A somewhat puzzling result was found when cells where sonicated in malt extract broth in the h-shape separator. A stimulated replication was indicated by an increase of the cell counts 18 hours post-experiment when compared to cell concentration measurements right after the experiment. This growth was significant only for samples retrieved by the retentate outlet, increases of bio-mass detected in the other samples were only insignificantly higher. The mentioned surprise came from the fact, that cells had been left in the incubator until no further growth took place (stationary phase). As the suspending medium was not changed no additional replication was expected anymore.

We have to admit that this is in contradiction to other investigations (data not shown) which indicated that lag time (i.e. the time occurring before cells duplicate) observed in sonicated cells is longer than in the control sample. This was supported by earlier observations [64] that the structure of the elements, responsible for the processes of the cell division, may be partially damaged or passivated, as well.

7.5 References

[1] KUNDT, A.; LEHMANN, O. Longitudinal vibrations and acoustic figures in cylindrical columns of liquids. *Annalen der Physik und Chemie (Poggendorff's Annalen).* 1874, 153, pp. 1-12.

[2] GRÖSCHL, M. Ultrasonic separation of suspended particles - Part I: Fundamentals. *Acustica - acta acustica*. 1998, 84, pp. 432-447.

[3] GRÖSCHL, M. et al. Ultrasonic separation of suspended particles – Part III: Application in biotechnology. *Acustica - acta acustica*. 1998, 84(5), pp. 815-822.

[4] WOODSIDE, S.M.; BOWEN, B. and PIRET, J. Mammalian cell retention devices for stirred perfusion bioreactors. *Cytotechnology*. 1998, 28(1), pp. 163-175.

[5] BARNES, R.A.; JENKINS, P. and COAKLEY, W.T. Preliminary clinical evaluation of meningococcal disease and bacterial meningitis by ultrasonic enhancement. *Arch Disease Child*. 1998, 78, pp. 58.

[6] DOBLHOFF-DIER, O. et al. A novel ultrasonic resonance field device for the retention of animal cells. *Biotechnology Progress*. 1994, 10(4), pp. 428-432.

[7] GAIDA, T. et al. *Scale-up of ultrasonic resonance field cell separation devices used in animal cell technology.* Dordrecht : Kluwer, 1995, pp. 699-703.

[8] PUI, P.W.S. et al. Batch and semicontinuous aggregation and sedimentation of hybridoma cells by acoustic resonance fields. *Biotechnol. Prog.* 1995, 11(2), pp. 146-152.

[9] BIERAU, H. et al. A comparison of intensive cell culture bioreactors operating with Hybridomas modified for inhibited apoptotic response. *Journal of Biotechnology*, 1998, 62, pp. 195.

[10] BÖHM, H. et al. Viability of plant cell suspensions exposed to homogeneous ultrasonic fields of different energy density and wave type. *Ultrasonics*. 2000, 38, pp. 629-632.

[11] COUSINS, C.M. et al. Clarification of plasma from whole human blood using ultrasound. *Ultrasonics*. 2000, 38, pp. 654-656.

[12] YASUDA, K. et al. Deoxyribonucleic acid concentration using acoustic radiation force. *Journal of Acoustical Society of America*. 1995, 99(2), pp. 1248-1251.

[13] HAWKES, J.J.; BARROW, D. and COAKLEY, W.T. Microparticle manipulation in millimetre scale ultrasonic standing wave chambers. *Ultrasonics*. 1998, 36, pp. 925-931.

[14] SPENGLER, J.F. and COAKLEY, W.T. Ultrasonic trap to monitor morphology and stability of developing microparticle aggregates. *ACS Journal of Surfaces and Colloids – Langmuir*. 2003, 19(9), pp. 3635-3642.

[15] GHERARDINI, L. et al. A study of the spatial organisation of microbial cells in a gel matrix subjected to treatment with ultrasound standing waves. *Bioseparation*. 2002, 10, pp. 153-162.

[16] GHERARDINI, L. et al. A new immobilisation method to arrange particles in a gel matrix by ultrasound standing waves. *Ultrasound Med Biol*. 2005, 31(2), pp. 261-272.

[17] WIKLUND, M.; NILSSON, S. and HERTZ, H.M. Ultrasonic trapping in capillaries for trace amount biomedical analysis. *J Appl Phys*. 2001, 90, pp. 421.

[18] LAURELL, T.; PETERSSON, F. and NILSSON, A. Chip integrated strategies for acoustic separation and manipulation of cells and particles. *Chem. Soc. Rev.* 2007, 36(3), pp. 492-506.

[19] HAWKES, J. et al. Continuous cell washing and mixing driven by an ultrasound standing wave within a microfluidic channel. *Lab on a Chip*. 2004, 4(5), pp. 446-452.

[20] HULTSTRÖM, J. et al. Proliferation and viability of adherent cells manipulated by standing-wave ultrasound in a microfluidic chip. *Ultrasound in Medicine & Biology*. 2007, 33(1), pp. 145-151.

[21] BENES, E. et al. Ultrasonic separation of suspended particles. In *IEEE Ultrasonics Symposium 2001.* Atlanta, USA : IEEE Inst. of Electrical & Electronics Engineers, 2001.

[22] KEIJZER, T.M.P. et al. Integrating acoustic perfusion in mammalian cell culture. Scale-up and performance characterisation. In *Cell Culture Engineering VII*. Snowmass Village, Colorado, USA : United Engineering Foundation, Inc., 2002.

[23] HAWKES, J.J.; LIMAYE, M.S. and COAKLEY W.T. Filtration of bacteria and yeast by ultrasound enhanced sedimentation. *Journal of Applied Microbiology*. 1997, 82, pp. 39-47.

[24] HAWKES, J.J. et al. Ultrasonic manipulation of particles in microgravity. *Journal of Physics D: Applied Physics*. 1998, 31, pp. 1673-1680.

[25] MANARESI, N. et al. A CMOS chip for individual cell manipulation and detection. *Solid-State Circuits Conference, 2003. Digest of Technical Papers. ISSCC. 2003 IEEE International*. 2003, pp. 192- 487 vol.1.

[26] LŐRINCZ, A. Ultrasonic cellular disruption of yeast in water-based suspensions. *Biosystems Engineering.* 2004, 89(3), pp. 297-308.

[27] TOLT, T.L. and FEKE, D.L. Separation of dispersed phases from liquids in acoustically driven chambers. *Chemical Engineering Science*. 1993, 48(3), pp. 527-540.

[28] GALLEGO-JUÁREZ, J.A.; GONZÁLEZ, I. and RIERA, E. Separation of fine aerosol particles by high power ultrasounds. In *137 Meeting of the Acoustical Society of America and the second Convention of the*

European Acoustic Association: Forum Acusticum. Berlin, Germany, 1999.

[29] KING, L.V. On the acoustic radiation pressure on spheres. *Proc. R. Soc. London*. 1934, A147, pp. 212-240.

[30] KÖNIG, W. Hydrodynamisch-akustische Untersuchungen: II. Über die Kräfte zwischen zwei Kugeln in einer schwingenden Flüssigkeit und über die Entstehung der Kundtschen Staubfiguren. *Annalen der Physik und Chemie*. 1891, 42(4), pp. 549-563.

[31] BJERKNES, V.F.K. *Die Kraftfelder*. Braunschweig : Vieweg und Sohn, 1909.

[32] WEISER, M.A.H. and APFEL, R.E. Interparticle forces on red cells in a standing wave field. *Acustica - acta acustica*. 1984, 56, pp. 114-119.

[33] GRÖSCHL, M. et al. Ultrasonic separation of suspended particles - Part III: Application in biotechnology. *Acustica - acta acustica*. 1998, 84, pp. 815-822.

[34] ZHANG, J. et al. High-density perfusion culture of insect cells with a Biosep ultrasonic filter. *Biotechnology and Bioengineering*. 1998, 59(3), pp. 351-359.

[35] RADEL, S. Influence of biomass, throughput and true electric power input on the separation efficiency of a 60 mL acoustic filter. *Elektrotechnik*. 2009, 126(1/2), pp. 51-57.

[36] BÖHM, H. et al. Quantification of a novel h-shaped ultrasonic resonator for separation of biomaterials under terrestrial gravity and microgravity conditions. *Biotechnol. Bioeng.* 2003, 82(1), pp. 74-85.

[37] BENES, E. et al. Ultrasonic separation of suspended particles. *2001 IEEE Ultrasonics Symposium*. 2001, 1, pp. 649-659.

[38] BLACK, J.T. *The scanning electron microscope: Operating principle.* New York : Van Nostrand Reinhold Co., 1974, pp. 1-43.

[39] MCLOUGHLIN, A.J. Controlled release of immobilized cells as a strategy to regulate ecological competence of inocula. *Advances in Biochemical Engineering/Biotechnology*. 1994, 51, pp. 1-45.

[40] GHERARDINI, L. et al. A study of the spatial organisation of microbial cells in a gel matrix subjected to treatment with …. *Bioseparation*. 2001.

[41] GAIDA, T. et al. Selective retention of viable cells in ultrasonic resonance field devices. *Biotechnology Progress*. 1996, 12, pp. 73-76.

[42] RADEL, S. et al. Breakdown of immobilisation/separation and morphology changes of yeast suspended in water-rich ethanol mixtures exposed to ultrasonic plane standing waves. *Bioseparation*. 2000, 9(6), pp. 369-377.

[43] RADEL, S. et al. Viability of yeast cells in well controlled propagating and standing ultrasonic plane waves. *Ultrasonics*. 2000, 38(1-8), pp. 633-637.

[44] WU, J. and NYBORG, W. Ultrasound, cavitation bubbles and their interaction with cells. *Advanced Drug Delivery Reviews*. 2008.

[45] APFEL, R.E. Sonic effervescence: A tutorial on acoustic cavitation. *Journal of Acoustical Society of America*. 1997, 101(3), pp. 1227-1237.

[46] DAKUBU, S. Cell inactivation by ultrasound. *Biotechnol. Bioeng.* 1976, 18, pp. 165-171.

[47] THACKER, J. An approach to the mechanism of killing of cells in suspension by ultrasound. *Biochimica et Biophysica Acta (BBA) - General Subjects*. 1973, 304(2), pp. 240-248.

[48] APFEL, R.E. Acoustic cavitation prediction. *J. Acoust. Soc. Am.* 1981, 69(6), pp. 1624-1633.

[49] APFEL, R.E. Acoustic cavitation series. Part four: Acoustic cavitation inception. *Ultrasonics.* 1984, 22, pp. 167-173.

[50] GOULD, R.K.; COAKLEY, W.T. and GRUNDY, M.A. Upper sound pressure limits on particle concentration in fields of ultrasonic standing-wave at megahertz frequencies. *Ultrasonics*. 1992, 30(4), pp. 239-244.

[51] BERTOLINI, D.; CASSELIARI, M. and SALVETTI, G. The dielectric properties of alcohols-water solutions: 1. The alcohol rich region. *Journal of Chemical Physics*. 1983, 78, pp. 365-372.

[52] COAKLEY, W.T. and SANDERS, M.F. Sonochemical yields of cavitation centres at 1 MHz. *Journal of Sound and Vibration*. 1973, 28(1), pp. 73-85.

[53] MILLER, D. and DOU, C. Membrane damage thresholds for pulsed or continuous ultrasound in phagocytic cells loaded with contrast agent gas bodies. *Ultrasound in Medicine & Biology*. 2004, 30(3), pp. 405-411.

[54] OHL, C. et al. Sonoporation from jetting cavitation bubbles. *Biophysical Journal*. 2006, 91(11), pp. 4285-4295.

[55] FRENKEL, V. Ultrasound mediated delivery of drugs and genes to solid tumors. *Advanced Drug Delivery Reviews*. 2008.

[56] CHISTI, Y. Sonobioreactors: using ultrasound for enhanced microbial productivity. *Trends in Biotechnology*. 2003.

[57] VERBELEN, P. et al. Immobilized yeast cell systems for continuous fermentation applications. *Biotechnology Letters*. 2006, 28(19), pp. 1515-1525.

[58] LARA, J. and DESNOYERS, J.E. Isentropic compressibilities of alcohol-water mixtures at 25°C. *Journal of Solution Chemistry*. 1981, 10(7), pp. 465-478.

[59] NORTON, S.; WATSON, K. and D'AMORE, T. Ethanol tolerance of immobilized brewers' yeast cells. *Applied Microbiology and Biotechnology*. 1995, 43(1), pp. 18-24.

[60] HIROMI KOBORI, M.S. Ultrastructural effects of pressure stress to the nucleus in *Saccharomyces cerevisiae*: a study by immunoelectron microscopy using frozen thin sections. *FEMS Microbiology Letters*. 1995, 132(3), pp. 253-258.

[61] MAMIKO SATO, H.K. Pressure-stress effects on the ultrastructure of cells of the dimorphic yeast *Candida tropicalis*. *FEMS Microbiology Letters*. 1995, 131(1), pp. 11-15.

[62] FERNANDES, P.; FARINA, M. and KURTENBACH, E. Effect of hydrostatic pressure on the morphology and ultrastructure of wild-type and trehalose synthase mutant cells of Saccharomyces cerevisiae. *Letters in applied microbiology*. 2001, 32(1), pp. 42-46.

[63] PERRIER-CORNET, J.; HAYERT, M. and GERVAIS, P. Yeast cell mortality related to a high-pressure shift: occurrence of cell membrane permeabilization. *Journal of applied microbiology.* 1999, 87(1), pp. 1-7.

[64] TRAMPLER, F. et al. Acoustic cell filter for high density perfusion culture of hybridoma cells. *Bio/Technology*. 1994, 12(3), pp. 281-284.

8 The effect of Photodynamic and Sonodynamic treatment on B16FO cell line

Kateřina Tománková, Hana Kolářová

Photodynamic therapy (PDT) of cell lines is sometimes associated with the rapid initiation of apoptosis, a mode of cell death that results in a distinct pattern of cellular and DNA fragmentation. The apoptotic response appears to be a function of a sensitizer and the cell line. PDT on malignancies is a widely used technique based on photochemical sensitization induced by combining a tumour-localizing photosensitizer and visible light [1]. Photodynamic therapy of tumour cells is sometimes associated with rapid initiation of apoptosis. Sonodynamic therapy is a newer concept, which relates to the ability of ultrasound to evoke a cytotoxic effect on cell lines [2]. The cytotoxicity of SDT can be enhanced by the presence of sonosensitizing drugs. Ultrasound can be focused into a small region of tumour to activate the sonosensitizing drug and, in contrast with PDT, can penetrate deeply into the tissue [3]. Kessel et al [4] suppose that the cytotoxic effect of SDT is mediated largely by inertial cavitation. Inertial cavitation is a process where a gas bubble created by ultrasound in a liquid rapidly collapses, producing a shock wave with intense temperature change (of several thousand degrees Kelvin) [5]. The water molecules surrounding the cavitation decompose into their ·H and ·OH constituents (water pyrolysis), these either recombine, forming H_2O, H_2O_2, and H_2, directly oxidize or reduce solute molecules, sonosensitizing drugs or the cell biomolecules [6]. It is expected that the affinity of the sonosensing agent to tumours and its ability to generate singlet oxygen is very important in understanding the mechanism of SDT [7].

In the past two decades there has been an explosive interest in the role of oxygen-free radicals more generally known as reactive oxygen species (ROS) in experimental and clinical medicine. ROS are generated during irradiation by UV light, X-rays and by gamma-rays. ROS are products of metal-catalyzed reactions; they are present as pollutants in the atmosphere, they are induced by neutrophils and macrophages during

inflammation, they may be generated as by-products of mitochondria-catalyzed electron transport reactions and other mechanisms [8]. Reactive oxygen species are formed and degraded by all aerobic organisms, leading to either physiological concentrations required for normal cell function or in excessive quantities, resulting in the state called oxidative stress. As the term ROS implies, intracellular production of those oxygen intermediates threatens the integrity of various biomolecules including proteins, lipids as well as lipoproteins involved in arterosclerosis and DNA [9]. Oxidative stress may also be involved in the process of aging by inducing damage to mitochondrial DNA and by other mechanisms [9]. Free radicals can be defined as molecules or molecular fragments containing one or more unpaired electron. The presence of unpaired electrons usually confers a considerable degree of reactivity upon a free radical. The derived oxygen radicals, that are derived from oxygen, represent the most important class of such species generated in living systems.

8.1 Materials and Methods

8.1.1 Materials and instruments

Cell line B16FO (mouse melanoma cells) was used as a biological material. The chemicals used included Dulbecco´s Modified Eagle Medium (DMEM), sensitizer $ClAlPcS_2$ (prepared by Jan Rakusan at the Research Institute for Organic Syntheses in Rybitvi, Czech Republic), CM-H_2DCFDA (Invitrogen Co., USA), 3-(4,5-dimethyl-2-thiazolyl)-2,5-diphenyl-2H-tetrazolium bromide (MTT, Sigma Aldrich), dimethyl sulfoxide (DMSO, Sigma Aldrich). Measurements were carried out on detection microplate reader Synergy HT (BioTek, USA), therapeutic ultrasound (BTL 4000, USA), LED diodes L53SRC-F, maximum 660 nm, FWHM 24 nm (Kingbright Corporation, Taiwan), Olympus IX80 microscope with DSU unit (Tokyo, Japan). 35 mm Petri dishes for cultivation of the cell lines were used.

8.1.2 Photodynamic and Sonodynamic therapy

3.3×10^5 B16FO cells were seeded into the 35 mm Petri dishes containing 2 ml of cultivation medium (DMEM) - with photosensitizer $ClAlPcS_2$ added in concentrations 0 (control), 0.5, 1, 5, 10, 50 and 100 μM. The cells were incubated in a thermobox at 37 °C, 5 % CO_2 atmosphere for

24h. Before starting the experiments DMEM was replaced by PBS containing 5 mM glucose adding 20 µl of 500 mM CM-H_2DCFDA (dissolved in DMSO). One dish was a control (cells in the absence of sensitizer), one dish was a negative control (cells in the absence of sensitizer and irradiated with a dose 15 J.cm^{-2}). Other dishes, i. e. cells in the presence of 0.5, 1, 5, 10, 50 and 100 µM ClAlPcS_2, were irradiated with total dose of 15 J.cm^{-2}. For the irradiation, we used light emitting diodes with the emission wavelength maximum at 660 nm, FWHM 25 nm. The light intensity was set to 0.1 mW.cm^{-2} (internal irradiator) and 12 mW.cm^{-2} for subsequent irradiation up to the total dose of 15 J.cm^{-2} using an external LED irradiator. The arrangement of the experiments was as follows: CM-H_2DCFDA incubation for 30 min, the rate of ROS production was measured during PDT at 30 seconds, 10 minutes and the final concentration taken at termination, using the total irradiation dose of 15 J.cm^{-2}. In experiments with SDT, we performed ultrasound irradiation before starting the measurement of kinetic ROS production. The parameters of the ultrasound exposure were: frequency 1 MHz, intensity 2 W.cm^{-2} with a duration of 10 min. After these treatments, cells were cultivated for the next 24 h under the same conditions in fresh DMEM medium.

8.1.3 Microscopic study

Cell viability and morphological changes after PDT were visualized by Olympus IX80 microscope with DSU unit. The measurement was carried out using 35 mm Petri dishes. After treatment, cells were incubated at 37 °C and 5 % CO_2 for 24h in fresh DMEM. Images were recorded by CCD camera and Cell^R software.

8.1.4 Measurement of ROS production

ROS were generated due to PDT and SDT influence. We determined ROS production during PDT using CM-H_2DCFDA and microplate reader Synergy HT. Excitation wavelength of 485 nm and emission wavelength of 548 nm were used. The time course of ROS generation was recorded for 10 minutes using the light intensity of 0.1 mW.cm^{-2}, produced by LEDs with internal irradiator inserted into the microplate reader. The total ROS production was measured after termination; for termination a 20-minute irradiation with a microplate reader and an external irradiator inserted

onto the thermobox was used at a greater intensity of 12 $mW.cm^{-2}$ with a final dose of 15 $J.cm^{-2}$.

8.1.5 Cancer cell cytotoxicity assay

The cytotoxic effect of the sensitizer $ClAlPcS_2$ in combination with irradiation and ultrasound on B16FO cells was determined using the MTT assay. After treatment, cells were incubated at 37 °C and 5 % CO_2 for 24 h in fresh DMEM. Than starting the experiments we replaced DMEM by PBS containing 5 mM glucose, added 222 µl 20 mM MTT (dissolved in PBS) and incubated the cells for 3 h at 37 °C and 5 % CO_2. The MTT solution was carefully removed and 1 ml DMSO was added in order to solubilize the violet formazan crystals. The absorbance of the resulting solution was measured in 96-well microplate reader Synergy HT at 570 nm and 690 nm. The cell viability of the samples was determined as percentage of control cell viability (100× average of test group/average of control group).

8.2 Results and Discussion

Our results revealed changes in B16FO cells after application of PDT induced by red light at the dose of 15 $J.cm^{-2}$ in the presence of 0 (control), 0.5, 1, 5, 10, 50 and 100 µM $ClAlPcS_2$. The production of ROS during photodynamic therapy was measured, with the detected final ROS production seen at a dose of 15 $J.cm^{-2}$. The results during the first 30 seconds, 10 minutes as well as the final production of ROS, are summarized in Tables 1 and 2. The ROS production increased with rising concentrations of the photosensitizer and decreased with time in the B16FO cell line.

Table 2 shows the production of ROS under the same conditions with additional ultrasound exposure. The ultrasound exposure enhanced the production of ROS. The increase in the production of ROS with concentration of $ClAlPcS_2$ was retained. Cell viability of the B16FO cell line 24 h after PDT and SDT with $ClAlPcS_2$ sensitizer is shown in Graph 1. It is noticeable, that the lower the ROS production is, after treatment, then the higher the viability of the cells (see Graph 1 and Tables 1 and 2).

The effect of PD and SD treatment on B16FO cell line

Table 1 Kinetic production of ROS at the first 30 seconds, 10 minutes and at final concentration ROS using a dose of 15 J.cm^{-2} in μM.s^{-1} H_2O_2 per 10^4 B16FO cells. Control = without sensitizer and without light irradiation. Negative control = without sensitizer and with light irradiation.

Concentration of $ClAlPcS_2$ [μM]	ROS production [μM.s^{-1} H_2O_2] in first 30 sec.	ROS production [μM.s^{-1} H_2O_2] in 10 min.	ROS concentration at dose of 15 J.cm^{-2} [μM H_2O_2]
0,5	0.32 ± 0.1	1.01 ± 0.4	777.51 ± 145.0
1	0.62 ± 0.2	2.08 ± 0.3	1088.14 ± 483.9
5	2.77 ± 0.6	8.11 ± 0.3	2546.56 ± 181.7
10	2.80 ± 1.3	9.11 ± 0.9	2830.90 ± 125.6
50	6.07 ± 1.4	10.26 ± 0.9	3140.82 ± 252.4
100	9.87 ± 2.1	11.10 ± 0.8	3746.06 ± 483.1
Negative Control	1.92 ± 1.8	1.14 ± 0.5	457.01 ± 61.5
Control	1.13 ± 0.5	0.75 ± 0.2	182.67 ± 11.9

Table 2 Kinetic production of ROS at the first 30 seconds, 10 minutes and at final concentration ROS using a dose of 15 J.cm^{-2} in μM.s^{-1} H_2O_2 per 10^4 B16FO cells after ultrasound exposure. Control = without sensitizer and without light irradiation and with ultrasound irradiation. Negative control = without sensitizer and with light irradiation and with ultrasound irradiation.

Concentration of $ClAlPcS_2$ [μM]	ROS production [μM.s^{-1} H_2O_2] in first 30 sec.	ROS production [μM.s^{-1} H_2O_2] in 10 min.	ROS concentration at dose of 15 J.cm^{-2} [μM H_2O_2]
0,5	2.50 ± 1.1	4.74 ± 1.5	939.52 ± 225.2
1	2.64 ± 1.2	4.83 ± 1.6	1313.22 ± 344.9
5	3.77 ± 1.2	15.41 ± 2.9	2580.74 ± 193.37
10	3.90 ± 1.3	16.87 ± 2.5	3540.49 ± 156.6
50	5.94 ± 2.6	19.00 ± 1.9	3670.14 ± 339.3
100	7.80 ± 0.9	21.02 ± 3.2	3766.85 ± 299.6
Negative Control	3.50 ± 1.0	2.21 ± 6.26	748.21 ± 159.6
Control	1.54 ± 0.7	0.58 ± 0.1	171.72 ± 24.5

Ultrasound treatment increases the production of ROS. These processes are marked particularly in higher concentrations of $ClAlPcS_2$. The sequence of the treatments affects the production of ROS. The highest production of ROS is acquired by application of SDT after PDT [10]. The decreased production of ROS (for example in lower concentration of sensitizer) leads to an increase of cell viability, while the increase of ROS production by ultrasound exposure leads to a decreased cell viability. These effects are evident in all concentrations of the sensitizer.

A microscopic study (Figure 1) shows morphological changes in the cell generally, before and after photodynamic treatment. Figure 1A presents undamaged control pigment mouse melanoma cell line B16FO without irradiation; Figure 1B shows photodamaged B16FO cells after PDT with $ClAlPcS_2$ at concentration 5 μM and dose of light irradiation of 15 $J.cm^{-2}$.

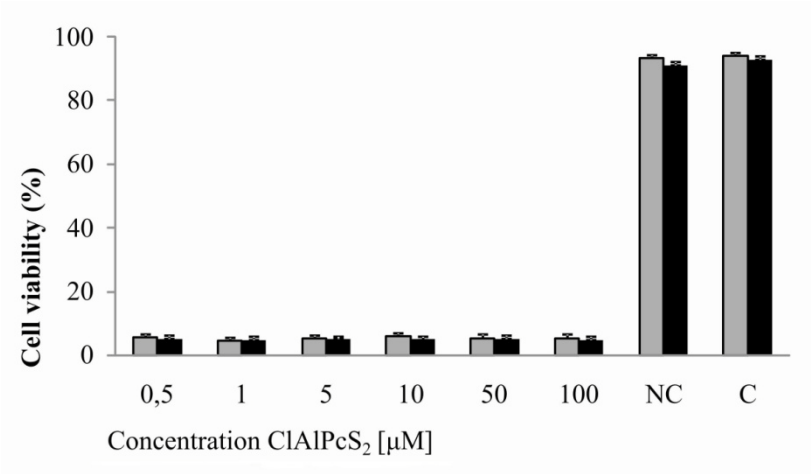

Graph 1 Cell viability of the B16FO cell line 24 h after PDT with $ClAlPcS_2$ sensitizer at concentration of 0.5, 1, 5, 10, 50, 100 μM and with a light dose of 15 $J.cm^{-2}$ (grey columns) and by comparison at the same concentrations with SDT (black columns). C = control without sensitizer and without light irradiation (grey column) and with ultrasound exposure (black column), NC = negative control without sensitizer and with light irradiation (grey column) and with ultrasound exposure (black column).

The effect of PD and SD treatment on B16FO cell line

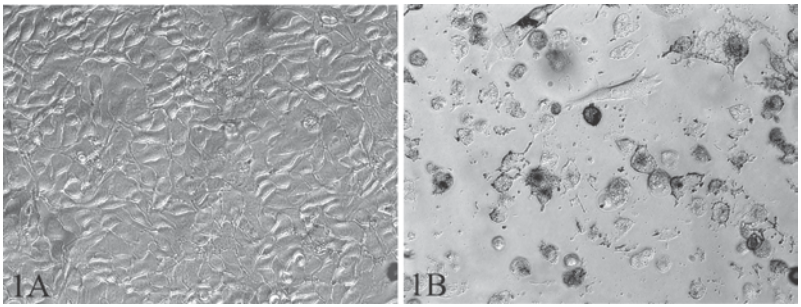

Figure 1 B16FO observed in transmitted light microscopy at 100× magnification. **A.** Control B16FO cells without irradiation. **B.** Photodamaged cells after PDT in presence of $ClAlPcS_2$ (concentration 5 μM, irradiation dose of 15 $J.cm^{-2}$.

We can see the morphological changes after PDT. The live B16FO cell line is spread in a monolayer on the substrate, with the cytoplasm of the individual cells approaching each other. On the other hand, the photodynamically treated cells undergo cell death, here the pigment of B16FO cells is more visible. The live undamaged cells (Figure 1A) have an elongated shape in comparison with photodynamically damaged cells. In general, the shape of the cells depends on the type and also on the state of the cell; for example, dead cells are characterized by circular or elliptic shape (Figure 1B) in comparison with the oblong shape of live cells.

In summary, the tumor cell line B16FO has a sensitivity to PDT, and the combination of photodynamic and sonodynamic treatments leads to cell death which can be seen in Graph 1. Cells given sonodynamic therapy after photodynamic therapy are more susceptible to ROS damage. This damage can lead to apoptosis. This phenomenon is to explain as a redistribution of sensitizer to more appropriate functional places in cell and formation of cavitation [2, 5]. Together with free radical and principally the most cytotoxic singlet oxygen, these treatments are highly effective in damaging cancer cells.

8.3 References

[1] NAKASEKO, H.; KOBAZASHI, M.; AKITA, Z.; TAMADA, Y.; MATSUMOTO, Y. Histological changes and involvement of apoptosis after photodynamic therapy for actinic keratoses. *British Journal of Dermatology.* Blackwell, England, 2003, 148, pp. 122-127.

[2] KESSEL, D.; JEFFERS, R.; FOWLKES, J.B.; CAIN, C. Effects of sonodynamic and photodynamic treatment on cellular thiol levels. *Journal of Photochemistry and Photobiology B*. Elsevier, Switzerland, 1996, 32, pp. 103-106.

[3] YUMITA, N.; UMEMURA, S. Sonodynamic therapy with photofrin II on AH130 solid tumor. Pharmacokinetics, tissue distribution and sonodynamic antitumoral efficacy of photofrin II. *Cancer Chemotherapy and Pharmacology*. Springer, USA, 2003, 51, pp. 174-178.

[4] KESSEL, D.; JEFFERS, R.; FOWLKES, J.B.; CAIN, C. Porphyrin-induced enhancement of ultrasound cytotoxicity. *International Journal of Radiation Biology.* Taylor and Francis, England, 1994, 66, pp. 221-228.

[5] WORTINGTON, A.E.; THOMPSON, J.; RAUTH, A.M.; HUNT, J.W. Mechanism of ultrasound enhanced porphyrin cytotoxicity. Part I: A search for free radical effects. *Ultrasound in Medicine and Biology.* Elsevier, England, 1997, 23, pp. 1095-1105.

[6] SUSLICK, K.S. Sonochemistry. *Science.* Amer Assoc Advancement Science, 1990, 247, pp. 1439-1445.

[7] SADZUKA, Y.; TOKUTOMI, K.; IWASAKI, F.; SUGIYAMA, I.; HIRANO, T.; KONNO, H.; OKU, N.; SONOBE, T. The phototoxicity of photofrin was enhanced by PEGylated liposome in vitro. *Cancer Letters*. Elsevier, Ireland, 2006, 241, pp. 42-48.

[8] VALKO, M.; RHODES, C.J.; MONOCOL, J.; IZAKOVIC, M.; MAZUR, M. Free radicals, metals and antioxidants in oxidative stress-induced cancer. *Chemico-Biological Interactions*. Elsevier, Ireland, 2006, 160, pp. 1-40.

[9] NORDBERG, J.; ARNÉR, S.J. Reactive oxygen species, antioxidants and the mammalian thioredoxin system. *Free Radical Biology and Medicine*. Elsevier, England, 2001, 31, pp. 1287-1312.

[10] TOMANKOVA, K.; KOLAROVA, H.; BAJGAR, R. Study of photodynamic and sonodynamic effect on A549 cell line by AFM and measurement

of ROS production. *Physica Status Solidy A*. Wiley, Germany, 2008, 205, pp. 1472 – 1477.

Index